IAEA-TECDOC-992

Nuclear data for neutron therapy: Status and future needs

IAEA

29 - 17

NUCLEAR DATA FOR NEUTRON THERAPY:
STATUS AND FUTURE NEEDS
IAEA-TECDOC-992

FOREWORD

During the past decade the IAEA has devoted much attention to developing nuclear and atomic databases for medical applications. The programme has covered the following topics:

1. Atomic and molecular data for radiotherapy and radiation research. (Results were published as IAEA-TECDOC-799 in 1995)

2. Nuclear data for medical isotope production.

3. Nuclear data for neutron therapy.

The present report summarizes the results of the programme for the last topic. The starting point was an Advisory Group meeting on Nuclear and Atomic Data for Radiotherapy and Related Radiobiology held at TNO Rijswijk, Netherlands, in September 1986. The meeting participants emphasized the growing number of neutron therapy clinics throughout the world and also noted that the energy of neutron beams was shifting to higher neutron energies: to the range from 14 to 70 MeV. The meeting has reviewed the status of data at that time and concluded that the following information was required for neutron therapy:

1. Kerma factors for the neutron energy range between 15 and 100 MeV and partial and total cross sections for biologically important elements, especially for carbon and oxygen.

2. Improvement of neutron transport calculations for in-phantom conditions, including the effect of inhomogeneities.

3. Primary and secondary charged-particle spectra needed for calculations of absorbed dose during treatment of patients.

In order to address these needs the IAEA organized a Co-ordinated Research Programme (CRP) on Nuclear Data Needed for Neutron Therapy. In the framework of this CRP three research co-ordination meetings were held during 1987-1993. The CRP participants concentrated on the problems of microdosimetry and protocols for the determination of absorbed doses, neutron source properties (for the Be(p,n)reaction up to 100 MeV), beam collimation and shielding, measurements of kerma factors for biologically important elements, and a comparative characterization of radiation quality (i.e. biological effect per unit dose) of neutron beams used in various therapy centres.

The work on summarizing the results of the CRP was continued after its official termination in 1993 and a report was prepared by the participants in 1995 for final review by a group of consultants.

EDITORIAL NOTE

Contents

1 Nuclear Data Needed for Neutron Therapy

1.1 Introduction

Neutron therapy is applied at present in eighteen centers worldwide. The considerable number of patients, exceeding 15,000, and their follow-up, extending over a period of twenty years in the longest series, allow some conclusions concerning the value of fast neutron therapy to be drawn.

Although the first patients were treated with neutrons with too low energies produced in cyclotrons or (D-T) generators, a clinical benefit was observed for some tumor types, especially for slowly growing, well-differentiated tumors, which are currently considered to be resistent to photon radiation (as well as to chemotherapy).

The most encouraging results were actually obtained for locally extended salivary gland tumors and prostatic adenocarcinomas, but also for some advanced tumors of the head and neck area as well as for well differentiated soft tissue sarcomas, osteo- and chondrosarcomas.

It is difficult today to evaluate the proportion of the patients currently referred to radiotherapy and who could in the future benefit from fast neutron therapy. However, the survey of the available clinical data allows us to expect that this proportion would exceed 10%. In fact this proportion is probably a lower limit since the patients treated in the past with neutrons were often treated in "suboptimal" technical conditions (poorly penetrating beams, fixed beams, fixed inserts, etc.). In addition, the greater efficiency of neutrons observed for some types of slowly growing tumors could extend the borders of the indications of radiation therapy, and allow the therapist to consider irradiation of tumor types traditionally considered as being resistant to photons.

The main problem for the therapist remains the selection of the patients suitable for neutron therapy. Much effort is spent to that end, and development of predictive tests is promising.

From a technical point of view, fast neutron therapy is undergoing important changes, especially with the introduction of high-energy, hospital-based, therapy-dedicated cyclotrons. The high-energy neutron beams available at present (50 to 65-MeV protons on Be target) have beam characteristics very similar to the current photon beams as far as dose distribution is concerned, i.e. penetration, skin sparing, penumbra, etc. In addition, these neutron machines are equipped with variable-often multileaf-collimators and isocentric gantries. They are entirely dedicated to treatment and are as reliable in their operation as modern linear electron accelerators for photon therapy. Consequently, one can assume that with the new generation of therapy-dedicated cyclotrons, patients can be treated with fast neutrons under conditions very similar to those at modern linear electron accelerators.

There is clinical and radiobiological evidence that the accuracy required for clinical dosimetry for neutrons is at least as high as that in photon clinical dosimetry. In general, an accuracy of +/- 3.5% is required (Mijnheer et al., 1987).

Neutron dosimetry for clinical purposes is carried out mainly with ionization chambers made of "tissue-equivalent" (wall and gas) material. The energy deposition by fast neutrons results from a two-step process. In the first, interactions between neutrons and target nuclides lead to the release of energetic charged particles, mainly protons, alpha particles and heavier ions. The second step is the subsequent interaction of these charged particles with matter by ionization and excitation.

The neutron interactions are highly nuclide-specific and strongly dependent on neutron energy within the energy range of interest for neutron therapy. The physical parameters describing these neutron interactions are microscopic cross sections, charged-particle spectra, and kerma, *i.e.* the total kinetic energy transfered to charged particles. For accurate dosimetry these parameters should be known for all nuclides that comprise tissue and detector materials. In practice, uncertainties are considerable, especially for neutron energies exceeding 15 MeV. The introduction of higher energy cyclotrons to produce neutrons with improved beam characteristics has therefore created additional problems for clinical dosimetry. Nuclide specificity and the strong energy dependence of the nuclear interactions make it impossible to construct ionization chambers or other dosimeters that are truly tissue-equivalent. Determination of absorbed dose in tissue depends upon the knowledge of the kerma for the constitutive elements of tissue and the dosimeter to be able to evaluate kerma factor ratios. Therefore, clinical neutron dosimetry requires comprehensive and accurate knowledge of kerma factor values for nuclides and materials relevant to the neutron energy range of interest. Furthermore, the application of kerma factors (ratios) requires adequate knowledge of the neutron energy spectrum.

This report discusses the status and success of neutron therapy and some of the problems in clinical neutron dosimetry. Existing neutron interaction data, in particular results of kerma factor measurements and data evaluations, are reviewed. Nuclear data relevant for neutron source reactions, collimation, and shielding are also discussed. Finally, physical aspects of the variation of biological effectiveness of neutrons with neutron energy ("radiation quality") are set out.

Exchange of information between neutron therapy centers is essential, since only clinical experience can determine the optimal absorbed dose, fractionation, target volume, and clinical indications/contra-indications for neutron therapy.

This exchange of information implies uniformity in specification of dose as well as radiation quality. In order to achieve this, the ECNEU (European Clinical NEUtron dosimetry group) and AAPM (American Association of Physicists in Medicine) independently designed clinical neutron dosimetry protocols. Application of these protocols ensured reasonable dosimetric uniformity within European and US centers. However, differences in the European and American dosimetric approaches, as well in the selection of numerical values for some parameters, could result in differences in the evaluated absorbed dose as large as 8% between the two protocols. Such discrepancies are highly significant clinically. Therefore a Reporting Committee set up by the ICRU, issued a unified protocol (ICRU Report 45, April 1989).

Although the agreement on a common protocol worldwide guarantees a uniform method of dose determination and of dose reporting, several problems remain to be solved. They are related to the fact that a change in neutron energy implies a change in the cross-sections and the responses of the detectors and also alters the biological effectiveness. This latter aspect is specific to neutron therapy, since RBE differences as high as 40% have been reported between the highest and the lowest energy beams used in therapy. By contrast, in the field of conventional photon therapy, there is no significant variation in RBE. A practical difficulty arises when transferring, at the new high-energy facilities, the experience previously gained with low-energy machines. The uncertainty in the kerma or W (energy per ion pair) values at high energy, as well as on the kerma and W ratios between high and low energy, will be reflected in the uncertainty in the "clinical RBE" used at high-energy machines. Discrepancies as high as 10% were reported on RBE variation between high and low neutron energies.

Of course animal experiments could be performed to provide the ultimate check on the optimum dose to be delivered to patients. However it is important, both for safety as well as for data interpretation, to separate what is due to differences in kerma and W, *i.e.* pure physical aspects, and what is due to biological effectiveness.

Differences in dose distribution as a function of tissue composition are probably more important with neutrons than with photons. Determining the exact absorbed dose in some relevant organs, or at least a clear indication of the possible differences, is essential for the interpretation of some clinical data. This also applies to some radio-biological experiments designed to derive some information to be used clinically (*e.g.*, on mammalian cells irradiated in monolayers attached to different plastic materials).

In that respect one of the advantages of neutron beams is related to the fact that the kerma in bone material is lower than in soft tissues. Knowledge of the absorbed dose near the bone-soft-tissue interface and at the level of the bone cavities is important in analyzing the existence or the absence of a bone necrosis and to set a dose limit to avoid bone necrosis.

Finally, correct interpretation of clinical data, which is the basic condition for improving therapy, requires the accurate determination of dose to the relevant organs. As indicated above, it is recognized that in photon therapy differences in dose as small as a few percent can be detected clinically in certain conditions: therefore an accurancy of 3.5% is required. All available clinical and radiobiological data indicate that for neutrons the dose effect curves for tumor control and normal tissue complications are at least as steep as for photons. The same accuracy on dose delivery should then be required. Today we are still far from that goal for absolute dose values or when different neutron energies or tissue compositions are involved.

2 Status and Success of Neutron Therapy

2.1 Introduction

Fast neutron therapy is applied today routinely in 18 centers throughout the world (Table I). More than 15,000 patients have been treated so far with neutrons, either as the sole irradiation modality or in combination with other radiotherapy techniques. The available clinical data now enable us to identify some tumor types (or sites) for which neutrons were shown to bring a benefit, as well as to discuss other tumor sites for which neutrons could be useful (Breit *et al.*, 1985; Chauvel and Wambersie, 1989; Schmitt and Wambersie, 1990; Wambersie, 1990; Wambersie and Battermann, 1985; and Wambersie *et al.*, 1986). Since fast neutrons were introduced in radiotherapy on the basis of radiobiological arguments, it is essential to review briefly some radiobiological data in order to properly interpret the clinical observations.

2.2 Rationale for Using Fast Neutrons in Radiation Therapy: Radiobiological Considerations

Historically, the oxygen effect was the rationale for the use of neutrons (and other high-LET radiations) in radiotherapy. The advantage expected from fast neutrons rests on the following experimental data (Tubiana *et al.*, 1990):

1. The presence of hypoxic cells in malignant tumors;

2. The selective radioresistance of hypoxic cells when irradiated with low-LET radiations. This is expressed by the Oxygen Enhancement Ratio (OER), which is the ratio of doses required, for a given biological effect, when delivered under hypoxic or aerobic conditions. For X rays the OER is about 3.

3. A reduction of the OER with high-LET radiations. For fast neutrons the OER is about 1.6.

The term Hypoxic Gain Factor (HGF) has been used to quantify this advantage: it is defined as the ratio of OER values for the compared radiation qualities. When fast neutrons are used instead of X rays, the HGF is equal to $3/1.6 = 1.9$. The HGF represents the therapeutic gain if the hypoxic cells were the determining factor in tumor resistance. In practice, therapeutic gain is less than the HGF as tumor reoxygenation during fractionated irradiation reduces the population of hypoxic cells.

Therefore, as one must accept that hypoxic cells play a role in the radioresistance of some tumors, it is not reasonable today to ascribe the radioresistance of all malignant tumors to this cause (Adams, 1990).

There are other factors besides the oxygen effect which may also influence the therapeutic gain with high-LET radiations. A wider approach to the rationale of neutron therapy suggests that with increasing LET there is a general reduction in differences in radiosensitivity between cell populations. Some experimental results are presented here in order to support this hypothesis, which is based to some extent on the comparison of the microdosimetric characteristics of the neutron and X-ray beams. After neutron irradiation, recoil protons and other secondary particles deposit about 50-100 times more energy per unit path length than do electrons (Figure 1). When a cell nucleus (or a critical subcellular structure) is crossed by such particles,

Table I: Fast neutron therapy facilities presently operating in the world.
Updated from ICRU (1989), Tsunemoto *et al.*, (1989), and Schmitt and Wambersie (1990).

Center		Neutron Producing Reaction	Comments
EUROPE			
U.K.	MRC-Clatterbridge	p(62)+Be	rotational gantry variable collimator
France	Orléans	p(34)+Be	vertical beam
Belgium	UCL-Louvain-la-Neuve	p(65)+Be	vertical beam (multileaf collimator and horizontal beam in preparation)
Germany	Hamburg	(d+T)	rotational gantry
	Heidelberg	(d+T)	rotational gantry
	Munster	(d+T)	rotational gantry
	Essen	d(14)+Be	rotational gantry
	Garching–T.U. München	reactor neutrons (av. energy 2 MeV)	mixed beam
UNITED STATES			
Texas	M.D. Anderson-Houston	p(42)+Be	rotational gantry variable collimator
Ohio	Cleveland	p(43)+Be	horizontal beam
California	UCLA–Los Angeles	p(46)+Be	rotational gantry variable collimator
Michigan	Harper-Grace Hospital, Detroit	d(50)+Be	rotational gantry multirod collimator
Washington	Seattle	p(50)+Be	rotational gantry multileaf collimator
Illinois	Fermilab	p(66)+Be	horizontal beam
ASIA			
Japan	National Institute of Radiological Sciences Chiba	d(30)+Be	vertical beam multileaf collimator
	Institute for Medical Sciences Tokyo	d(14)+Be	horizontal beam
Korea	Korea Cancer Center Hospital Seoul	d(50.5)+Be	rotational gantry
Saudi Arabia	King Faisal Hospital-Riyadh	p(26)+Be	rotational gantry
AFRICA			
South Africa	National Accelerator Centre (NAC), Faure	p(66)+Be	rotational gantry variable collimator

there is much greater probability of lethal damage than when the nucleus is crossed by recoil electrons (Wambersie *et al.*, 1984).

Studies on the survival of irradiated cell cultures shed light on the effectiveness of irradiations with differing LET. In 1977, Barendsen and Broerse compared cell survival curves of five cell lines *in vitro* after irradiation with 300 keV X rays and 15 MeV neutrons. A general reduction in the differences of radiosensitivity was observed with neutrons. Somewhat different conclusions were reached by Fertil *et al.* (1982) who showed that the ranking of radiosensitivity of some cell lines could be altered when X rays were replaced by fast neutrons (Figure 2).
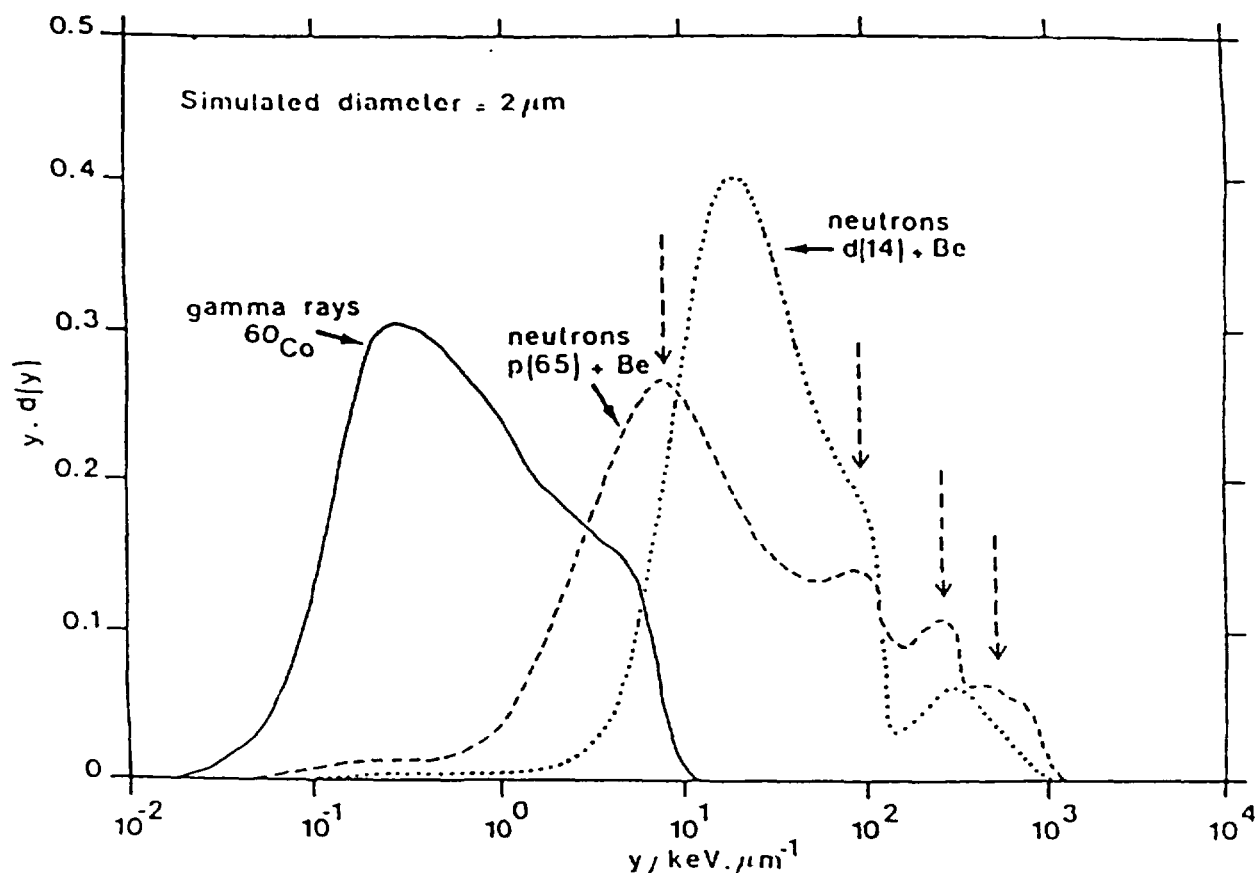
Figure 1: Comparison of energy depositions after irradiation with fast neutrons and γ-rays. The curves indicate distributions of individual energy-deposition events in a simulated volume of tissue 2 mm in diameter; the parameter y (lineal energy) represents the energy deposited by a single charged particle traversing the sphere, divided by the mean cord length. The maximum with γ-rays is at 0.3 keV·μm^{-1} and with d(14)Be neutrons at 20 keV·μm^{-1}. The spectrum for p(65)Be neutrons shows four peaks: the first is at 8 keV·μm^{-1} and corresponds to high energy protons, the second at 100 keV·μm^{-1} corresponds to low energy protons, the third at 300 keV·μm^{-1} is due to α-particles and the last is due to recoil nuclei at 700 keV·μm^{-1} (Menzel et al., 1990; Pihet et al., 1990).
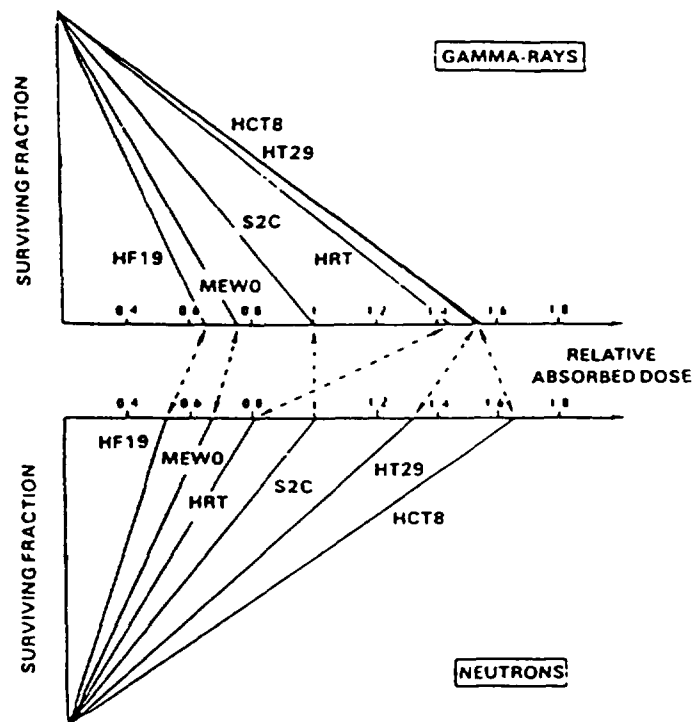
Figure 2: Comparison of surviving fractions for six cell lines irradiated with ^{60}Co γ-rays and d(50)Be neutrons. Survival of the six populations has been calculated for a fractionated irradiation given with fractions of 2 Gy (γ-equivalent). The $_{eff}D_o$ values were deduced from the α and β-coefficients derived from the survival curves observed in vitro. To facilitate the comparison, relative absorbed doses are indicated on the abscissa, the SZC cells being taken as the reference. The variations of radiosensitivity are as important with neutrons as with photons, but the order of radiosensitivities is altered (calculated from the data of Fertil *et al.*, 1982).

Another factor favoring high LET radiation is that repair phenomena are in general less important with neutrons, and consequently differences in repair capacity are of less significance (Tubiana *et al.*, 1960).

A third difference in the biological effects produced by neutrons compared to X rays is a reduction in the variation of radiosensitivity with the phase of the cell cycle and consequently a variation in neutron RBE, depending on the phase (Figure 3) (Chapman, 1988).

Withers and Peters (1979) introduced the concept of the Kinetics Gain Factor (KGF) defined as the ratio of the RBE values for effects on the tumor and normal tissues, evaluated by taking account only of the fluctuations in radiosensitivity with the phase of the cycle. Basing their calculations on data such as those of Gragg *et al.* (1978), they obtained Kinetics Gain Factors which could under certain conditions be as great as 3, *i.e.* of the same order as the Hypoxic Gain Factor. However, a reduction in OER is always an advantage because only malignant cells are hypoxic, whereas the KGF may, depending on the situation, represent a gain or a loss. There may be a gain (KGF > 1) for tumors in which cell redistribution is slow, leading to the accumulation of cells in resistant phases of the cell cycle during a fractionated treatment. It may also be effective for tumors whose cells have a long radioresistant G_1 phase. These radiobiological considerations can be correlated with slowly growing, well-differentiated tumors.

In summary, with photons there are large variations of radiosensitivity between different cell lines or tissues, whether they are normal or malignant. These variations are amplified by fractionation because of differences in repair patterns. With neutrons these variations in radiosensitivity are reduced. The reduction in OER with neutrons is an example of the more general phenomenon of radiosensitivity leveling. Although a reduction in OER is always advantageous, a reduction of differences in radiosensitivity related to cell line, position in the mitotic cycle and repair capacity could be an advantage or a disadvantage, depending on the characteristics of the tumor cell population and the normal cell population(s) at risk. This raises the important problem of patient selection (Figure 4).

Another conclusion which can be derived from the radiobiological data is the importance of the physical selectivity with LET radiations. As a matter of fact, since there is a reduction in the differential effect between the different cell populations, high-physical selectivity plays a more important role for improving the therapeutic gain.

It can therefore be concluded from the available radiobiological data that high-LET radiations could be advantageous for some tumor types or sites. In addition, radiobiology suggests some mechanisms which could be responsible for this therapeutic gain, as well as ways to select the patients suitable for neutron therapy. On the other hand, analysis of the clinical data is needed to identify the tumor types for which fast neutrons bring a benefit and furthermore to evaluate quantitatively the therapeutic gain.

2.3 Review of the Clinical Neutron Therapy Data

A review of the clinical data is presented here. Data have to be analyzed keeping in mind the important problem of patient selection (neutrons certainly do not provide the solution for all tumors!), and the role of the technical factors which are of special importance when high-LET radiations are used.
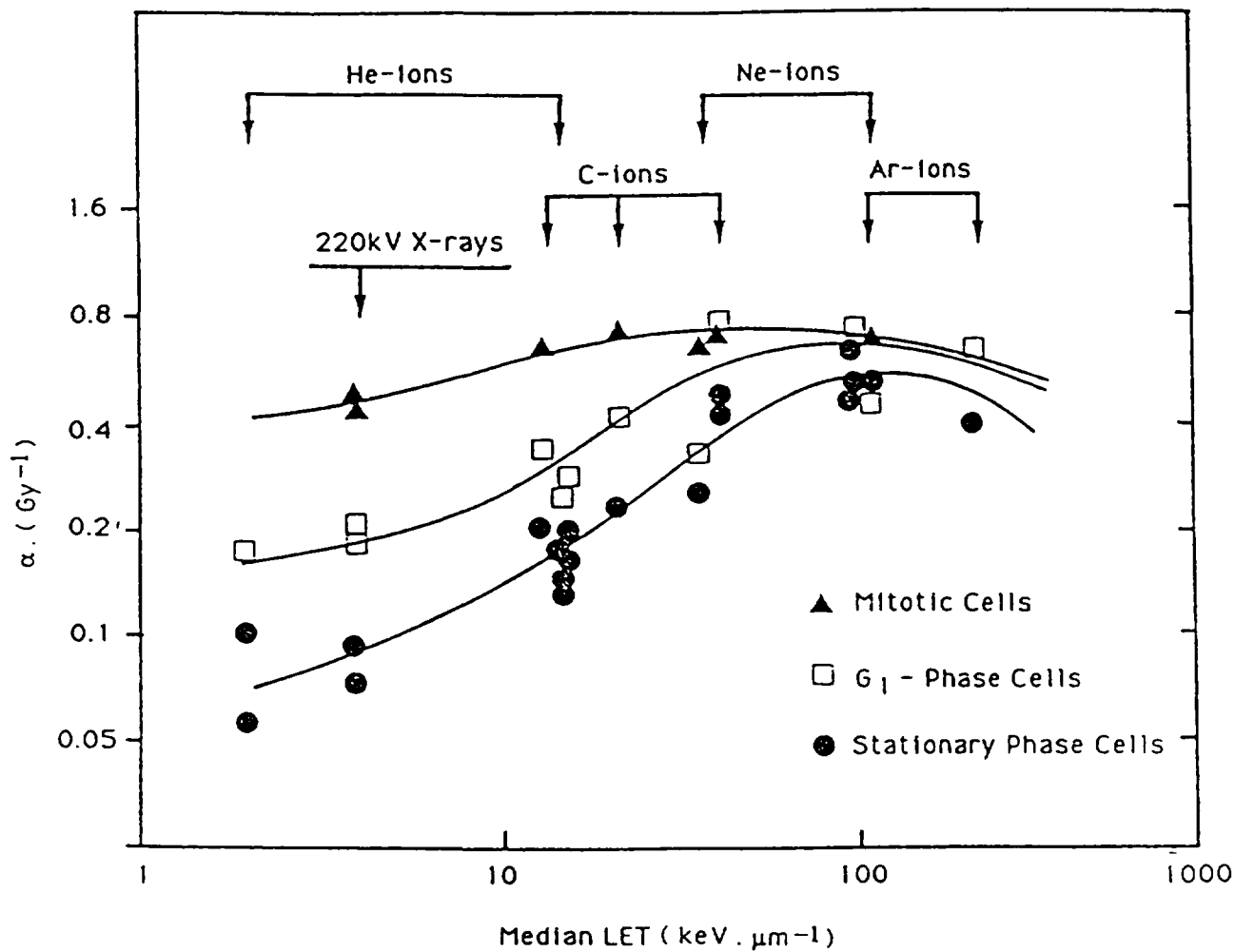
Figure 3: Single-hit inactivation coefficients (α) for homogeneous populations of Chinese hamster cells irradiated in mitosis, G_1 phase and stationary phase, with 220 kV X rays and various beams of charged particles. The α-coefficients are plotted as a function of the median LET (in keV·μm^{-1}). After Chapman (1988).
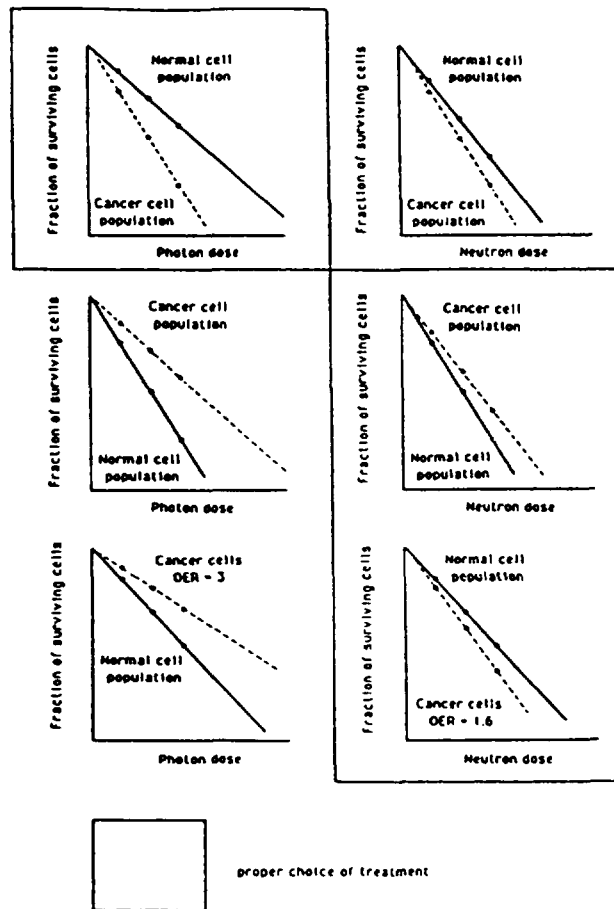
Figure 4: Importance of patient selection for fast neutron therapy. Three possible clinical situations are considered. In the first (a), the cancer cells are more sensitive to X rays than the normal cell populations at risk, and there is no argument at all for using neutrons which would reduce a favorable differential effect. In the second situation (b), neutrons bring a benefit by reducing a difference in radiosensitivity which would selectively protect the cancer cell population. A third more favorable situation is shown (c) where the relative radiosensitivities are reversed (e.g., if OER is the relevant factor, or according to Fertil et al.) It has been assumed in the figure that the survival curves are exponential after fractionated irradiation, i.e. a constant proportion of the cells is killed at each session. However, the exact shape of the cell survival curve is not essential for the present discussion (Tubiana et al., 1990).

2.3.1 Salivary Gland Tumors

Locally extended inoperable salivary gland tumors are the first type of tumors for which the superiority of fast neutrons, compared to conventional low-LET radiations, has been recognized. Griffin *et al.* (1979) reported promising results from the University of Washington in Seattle. In Europe, the two most important series were obtained in Hammersmith (Catterall and Errington, 1987) and in Amsterdam (Battermann and Mijnheer, 1986) with persistent local controls of 77% and 66%, respectively. These results were confirmed by the further publications from the Seattle group (Table II) (B.R. Griffin *et al.*, 1988).

Table II: Neutron therapy of salivary gland tumors loco-regional control rate versus tumor histology (minimum one year follow-up). Modified from Griffin *et al.* (1988).

Tumor histology	Number of patients	Loco-regional control
Adenoid cystic	17	15
Mucoepidermoid	9	6
Malignant mixed	2	2
Undifferentiated	4	3
Overall	32	26 (81%)

At the NIRS in Japan, 21 patients with inoperable or recurrent parotid gland tumor were treated with fast neutrons; local control was achieved in 13 cases (62%). In addition, 14 patients were treated after radical surgery; no local recurrence was observed. Of the total number of 35 patients treated with neutrons, 4 complications were scored (Tsunemoto *et al.*, 1989). A recent review of all the patient series treated worldwide (Table III) indicates an overall local control rate of 67%, while the overall local control rate for "similar" patient series treated with low-LET radiation (photons, electrons, interstitial therapy) reaches only 24% (Griffin *et al.*, 1984).

Such a comparison of historical series is always questionable and only a randomized trial can bring a definite conclusion. A prospective randomized trial for inoperable primary or recurrent malignant salivary gland tumors was initiated by the RTOG in 1980 (Table IV).

The loco-regional control rates at two years were 67% for neutrons and 17% for photons. Although the numbers of patients were small (13 and 12, respectively), the study was closed in 1986 for ethical reasons when the statistical significance of the difference between treatments became apparent ($p < 0.005$) (T.W. Griffin *et al.*, 1988). One should point out that the local control rates observed in the randomized study are very similar to the average local control rates reported in the historical series.

Taken as a whole, the results of the non-random clinical studies and the prospective randomized trial overwhelmingly support the contention that fast neutrons offer a significant advance in the treatment of inoperable and unresectable primary or recurrent malignant salivary gland tumors.

Table III: Review of the loco-regional rates for malignant salivary gland tumors treated with radiation therapy. Updated from B.R. Griffin *et al.* (1989), T.W. Griffin *et al.* (1988), and Tsunemoto *et al.* (1989).

FAST NEUTRONS		
Authors	Number of patients *	Loco-regional control (%)
Saroja *et al.* (1987)	113	71 (63%)
Catterall and Errington (1987)	65	50 (77%)
Battermann and Mijnheer (1986)	32	21 (66%)
Griffin *et al.* (1988)	32	26 (81%)
Duncan *et al.* (1987)	22	12 (55%)
Tsunemoto *et al.* (1989)	21	13 (62%)
Maor *et al.* (1981)	9	6 (67%)
Ornitz *et al.* (1979)	8	3 (38%)
Eichhorn (1981)	5	3 (60%)
Skolyszewski (1982)	3	2 (67%)
Overall	310	207 (67%)
LOW-LET RADIOTHERAPY PHOTON AND/OR ELECTRON BEAMS, AND/OR RADIOACTIVE IMPLANTS		
Authors	Number of patients *	Loco-regional control (%)
Fitzpatrick and Theriault (1986)	50	6 (12%)
Vikramet *et al.* (1984)	49	2 (4%)
Borthne *et al.* (1986)	35	8 (23%)
Rafla (1977)	25	9 (36%)
Fu *et al.* (1977)	19	6 (32%)
Stewart *et al.* (1968)	19	9 (47%)
Dobrowsky *et al.* (1986)	17	7 (41%)
Shidnia *et al.* (1980)	16	6 (38%)
Elkon *et al.* (1978)	13	2 (15%)
Rossman (1975)	11	6 (54%)
Overall	254	61 (24%)

Table IV: Neutron therapy of inoperable salivary gland tumors: results of an RTOG/MRC prospective randomized trial. Modified from Griffin *et al.* (1988).

	Photons	Neutrons
Number of evaluable patients	12	13
Loco-regional control		
at 1 year	17 ± 11%	67 ± 14%
at 2 year	17 ± 11%	67 ± 14%
Survival		
at 1 year	67 ± 12%	77 ± 12%
at 2 year	25 ± 14%	62 ± 14%

* Patients treated *de novo* and for gross disease after a post-surgical recurrence are included, but not patients who were treated postoperatively for microscopic residual disease.

2.3.2 Paranasal Sinuses

Remarkably good results of neutron therapy have also been reported by Errington for locally extended tumors of the paranasal sinuses. In the series treated at the Hammersmith Hospital, 86% (37/43) of the patients showed complete remission, and relief of symptoms was noticed in all cases. Thirty percent of the patients survived at three years with a 50% local control rate (Errington, 1986). Several factors could explain these interesting results, indicating that paranasal sinuses could be a good indication for neutron therapy:

- The superficial location of these tumors (when only poorly penetrating beams are available);

- The diversity of differentiated histology: in the Errington's series, there were 14 squamous cell carcinomas, but also 11 adenoid-cystic carcinomas and 8 adenocarcinomas (Table V);

- The presence of bone structures, in or near the target volume, which reduces the absorbed dose to the cells located in the osseous cavities (Bewley, 1989; Catterall and Bewley, 1979). Similar results were reported more recently by Errington at the Clatterbridge cyclotron in U.K. (Errington, 1991).

Table V: Results of treatment with 7.5 MeV neutrons for advanced tumors of paranasal sinuses: histological types, responses, and complications.

Histological type	Regressing completely	Recurring	With complications
Squamous (n = 17)	14	3	3
Adenoid cystic (n = 11)	10	4	4
Adenocarcinoma (n = 8)	6	-	1
Transitional cell (n = 5)	5	1	2
Undifferentiated (n = 1)	1	-	-
Malignant melanoma (n = 1)	1	-	-
Total (n = 43)	37 (86%)	8 (18%)	* 10 (23%)

*2 of these from 8 patients who had received previous photon radiotherapy (Errington, 1986).

2.3.3 Other Head and Neck Tumors

Conflicting results have been reported in Europe for neutron therapy of advanced squamous cell carcinomas of the head and neck. The first study conducted by Catterall et al. (1977) showed a highly significant advantage of neutrons over photons with respect to local control and survival. However, these results were not substantiated in a European multi-center, randomly controlled trial. The disease-free survival rate at 12 months was 34% (34/100) for the neutron group and 38.9% (37/95) for the photon group. The recurrence rates were 37% and 39.7%, respectively (Duncan et al., 1984). In Japan, 13 patients with tumor of the supraglottis were treated with

fast neutrons at the NIRS. Local control was reported in 11 cases (84%), while with photons for similar patients local control was achieved in only 25% of the cases. In the same center, no difference in local control after neutron or photon irradiation was reported for carcinoma of the glottis and subglottis (Tsunemoto, 1989). In the United States, an RTOG trial with a small number of patients with advanced disease revealed a local control of 52% (12/23) for the neutron group, compared with 17% (2/12) for the photon group. Although the number of patients was small, the benefit due to neutrons for these advanced cases was statistically significant (p = 0.035). The actuarial survival rate at two years was 25% in the neutron group and 0% in the photon group (Griffin et $al.$, 1984).

Another RTOG randomized trial compared mixed schedule irradiation (2 neutron + 3 photon fractions per week) with conventional photon irradiation in unresectable squamous cell carcinomas of the head and neck (Griffin et $al.$, 1989). A total number of 327 patients entered in the study: 163 patients of the mixed schedule group and 134 patients of the photon group were eligible for analysis. The minimum at-risk follow-up period was six years. The study results reveal no significant differences in overall loco-regional tumor control rates of survival. However, subgroup analysis reveals significant differences based on whether or not patients presented with positive lymph nodes. Loco-regional tumor control rates for patients presenting with positive lymph nodes were 30% for mixed schedule treated patients versus 18% for photon-treated patients (ps = 0.05). In contrast, loco-regional tumor control rates for patients presenting without positive lymph nodes were 64% for photon-treated patients and 33% for mixed-beam-treated patients (p = 0.004). It is important to stress that control of the metastatic lymph nodes favored mixed schedule over photons by a margin of 45% (49/109) to 26% (23/87) with a significance of p = 0.004 (Figure 5).
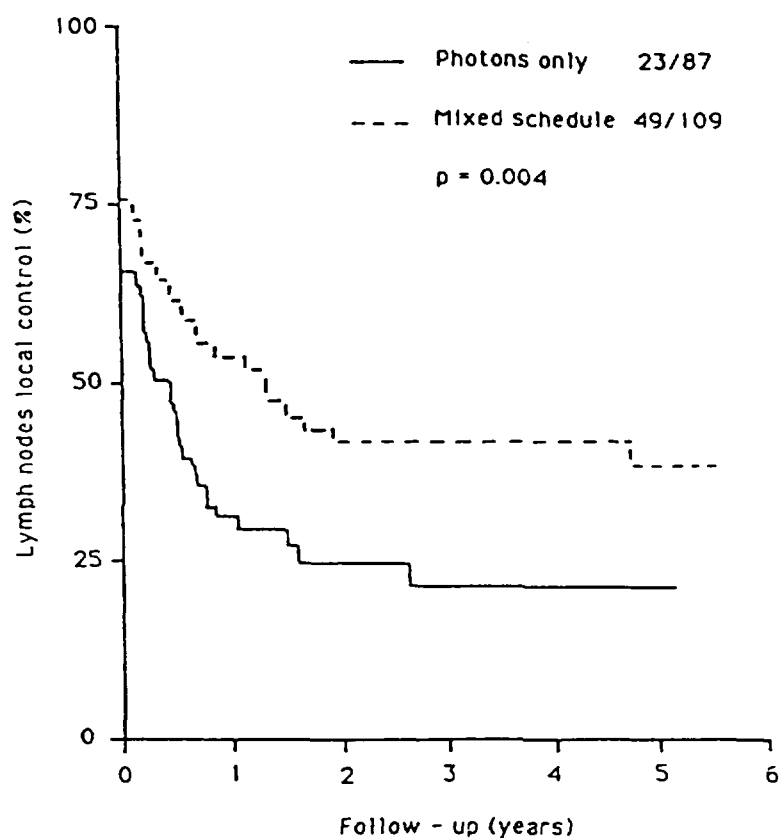
Figure 5: Comparison of the tumor local control rates at the level of the lymph nodes after photon and mixed scheduled irradiation. After Griffin et $al.$ (1989).

14

A similar difference of 12.5% in favour of the neutron-treated patients was found in the Edinburgh series for the local control of lymph nodes metastases of more than 3 cm in diameter (Duncan *et al.*, 1982). A possible explanation for the observed discrepancy of the results between patients presenting with or without positive lymph nodes could be related to the physical distribution of the dose. The suboptimal technical conditions (fixed horizontal beam, lack of adequate port verification, poor beam penetration) could be responsible for a geographic miss of part of the primary tumor in patients presented with negative lymph nodes. The large field sizes required for patients presenting with positive nodes could have increased the chance of adequate coverage of the primary site. On the other hand, the rather poor depth dose characteristics of the neutron beams available for this study could have resulted in an increased irradiation of the neck (lymph nodes) compared to the deeper primary site. These physical characteristics of the neutron beams could explain an increase rate of nodal tumor control versus primary tumor control.

It seems reasonable to conclude that fast neutrons can bring a significant benefit in well-defined patient series with tumors in the head and neck area, especially locally advanced tumors with fixed metastatic lymph nodes. However, there is no argument at present for recommending neutron therapy as a general treatment policy for all tumors of the head and neck area. In particular, it seems reasonable to keep the classical treatments for tumor types which are efficiently controlled with photons (such as T_{1-2} tumors of the larynx) (Wells *et al.*, 1989).

2.3.4 Brain Tumors

The marked radioresistance of the majority of brain tumors of the adult to photon irradiation was the rationale for treating them with fast neutrons. No prolongation of survival and no benefit in terms of quality of life was observed for the neutron treated patients. This was observed in most of the centers, and underlines the high or low RBE radiation in the CNS, which obviously prevents achieving a sufficient therapeutic gain factor for brain tumors (Saroja *et al.*, 1993; Schmitt and Wambersie, 1990)

At the NIRS in Japan, grade III (15 patients) and grade IV (22 patients) astrocytomas were treated with fast neutrons either as mixed schedule or as boost. Cumulative five-year survivals of 36% and 16%, respectively, were reported (Tsunemoto, 1989). The corresponding survival rate for grade IV astrocytoma in the Brain Registry in Japan is 9.8%. Malignant meningioma is also considered as a good indication for fast neutrons at the NIRS.

A recent study by B.R. Griffin *et al.* (1989) confirms that although neutrons could have an increased antitumor effect against malignant gliomas compared to photons, no benefit in survival could be expected. The authors conclude from their study that anaplastic astrocytomas should be excluded from pilot studies involving fast neutrons. For patients with newly diagnosed glioblastomas multiforme or recurrent malignant gliomas, a possible new approach could be the combination of neutron irradiation with agents designed to selectively protect the normal brain or with agents aimed at selectively increasing the dose to the tumor cells (*e.g.*, target antibodies).

Another possible approach could be the use of heavy ions which combine the potential high-LET advantage with a superior physical selectivity (Castro *et al.*, 1985). Heavy ions could be used as a boost irradiation. A similar rationale was followed by Breteau in Orleans who observed after neutron boost a slight improvement in survival for grade IV astrocytoma for non-operated patients and for patients who had incomplete resection (Breteau *et al.*, 1989).

As far as differentiated tumors of the spinal cord are concerned, Schmitt reported the result obtained for ten extensive and inoperable low grade astrocytomas (Schmitt et al., 1987). These patients were treated in Essen between 1980 and 1986 with neutron doses of 8 Gy in ten fractions. Objective neurological improvements were seen in six cases with follow-up periods of 12–71 months. Complete remission occurred in two of them and no change of symptoms in two other patients. Two patients died from progressive disease. This pilot study will be continued to determine the optimum dose for long term control. For these tumors also, the high physical selectivity of heavy ions could provide a promising alternative (Chauvel and Wambersie, 1989).

2.3.5 Sarcomas of Soft Tissue, Bone and Cartilage

Soft tissue sarcomas were treated in most of the neutron therapy centers, mainly because they are often resistant to X rays and also because of the excellent results reported from Hammersmith (Catterall and Bewley, 1979). When evaluating the results of neutron therapy, comparison with historical series should be made very carefully since the series could differ by histology, degree of differentiation, local extent, localization, etc. Furthermore, patient recruitment is influenced by the general treatment policy in a given center (i.e., the relative place of surgery and/or chemotherapy). Therefore, randomized trials that would be ideally needed have been difficult to achieve so far for practical reasons.

The largest patient series was treated in Essen. Neutrons only were used first and a 76.5% local control rate was achieved. However, a high percentage of complications was observed (22%), which could be related to the poor beam penetration and the high skin doses. Therefore, in a second phase neutrons were applied as boost, resulting in a local control rate of 61.9% and a complication rate of 15%. The results of this study are reported in detail by Schmitt et al. (1989, 1990).

A review of the results reported from the different centers (Table VI) indicates an overall local control rate after neutron therapy of 53% for inoperable soft tissue sarcomas. This value is higher than the 38% local control rate currently observed after low-LET radiation for similar patient series (Laramore et al., 1989; 1986).

Taking into account the difficulties in initiating a randomized trial for soft tissue sarcomas, the German Neutron Therapy Group (M. Wannenmacher) together with the EORTC (European Organization for Research on Treatment of Cancer) Heavy-Particle Therapy Group initiated a collaborative study in order to collect all the data from the different participating neutron therapy centers. The data are to be reported according to strict rules in terms of tumor description, follow-up, treatment technique, dose specification, etc.

The proposed indications of neutron therapy (and/or photon therapy) for low grade soft tissue sarcomas, are presented in Table VII after Pötter et al. (1990).

As far as primary bone tumors are concerned, conventional radiotherapy generally fails to control bulky tumors, as appropriate doses inevitably induce osteoradionecrosis. The low neutron kerma in bone reduces the absorbed dose by 25% or more to cells in osseous cavities (Bewley, 1989) and allows application of an adequate dose with a reduced probability of late normal bone injury. Hence, differentiated primary bone tumors of the adult were part of many clinical neutron programs.

The review of the published data indicates that for 88 patients with osteosarcoma treated at different institutions, persisting local control of 54% (52/97) was achieved (Laramore et al., 1989; Richter et al., 1984). Most of these patients had inoperable

Table VI: Review of the local control rates for soft-tissue sarcomas treated with radiation therapy. Modified from Laramore et al. (1989, 1986).

NEUTRONS		
Institutions	Number of patients*	Local control (%)**
Essen + Heidelberg, 1983	60	31 (52%)
Hammersmith, 1987	50	26 (52%)
Hamburg, 1987	45	27 (60%)
TAMVEC, 1980	29	18 (62%)
Fermilab, 1984	26	13 (50%)
Seattle, 1986	21	15 (71%)
Louvain-la-Neuve, 1982	19	4 (21%)
Amsterdam, 1981	13	8 (61%)
NIRS, 1979	12	7 (58%)
Edinburgh, 1986	12	5 (42%)
MANTA, 1980	10	4 (40%)
Overall	297	158 (53%)
PHOTONS/ELECTRONS		
Authors	Number of patients*	Local control (%)
Tepper & Suit (1985)	51	17 (33%)
Duncan & Dewar (1985)	25	5 (20%)
McNeer et al. (1968)	25	14 (56%)
Windeyer et al. (1966)	22	13 (59%)
Leibel et al. (1983)	5	0 (33%)
Overall	128	49 (38%)

* Patients treated de novo or for gross disease after surgery are included but not patients treated postoperatively for microscopic residual disease or for limited macroscopic residual disease.
**Two-year actuarial data. Modified from Laramore et al. (1989, 1986).

tumors or refused amputation (Table VIII). An overall local control rate of 21% after photon irradiation is currently reported for similar patient series. However, due to the large treatment volumes, and often preceeding chemotherapy, a complication rate up to 36% was registered for neutron irradiation (Schmitt et al., 1982).

As far as differentiated chondrosarcomas are concerned, the review of the results reported from the same institutions indicates a persisting local control after neutron therapy in 49% (25/51) of the patients (Laramore et al., 1989; Richter et al., 1984). This value compares well with the 33% (10/30) local control rate achieved after photon irradiation (Table IX). Debulking surgery followed by appropriate neutron- or neutron-boost irradiation then may become an alternative to ablative or mutilating surgery.

In conclusion, fast neutrons (and high LET radiation) may be considered the best radiation quality for differentiated, slowly growing, soft tissue sarcomas, especially locally extended inoperable or recurrent tumors. A similar conclusion may apply to osteosarcomas and chondrosarcomas.

2.3.6 Prostatic Adenocarcinomas

Prostatic adenocarcinomas, having in general a long doubling time, should be a good indication for neutron therapy taking into account the available radiobiological data (Battermann, 1981). In fact, the benefit of neutron therapy was rapidly recognized in several centers and initially in Hamburg by Franke *et al.* (1980). Excellent results were also achieved at Louvain-la-Neuve using mixed schedule (3 neutron and 2 photon fractions per week) (Richard *et al.*, 1986). At NIRS in Chiba, for prostatic adenocarcinomas Stage A2, B and C, local controls at three years of 3/3, 3/5 and 8/14, respectively, were reported (Tsunemoto, 1989).

The most convincing data are the result of a randomized trial, initiated by the RTOG, on locally advanced (C,D1) adenocarcinomas of the prostate gland (Figure 6) (Russell *et al.*, 1987).

The local control rate was 77% for patients treated with mixed schedule (55 patients) and only 31% for patients receiving photons alone (36 patients) (P < 0.01). Actuarial survival rates at eight years ("determinental" survivals, *i.e.* adjusted by exclusion of intercurrent deaths) were 82% and 54%, respectively, (P = 0.02).

Complications after radiation therapy have been studied by Russell *et al.* (1990). Among 132 patients treated for prostatic adenocarcinoma (94 with neutrons, 16 with mixed schedule, 22 with photons) and with a median follow-up of 14 months (range 1-101 months), 31 have experienced either sciatica beginning during or shortly after treatment, or diminished bladder or bowel continence developing at a median time of 6.5 months after treatment (26/94 after neutron, 3/16 after mixed schedule and 2/22 after photon irradiation). Sciatica responded to oral steroids and was usually self-limited, whereas sphincter dysfunction appears to be permanent. Seven patients have moderate (5 patients) or severe (2 patients) residual problems, all in the group receiving neutrons (6/7) or mixed schedule (1/7) irradiation. The total number of severely affected patients (2/110) represents a small percentage of the patients treated with fast neutrons only or with mixed schedule. These complications should not place a constraint on the use of neutrons, although it is conceivable that the incidence of complications will increase, as the follow-up of the patients is still short. Because survival and local control of locally advanced prostate cancer achieved with neutrons is superior to results with photons, this low incidence of severe neurological problems appears to be an acceptable risk to take for more effective treatment.

In the Louvain-la-Neuve experience, on a total number of more than 150 patients treated with mixed schedule irradiation following the RTOG protocol (but with 3 neutrons + 2 photons per week), the early tolerance was excellent and only one late complication, scored grade 3, was observed (urethral stricture in a patient who underwent several surgical procedures).

The RTOG has performed the second multicenter randomized trial comparing neutrons (alone) and photons in locally extended prostatic adenocarcinoma. Preliminary results indicate that neutrons are indeed more effective than photons for locally controlling the tumor, but this does not seem to affect the patient survival. As far as complications are concerned, they appear to be dependent to a large extent on the technical irradiation conditions (such as beam collimation: fixed inserts, variable collimator or multileaf variable collimator which is probably more effective with neutrons than with photons) (T.W. Griffin, 1991). The results of this clinical trial showing the selective efficiency of neutrons against slowly growing tumors, as well as a need for a high physical selectivity, is in full agreement with the radiobiological data
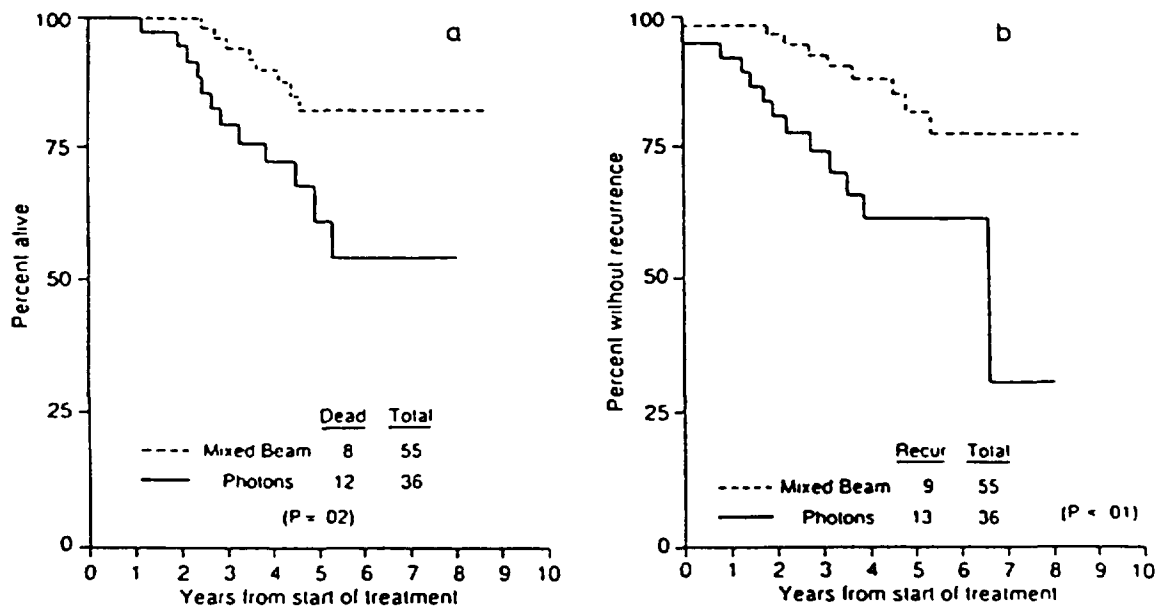
Figure 6: Locally extended prostatic adenocarcinoma. RTOG randomized trial comparing a combination of fast neutrons and photons ("mixed-beam") and conventional photon irradiation alone. (a) The actuarial survival rates at 8 years are indicated, adjusted by exclusion of intercurrent non-cancer death ("determinental" survival rates). (b) The local control rates are indicated, combining clinical and biopsy criteria (Russell et al., 1987).

discussed above (see Section 2.3). Of course, one has to take into account the slow natural history of prostatic adenocarcinoma and be careful before deriving definitive conclusions. However, the clinical data presently available indicate a significant benefit for fast neutrons, used alone or in a mixed photon/neutron schedule, as compared to the current photon irradiation modalities for locally advanced cases (Russell et al., 1989a).

2.3.7 Pancreatic Cancers

The poor prognosis currently observed with the conventional techniques was an argument for the radiotherapists to introduce fast neutrons in the treatment of pancreatic carcinoma, at least for patients medically or technically inoperable. Between 1980 and 1984, the RTOG conducted a trial in patients with untreated, unresectable localized carcinomas of the pancreas (Thomas et al., 1989).

Patients were randomly assigned to receive either 64 Gy with photons (control arm), the equivalent dose with mixed schedule (2 neutrons + 3 photons per week) or the equivalent dose with neutrons alone. The adopted "clinical RBE" was 3.3 for the University of Washington and the Cleveland Clinic Foundation and 3.0 for the Fermilab.

A total of 49 cases were evaluable: 23 treated with photons, 11 with mixed schedule and 15 with neutrons alone. The median survival times were 8.3 months, 7.8 months, and 5.6 months, respectively. The median local control durations were 2.6 months, 6.5 months and 6.7 months, respectively. These differences are not statis-

tically significant and the results are similar to those currently reported after photon irradiation or after heavy ion radiation therapy (Chauvel, 1989). As far as side effects and complications are concerned, acute toxicity was similar for the 3 groups. On the other hand, late complications were more severe and more frequent in the neutron arm compared to the photon and mixed schedule arms. In the neutron arm, 2 patients showed severe and life-threatening reactions (i.e., grade 4 or 5) and 1 patient showed reaction of grade 3. No patient in the photon or mixed schedule arms showed reaction of grade 3 or more.

Several technical factors could have contributed to higher complication rates with neutrons: the poorer depth doses and the wider penumbras. In addition, some patients were treated with neutrons in standing position because of the fixed horizontal beam. This may have allowed a greater volume of stomach and intestine to fall into the treatment volume compared to conventional supine position.

The RTOG study concluded that neutrons and mixed schedule irradiation do not bring a therapeutic benefit in the treament of inoperable pancreatic carcinoma as far as survival and local control are concerned. Furthermore, complication rate was higher in the neutron group.

More recently, a preliminary study from Fermilab indicates an improvement in survival for patients treated with a combination of neutrons and chemotherapy compared to neutrons alone. The median survial was 6.4 months in the neutron arm (21 patients), as compared to 13.5 months in a neutron-chemotherapy arm (17 patients). Chemotherapy consisted of 5-FU alone or in combination with Mitomycine, FAM or Adriamycine (Cohen et al., 1996).

2.3.8 Tumors of the Uterine Cervix

Neutron therapy of locally advanced tumors of the cervix was carried out at several centers. The rationale for this treatment was the high local recurrence rates observed with conventional techniques and the benefit observed from the use of hyperbaric oxygen, suggesting the role of hypoxic cells in tumor radioresistance. At several neutron facilities, the patients were treated in "suboptimal" conditions as far as physical selectivity was concerned. This has to be taken into account when analyzing the results and especially when analyzing complication rates.

A randomized trial was carried out by the RTOG for locally advanced cervical cancers, comparing mixed schedule irradiation (neutrons + photons) and photons only (Maor et al., 1988). A total of 146 patients were analyzed (stages IIB, III, and IVA with negative para-aortic nodes): 80 patients were treated with mixed schedule and 66 with photons. Tumor clearance was 52% and 72% for mixed schedule and photons, respectively; local control at two years was 45% and 52%. Median survival was 1.9 years for mixed schedule and 2.3 years for photons; severe complications occurred in 19% and 11% of the patients, respectively. The inferior outcome with neutrons resulted from "suboptimal" technical conditions, especially the use of fixed horizontal beams. Another randomized trial using high-energy hospital-based cyclotrons with gantry-mounted beam-delivery systems has been activated in order to evaluate more accurately the role of fast neutron therapy for advanced cervical cancers. However, accrual of suitable patients for that tumor site raised difficulties.

A similar study was performed by Tsunemoto et al. (1989) at the NIRS in Japan where 98 patients with stage IIIB squamous cell carcinoma were randomized between mixed schedule (neutrons + photons) and photons only (45 and 53 patients,

respectively). The local control rates were 73% after mixed schedule compared to 66% after photon irradiation. However, the cumulative five year survival was 49% in both series. This was due, according to the authors, to the frequent involvement of the para-aortic lymph nodes in stage IIIB cancers, which could obscure the effects of the greater efficiency of neutrons for the local control of pelvic lesions.

2.3.9 Bladder Carcinoma

As far as bladder tumors are concerned, the data reported from Amsterdam (Battermann, 1981; 1982; Battermann et al., 1981) and Edinburgh (Duncan et al., 1985; Duncan et al., 1982) give no indication that fast neutrons can produce better results than photons. However, in both centers the dose distributions achieved with neutrons were poor compared to those currently achieved with photons and explain the rather high complication rates.

A recent analysis of 58 patients treated for bladder carcinoma at Louvain-la-Neuve with p(65)Be neutrons gives a local control rate of 22% with a complication rate of 12% (Kirkove et al., in press). The patient series consisted in $12T_2$, $32T_3$ and $13T_1$, and as far as grade was concerned, $20G_2$ and $30G_3$. Patients were treated according to the RTOG protocol with mixed schedule (3 neutrons + 2 photons per week: "clinical RBE" 2.8). Although comparison with other published data are difficult taking into account differences in recruitment, this study clearly indicates that the tolerance to mixed schedule irradiation compares well with the conventional photon techniques when neutrons of sufficiently high-energy are used. Comparison of the complication rates observed at Louvain-la-Neuve, Amsterdam and Edinburgh stresses the importance of the physical selectivity in neutron therapy.

Further studies are needed in order to determine the value of fast neutrons in the treatment of bladder carcinoma. In particular, the use of predictive tests should be activated in order to select specific subgroups of patients eventually suitable for neutron therapy.

2.3.10 Melanomas

Although surgery when feasible is the treatment of choice for melanomas, radiation therapy may be required for some patients (discussion of the value of adjuvant chemotherapy is outside the scope of this paper). Melanomas are often resistant to photon irradiation; this can be related, from a radiobiological point of view, to the broad shoulder of the survival curves for several cell lines (Malaise et al., 1975; Tubiana et al., 1990). Therefore neutron therapy could be an alternative.

Encouraging results were obtained at the Hammersmith Hospital where 87 tumor sites in 48 patients were treated with fast neutrons (Catterall, 1991). They consist of metastatic tumors, recurrences after surgery, or sites unsuitable for surgery. Permanent local control was achieved in 62% of the sites (the minimum follow-up was three months). In addition, in 20 of the 25 patients good palliation was obtained. These results, as well as others (Duncan, 1982), indicate that fast neutron therapy can be an alternative in the treatment of some melanomas, especially where surgery cannot be performed, and for metastatic tumors.

2.3.11 Other Tumor Sites or Types

The value of fast neutrons has been assessed in other tumor types or sites such as rectum, bronchus or oesophagus carcinoma. No general and definitive conclusions can be drawn yet, but some of the results are promising (Bewley, 1989; Hall, et al., 1982; Schmitt and Wambersie, 1990; Tsunemoto et al., 1989; Wambersie, 1990; Wambersie et al., 1986).

As far as rectal adenocarcinoma is concerned, no valid conclusion can be derived from the Amsterdam and Edinburgh experiences since the dose distributions were not suitable for that type of localisation (Battermann, 1982; Battermann et al., 1981; Duncan et al., 1982). On the other hand, preliminary results of the pilot study recently initiated in Orleans using p(34)Be neutron beams should be mentioned (Breteau, et al., 1986). For recurrent or inoperable rectal adenocarcinoma, complete tumor regression was observed in 23/31 cases, and at 14 months persistent local control was achieved in 14/31 cases. Severe pelvic sclerosis was observed in two cases.

A prospective randomized trial comparing neutrons and photons for inoperable or recurrent rectal carcinoma has been initiated at the European level (Engenhardt and Pötter for the German Neutron Therapy Group and the EORTC Heavy-Particle Therapy Group, 1991).

Encouraging results for Pancoast tumors were obtained at the NIRS in Chiba where the cumulative survival rate at five years of 21 patients stage III or IV was 24%. It was 36% and 10% for stages III and IV, respectively (Tsunemoto, 1989).

The value of neutron irradiation for unresectable non-small-cell carcinoma of the lung has been reviewed by Stewart et al. (1989).

As far as the esophagus is concerned, 34 patients were irradiated at the NIRS with fast neutrons given either as boost or in mixed schedule. Local control was achieved in 15 of them (44%). In a comparable group of 81 patients treated with photons, the local control rate was 30% (24/81). For small lesions (< 8 cm in length) the local control rate after neutron irradiation was somewhat better than after photon irradiation, i.e., 50% (13/26) compared to 41% (17/41). The superiority of fast neutrons was less apparent for a small group of patients with large tumors (> 8 cm in length) where the local control rate was 29% (2/7) compared to 26% (7/27) for photons (Tsunemoto, 1989).

2.4 Discussion and Conclusions

Introduction of fast neutrons in radiation therapy was based on radiobiological arguments, historically focusing on the oxygen effect. The bulk of radiobiological data accumulated for more than 25 years indicate that (see Section 2.3):

1. Fast neutrons can indeed bring an advantage in the treatment of some tumor types. Radiobiological data also suggest mechanisms through which such an advantage could be achieved: Oxygen Gain Factor, Kinetics Gain Factor, etc.

2. Radiobiological data also indicate the need for proper patient selection. For example, neutrons should not be used for a patient where the normal tissues are more resistant to X rays than the tumor (and thus selectively protected).

3. The physical selectivity which was proven for decades to play an important role with X rays is even more important with neutrons due to the reduction of the radiobiological differential effect with increasing LET.

22

The arguments mentioned above for fast neutrons can be extended to the other forms of high-LET radiation, such as heavy ions. In particular, the requirements for a high physical selectivity is the justification of the heavy ion therapy programs (Lawrence Berkeley Laboratory in California, HIMAC in Japan, and EULIMA in Europe) (Chauvel and Wambersie, 1989).

The available clinical data indicate that indeed there exist some tumor types (or sites) for which fast neutrons were shown to bring a benefit when compared with conventional X rays. In that respect, one can schematically identify:

- Tumors for which fast neutrons were found to be superior to the conventional X rays. Examples are:

  1. salivary gland tumors (locally extended, well differentiated)

  2. paranasal sinuses (adenocarcinomas, adenoid cystic carcinomas, other histology (?))

  3. some tumors of the head and neck area (locally extended, metastatic adenopathies)

  4. soft tissue sarcomas, osteosarcomas, chondrosarcomas (especially slowly growing/well differentiated)

  5. prostatic adenocarcinomas (locally extended)

  6. melanomas (inoperable/recurrent)

- Tumors for which conflicting or incomplete results have been reported and for which additional studies are necessary.

- Tumors for which no benefit or even worse results were observed with fast neutrons.

As far as the first group of tumors is concerned, they are in general slowly growing and well differentiated as could be expected from the radiobiological data (Tubiana et al., 1990; Wambersie, 1990). This is in agreement with the observations of Batterman for lung metastases (Battermann, 1981).

The second group of tumors are those for which further clinical studies are necessary. However, when evaluating the results at least two factors must be taken into account:

1. Some of the conflicting results which were reported could be related to differences in patient recruitment and to the fact that, in some studies, the patient "subgroups" for which neutrons could bring a benefit could not be identified.

2. In many centers, neutron treatments were applied (especially in the past) in "sub-optimal" technical conditions (e.g., poor beam penetration, no skin sparing, fixed beams, poor patient positioning, etc.). These technical factors could bias the conclusions that one would derive concerning the value of fast neutrons or high-LET radiations in general. For example, one cannot derive valid conclusions from data on bladder tumors irradiated with d(16)Be beams (Duncan et al., 1985). Similarly, the difficulty of treating cervix tumors with a fixed horizontal beam was stressed at TAMVEC (Maor et al., 1988).

Some of the poor results, and especially the high complication rates, reported in patients treated with low-energy cyclotrons (or D-T generators) confirm once more

the importance of the physical selectivity in the outcome of radiation therapy. This indicates that an improved radiobiological differential effect cannot compensate for bad physical selectivity.

Negative results for brain tumors were reported from most of the centers. Such conclusions are again in agreement with the radiobiological data and especially with the observed high RBE value for CNS. However, a possible benefit for neutron boost should be investigated further (Battermann and Mijnheer, 1986).

Obviously, neutrons should not be used for tumors showing an exquisite radiosensitivity to X rays (e.g., seminomas; lymphomas; or in general poorly differentiated rapidly growing tumors). Neutron irradiation would then reduce a differential effect which selectively protects the normal tissues.

As far as the proportion of patients suitable for neutron therapy is concerned, figures ranging from 10 to 20% have been suggested. These percentages are probably at the lower limit since they were often based on results obtained with low energy cyclotrons and poor physical selectivity. It is likely that with high-energy, hospital-based modern cyclotrons, neutron therapy will be found useful for a larger proportion of patients. In addition, neutrons could extend the field of the indications of radiation therapy by allowing therapists to envisage the treatment of groups of tumors "traditionally" considered to be radioresistant (e.g., some types of adenocarcinomas).

Patient selection remains one of the main problems in clinical neutron therapy, since inappropriate application of neutrons will worsen clinical results. In that respect, the development of individual predictive tests is essential. If the subgroup suitable for neutron therapy in a group of patients has not been identified and if the entire group has been treated by neutrons, then the benefit obtained for the neutron subgroup will be diluted by the poorer results obtained in the remaining patients for which photons would have done better. This could explain in part some of the discrepancies that seem to exist between the published data (Wambersie, 1990).

Further and improved collaboration between the neutron therapy centers is essential in order to pool the available clinical information and to provide the centers with sufficient data as quickly as possible in order to allow them to select the patients for neutron therapy and to apply the best treatment modality (i.e., clinical RBE, fraction size, or overall time). This is the goal which is aimed at in the United States by the Neutron Therapy Section of the RTOG and in Europe by the Heavy-Particle Therapy Group of the EORTC.

The cost per neutron session can be estimated at three times the cost of a photon session (provided that the cyclotron has been designed for therapy applications and is used in optimal conditions). However, the total cost per treatment with neutrons is less than three times the cost per photon treatment since the number of fractions can be reduced with high LET-radiations.

The importance of the technical factors has been stressed. Although important progress recently has been achieved, especially with the introduction of new high-energy cyclotrons fully dedicated to therapy applications, some further improvements are needed before fast neutrons reach the same level of physical selectivity, reliability, and accuracy of dose delivery that modern electron linear accelerators (Figure 7) currently achieve. The available radiobiological and clinical data indicate that the dose response curves for tumor control and normal tissue complications are as steep for neutrons (or high-LET radiations) as for photons (or low-LET radiations) (Mijnheer et al., 1987). The same accuracy in dose delivery and physical selectivity should then be accomplished.

Table VII: Indications of neutron (and/or photon) radiotherapy for low grade soft tissue sarcoma (Pötter et al., 1990).

Type of Surgery	Plane of Dissection	Microscopic Appearance	Local Control After Surgery	Indication for Radiotherapy	Local Control After Combined Modality
Intracapsular	Within lesion	Tumor at margin	0%	Neutrons (photons)	30-50%
Marginal	Within reactive zone –extracapsular	Reactive tissue microsatellite tumor	10-20%	Neutrons (photons)	>50%
Wide	Beyond reactive zone through normal tissue within compartment	Normal tissue	50-60%	Photons	90%
Radical	Normal tissue extracompartmental	Normal tissue	80-90%	Photons (rare)	>90%

Table VIII: Review of the local control rates for osteosarcomas after neutron and photon therapy. Patients treated post-operatively for microscopic residual disease or for limited macroscopic residual disease are not included. Modified from Richter et al. (1984), and Laramore et al. (1989).

NEUTRONS		
Institutions	Number of patients	Local control (%)
NIRS	41	33 (80%)
Essen	24	12 (50%)
Seattle	13	3 (23%)*
Fermilab	9	2
Edinburgh	5	1 **
Amsterdam	3	0 **
MANTA	1	1
M.D. Anderson Hospital	1	0
Overall	97	52 (54%)
PHOTONS		
Authors	Number of patients	Local control (%)
De Moor	43	9 (33%)
Beck et al.	21	1 (5%)
Tudway	9	5 (56%)
Overall	73	15 (21%)

Two year actuarial data.
*Persistent mass and calcification treated as failure.

To reach this goal, several steps can be identified. Firstly, as far as clinical dosimetry is concerned, the ICRU has published Report 45 in which an agreement has been reached between the American and European Therapy Centers, allowing the same protocol to be used worldwide (ICRU, 1989). Secondly, since the RBE strongly depends on neutron energy (Figure 8), the specification of the beam quality is essential. The role of microdosimetry has been demonstrated especially in Europe by Menzel and Pihet (Menzel et al., 1990; Pihet et al., 1990). Systematic microdosimetric measurements were performed at all the European Neutron Therapy Centers, and a complete set of microdosimetric spectra are now available as a function of depth, field size, distance to the beam axis, etc.

Some basic physical data are still missing for the high-energy neutrons presently used in therapy. These data are needed:

- To evaluate the kerma and the absorbed dose in different human and biological tissues;

- To determine the response of different detectors (kerma and absorbed dose in the detector materials);

- To optimize the method of neutron production, the collimation, and the shielding systems, with the aim of improving the physical selectivity.

These subjects are reviewed in the following chapters.

Table IX: Review of the local control rates for chondrosarcomas after neutron and photon therapy. Patients treated post-operatively for microscopic residual disease or for limited macroscopic residual disease are not included. Modified from Richter *et al.* (1984), and Laramore *et al.* (1989).

NEUTRONS		
Institutions	Number of patients	Local control (%)
Fermilab	16	9
MANTA	9	7
Seattle	9	4 *
Amsterdam	6	0 **
Edinburgh	5	0 **
M.D. Anderson Hospital	4	4
NIRS	2	1
Overall	51	25 (49%)
PHOTONS		
Institutions	Number of patients	Local control (%)
Princess Margaret Hospital	20	7 (35%)
M.D. Anderson Hospital	10	3 (30%)
Overall	30	10 (33%)

*Two year actuarial data.
**Persistent mass and calcification treated as failure.
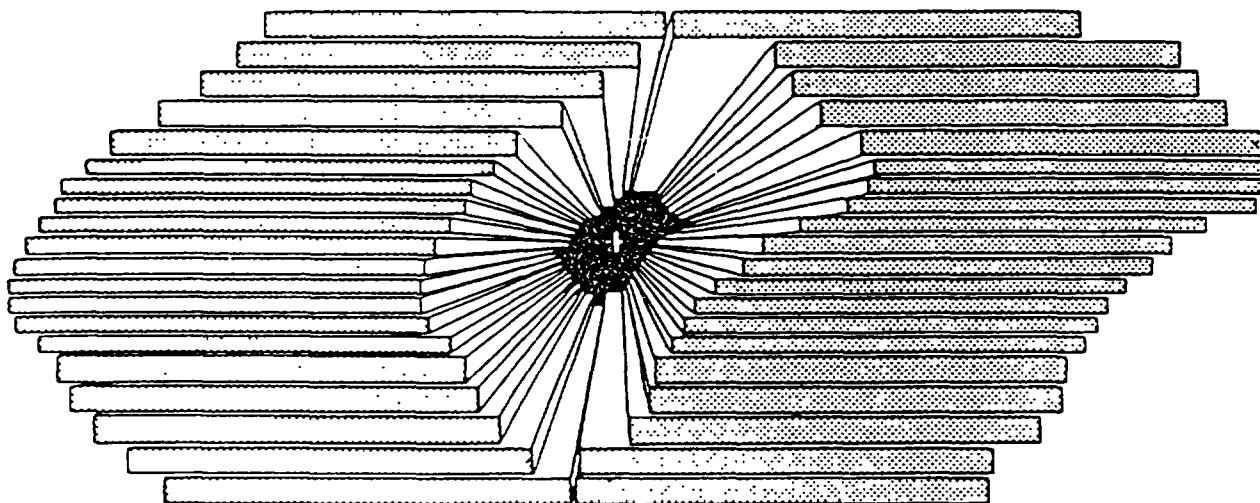
Figure 7: Variable multileaf collimator in neutron therapy. (a) Diagram of a variable multileaf collimator showing the lower end of the leaves and the collimation surfaces which are all aligned with the proton target (symbolized by the +). Each leaf has its own motor drive and position readout (after Brahme, cited in ICRU Report 45). (b) Diagram of one of the leaves of the variable multileaf collimator recently installed at the cyclotron of Louvain-la-Neuve. The collimator, which is used on a vertical neutron beam line, consists of 2 sets of 24 leaves made of steel and borated polyethylene. The leaves are 92 cm thick as needed for p(65)Be neutrons.
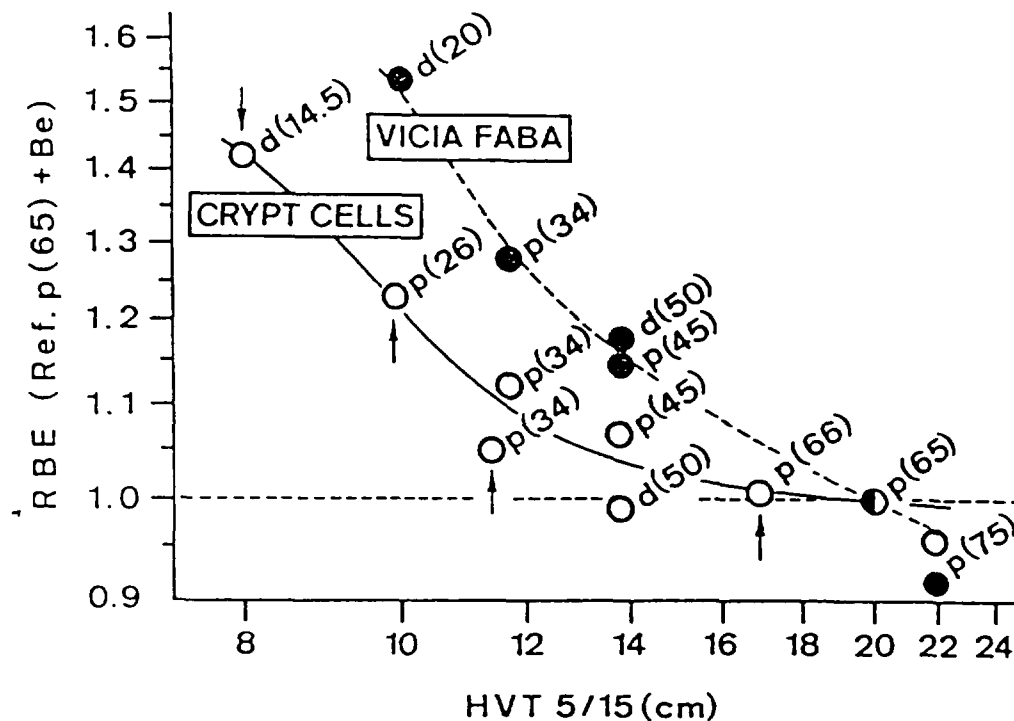
Figure 8: RBE variation as a function of the neutron energy determined for *vicia faba* and the intestinal crypt colony system. The energy of the neutron beams (in abcissa) is expressed by the parameter HVT (half value thickness measured, in reference conditions, between 5 and 15 cm); it covers the whole range actually used for therapy. The different neutron beams were produced at the Louvain-la-Neuve cyclotron. In addition, the intestinal crypt cell system was used for direct comparisons at other neutron therapy facilities (Beauduin et al., 1990).

28

References

Adams, G.E., "The Clinical Relevance of Tumour Hypoxia," *Eur. J. Cancer* **26**, 420-421 (1990).

Barendsen, G.W., and Broerse, J.J., "Differences in Radiosensitivity of Cells From Various Types of Experimental Tumors in Relation to the RBE of 15 MeV Neutrons," *Int. J. Radiat. Oncol. Biol. Phys.* **3**, 211-214 (1977).

Battermann, J.J., "Clinical Application of Fast Neutrons, the Amsterdam Experience." Ph.D. Thesis, University of Amsterdam (The Netherlands) (1981).

Battermann, J.J., "Results of d + T Fast Neutron Irradiation on Advanced Tumours of Bladder and Rectum," *Int. J. Radiat. Oncol. Biol. Phys.* **8**, 2159-2164 (1982).

Battermann, J.J., Hart, G.A.M., and Breur, K., "Dose-effect Relations for Tumour Control and Complication Rate After Fast Neutron Therapy for Pelvic Tumours," *Br. J. Radiol.* **54**, 899-904 (1981).

Battermann, J.J. and Mijnheer, B.J., "The Amsterdam Fast Neutron Radiotherapy Project: a Final Report," *Int. J. Radiat. Oncol. Biol. Phys.* **12**, 2093-2099 (1986).

Beauduin, M., Gueulette, J., Grégoire, V., De Coster, B., Vynckier, S., and Wambersie, A., "Radiobiological Comparison of Fast Neutron Beams Used in Therapy. Survey of the Published Data," *Strahlenther. Onk.* **166**, 18-21 (1990).

Bewley, D.K., *"The Physics and Radiobiology of Fast Neutron Beams,"* Adam Hilger, Bristol and New York (1989).

Breit, A., Burger, G., Scherer, E., and Wambersie, A, "Advances in Radiation Therapy with Heavy Particles," *Strahlenth. Onk.* **161**, **12**, 729-806 (1985).

Breteau, N., Destembert, B., Favre, A., Phéline, C., and Schlienger, M., "Fast Neutron Boost for the Treatment of Grade IV Astrocytomas," *Strahlenth. Onk.* **165**, 320-323 (1989).

Breteau, N., Destembert, B., Favre, A., Sabattier, R., and Schlienger, M., "An Interim Assessment of the Experience of Fast Neutron Boost in Inoperable Rectal Carcinomas in Orléans," *Bull. Cancer* (Paris) **73**, 591-595 (1986).

Castro, J.R., Saunders, W.M., Austin-Seymour, M.M., Woodruff, K.H., Gauger, G., Chen, G.T.Y., Collier, J.M., and Zink, S.R., "Heavy Charged Particles Irradiation of Glioma of the Brain," *Int. J. Radiat. Oncol. Biol. Phys.* **11**, 1795-1800 (1985).

Catterall, M., Private Communication (1991).

Catterall, M., and Bewley, D.K., *"Fast Neutrons in the Treatment of Cancer,"* London, Academic Press, New-York, Grune and Stratton (1979).

Catterall, M., Bewley, D.K., and Sutherland, I., "Second Report on a Randomized Clinical Trial of Fast Neutrons Compared With X- or Gamma-rays in Treatment of Advanced Head and Neck Cancers," *Br. Med. J.* (London) **1**, 1942 (1977).

Catterall, M. and Errington, R.D., "The Implications of Improved Treatment of Malignant Salivary Gland Tumors by Fast Neutron Radiotherapy," *Int. J. Radiat. Oncol. Biol. Phys.* **13**, 1313-1318 (1987).

Chapman, J.D., "Biophysical Models of Mammalian Cell Inactivation by Radiation," In: *Radiation Biology in Cancer Research*, R.E. Meyn, H.R. Withers, (eds.), pp. 21-32, Raven Press, New York (1988).

Chauvel, P. and Wambersie, A. (eds.), *EULIMA Workshop on the Potential Value of Light Ion Beam Therapy*, Publication EUR 12165 EN of the Commission of the European Communities, ECSC-EEC-EAEC, Brussels-Luxembourg (1989).

Cohen, L., Hendrickson, F.R., Lennox, A.J., Kroc, T.K., Hatcher, M.A., and Bennett, B.R. "Pancreatic Cancer: Treatment with Neutron Irradiation Alone and With Chemotherapy," *Radiology* **200**, 627-630 (1996).

Duncan, W., Arnott, S.J., Battermann, J.J., Orr, J.A., Schmitt, G., and Kerr, G.R., "Fast Neutrons in the Treatment of Head and Neck Cancers: the Results of a Multi-Centre Randomly Controlled Trial," *Radiother. Oncol.* **2**, 293-301 (1984).

Duncan, W., Arnott, S.J., Jack, W.J.L., MacDougall, R.H., Quilty, P.M., Rodger, A., Kerr, G.R., and Willimas, J.R., "A Report of a Randomized Trial of d(15)+Be Neutrons Compared with Megavoltage X-ray Therapy of Bladder Cancer," *Int. J. Radiat. Oncol. Biol. Phys.* **11**, 2043-2049 (1985).

Duncan, W., Arnott, S.J., Orr, J.A., and Kerr, G.R., "The Edinburgh Experience of Fast Neutron Therapy," *Int. J. Radiat. Onc. Biol. Phys.* (New York) **8**, 2155-2157 (1982).

Errington, R.D., "Advanced Carcinoma of the Paranasal Sinuses Treated with 7.5 MeV Fast Neutrons," *Bull. Cancer* (Paris) **73**, 569-576 (1986).

Errington, R.D., Private Communication (1991).

Fertil, B., Deschavanne, P.J., Gueulette, J., Possoz, A., Wambersie, A., and Malaise, E.P., "In Vitro Radiosensitivity of Six Human Cell Lines. II. Relation to the RBE of 50-MeV Neutrons," *Radiat. Res.* **90**, 526-537 (1982).

Franke, H.D., Langendorff, G., and Hess, A., "Die Strahlenbehandlung des Prostata-Carcinoms in Stadium C mit Schnellen Neutronen," *Verhandlungsbericht der Deutschen Gesellschaft für Urologie* **32**, Tagung 1980, Berlin, Heidelberg, New-York Springer-Verlag, 175-180 (1981).

Gragg, R.L., Humphrey, R.M., Thames, H.D., Meyn, R.E., "The Response of Chinese Hamster Ovary Cells to Fast Neutron Radiotherapy Beams. III. Variation in Relative Biological Effectiveness with Position in the Cell Cycle," *Radiat. Res.* **76**, 283-291 (1978).

Griffin, B.R., Laramore, G.E., Russell, K.J., Griffin, T.W., and Eenmaa, J., "Fast Neutron Radiotherapy for Advanced Malignant Salivary Gland Tumors," *Radioth. Onc.* **12**, 105-111 (1988).

Griffin, B.R., Berger, M.S., Laramore, G.E., Griffin, T.W., Shuman, W.P., Parker, R.G., Davis, L.W., and Diener-West, M., "Neutron Radiotherapy for Malignant Gliomas," *Am. J. Clin. Oncol. (CCT)* **12**, 311-315 (1989).

Griffin T., Blasko J., and Laramore G., "Results of Fast Neutron Beam Radiotherapy, Pilot Studies at the University of Washington," In: *High-LET Radiations in Clinical Radiotherapy,* G.W. Barendsen, J.J. Broerse, and K. Breur (eds.), *Eur. J. Cancer,* Suppl., 23-29 (1979).

Griffin, T.W., Davis, R., Laramore, G.E., Hussey, D.H., Hendrickson, F.R., and Rodriguez-Antunez, A., "Fast Neutron Irradiation of Metastatic Cervical Adenopathy. The Results of a Randomized RTOG Study," *Int. J. Radiol. Oncol. Biol. Phys.* **9**, 1267-1270 (1983).

Griffin, T.W., Davis, R., Hendrickson, F.R., Maor, M.H., Laramore, G.E., and Davis, L., "Fast Neutron Radiation Therapy for Unresectable Squamous Cell Carcinomas of the Head and Neck: the Results for a Randomized RTOG Study," *Int. J. Radiat. Oncol. Biol. Phys.* **10**, 2217-2223 (1984).

Griffin, T.W., Pajak, T.F., Laramore, G.E., Duncan, W., Richter, M.P., Hendrickson, F.R., and Maor, M.H., "Neutron vs. Photon Irradiation of Inoperable Salivary Gland Tumors: Results of an RTOG-MRC Cooperative Randomized Study," *Int. J. Radiol. Oncol. Biol. Phys.* **15**, 1085-1090 (1988).

Griffin, T.W., Pajak, T.F., Maor, M.H., Laramore, G.E., Hendrickson, F.R., Parker, R.G., Thomas, F.J., and Davis, L.W., "Mixed Neutron/Photon Irradiation of Unresectable Squamous Cell Carcinomas of the Head and Neck: the Final Report of a Randomized Cooperative Trial," *Int. J. Radiol. Oncol. Biol. Phys.* **17**, 959-965 (1989).

Griffin, T.W., Private Communication (1991).

Hall, E.J., Graves, R.G., Phillips, T.L., and Suit, H.D., "Particle Accelerators in Radiation Therapy," In: *Proc. of the CROS/RTOG Part III International Workshop,* Houston, February 10-11, 1982, *Int. J. Radiat. Oncol. Biol. Phys.* **8** (1982).

International Commission on Radiation Units and Measurements, *Clinical Neutron Dosimetry. Part I: Determination of Absorbed Dose in a Patient Treated by External Beams of Fast Neutrons,* Report 45, 85 pages, (International Commission on Radiation Units and Measurements, Bethesda, MD) (1989).

Kirkove C., Richard F., Van Cangh P.J., Ledent G., Octave-Prignot M., Wambersie A., "Neutron Therapy of bladder Carcinoma. Can a High Rate of Severe Complications be Avoided in Neutron Therapy?" *Eur. Urol.* **24**, 52-57 (1993).

Laramore, G.E., Griffeth, J.T., Boespflug, M., Pelton, J.G., Griffin, T.W., Griffin, B.R., Russell, K.J., and Koh, W., "Fast Neutron Radiotherapy for Sarcomas of Soft Tissue, Bone, and Cartilage," *Am. J. Clin. Oncol.* **12**, 320-326 (1989).

Laramore, G.E. and Griffin, T.W., "High-LET Radiotherapy," *Int. J. Radiat. Oncol. Biol. Phys.* **12**, Supp. 1, Abstract No. 505, p. 85 (1986).

Malaise, E.P., Weininger, J., Joly, A.M., and Guichard, M., "Measurements In Vitro With Three Cell Lines Derived from Melanomas," In: *Cell Survival After Low Doses of Radiation: Theoretical and Clinical Implications,* Alper T. Bristol (ed.), pp. 223-225, John Wiley & Sons, (1975).

Maor, M.H., Gillespie, B.W., Peters, L.J., Wambersie, A., Griffin, T.W., Thomas, F.J., Cohen, L., Conner, N., and Gardner, P., "Neutron Therapy in Cervical Cancer: Results of a Phase III RTOG Study," *Int. J. Radiat. Oncol. Biol. Phys.* 14, 885-891 (1988).

Menzel, H.G., Pihet, P., and Wambersie, A., "Microdosimetric Specification of Radiation Quality in Neutron Radiation Therapy," *Int. J. of Radiat. Biol.* 57, 865-883 (1990).

Mijnheer, B.J., Battermann, J.J., and Wambersie, A., "What Degree of Accuracy is Required and Can Be Delivered in Photon and Neutron Therapy?" *Radioth. Onc.* 8, 237-252 (1987).

Pihet, P., Menzel, H. G., Schmidt, R., Beauduin, M., and Wambersie, A., "Evaluation of a Microdosimetric Intercomparison of European Neutron Therapy Centres," *Radiation Protection Dosimetry, Microdosimetry* 31, 437-442 (1990).

Pötter, R., Knocke, T.H., Haverkamp, U., and Al-Dandashi, Chr., "Treatment Planning and Delivery in Neutron Radiotherapy of Soft Tissue Sarcomas," *Strahlenth. Onk.* 166, 102-106 (1990).

Richard, F., Renard, L., and Wambersie, A., "Current Results of Neutron Therapy at the UCL for Soft Tissue Sarcomas and Prostatic Adenocarcinomas," *Bull. Cancer* (Paris) 73, 562-568 (1986).

Richter, M.P., Laramore, G.E., Griffin, T.W., and Goodman, R.L., "Current Status of High Linear Energy Transfer Irradiation," *Cancer* 54, 2814-2822 (1984).

Russell, K.J., Laramore, G.E., Krall, J.M., Thomas, F.J., Maor, M.H., Hendrickson, F.R., Krieger, J.N., and Griffin, T.W., "Eight Years Experience with Neutron Radiotherapy in the Treatment of Stages C and D Prostate Cancer: Updated Results of the RTOG 7704 Randomized Clinical Trial," *The Prostate* 11, 183-193 (1987).

Russell, K.J., Laramore, G.E., Krieger, J.N., Wiens, L.W., Griffeth, J.T., Koh, W.J., Griffin, B.R., Austin-Seymour, M.M., Griffin, T.W., and Davis, L.W., "Transient and Chronic Neurological Complications of Fast Neutron Radiation for Adenocarcinoma of the Prostate," *Radioth. Onc.* 18, 257-265 (1990).

Russell, K.J., Laramore, G.E., Griffin, T.W., Parker, R.G., Maor, M.H., Davis, L.W., and Krall, J.M., "Fast Neutron Radiotherapy in the Treatment of Locally Advanced Adenocarcinoma of the Prostate, Clinical Experience and Future Directions," *Am. J. Clin. Oncol. (CCT)* 12(4), 307-310 (1989a).

Russell, K.J., Laramore, G.E., Griffin, T.W., Parker, R.G., Davis, L.W., and Krall, J.W., "Fast Neutron Radiotherapy for the Treatment of Carcinoma of the Urinary Bladder. A Review of Clinical Trials," *Am. J. Clin. Oncol. (CCT)* 12(4), 301-306 (1989b).

Saroja, K.R., Oesterling, J.E., Hendrickson, F., Cohen, L., Mansell, J.A., "The Prognostic Implications of Prostate Specific Antigen in Patients with Locally Advanced Prostate Cancer Treated with High Energy Neutron Beam Therapy: Preliminary Results," *Urology* **41**(6), 540-547 (1993).

Schmitt, G., Bamberg, M., and Budach, V., "Preliminary Results of Neutron Irradiation of Patients with Spinal Gliomas," *Br. J. Radiol.* **60**, 711, 1295-1297 (1987).

Schmitt, G., Mills, E.E.D., Levin, V., Pape, H., Smit, B.J., and Zamboglou, N., "The Role of Neutrons in the Treatment of Soft Tissue Sarcomas," *Cancer* **64**, 2064-2068 (1989).

Schmitt, G., Rehwald, U., and Bamberg, M., "Neutron Irradiation of Primary Bone Tumours," *J. Eur. Radiother.* **3**, 145-146 (1982).

Schmitt, G. and Wambersie, A., "Review of the Clinical Results of Fast Neutron Therapy," *Radioth. Onc.* **17**, 47-56 (1990).

Schmitt, G., Pape, H., and Zamboglou, N., "Long Term Results of Neutron- and Neutron-boost Irradiation of Soft Tissue Sarcomas," *Strahlenth. Onk.* **166**, 61-62 (1990).

Stewart, G., Griffin, T.W., Griffin, B.R., Laramore, G., Russell, K.J., Parker, R.G., Maor, M.N., and Davis, L.W., "Neutron Radiation Therapy for Unresectable Non-small-cell Carcinoma of the Lung," *Am. J. Clin. Oncol. (CCT)* **12**(4), 290-294 (1989).

Thomas, F.J., Krall, J., Hendrickson, F., Griffin, T.W., Saxton, J.P., Parker, R.G., and Davis, L.W., "Evaluation of Neutron Irradiation of Pancreatic Cancer," *Am. J. Clin. Oncol. (CCT)* **12**(4), 283-289 (1989).

Tsunemoto, H., Morita, S., Satoh, S., Iino, Y., and Yul, Yoo., "Present Status of Fast Neutron Therapy in Asian Countries," *Strahlenth. Onk.* **165**, 330-336 (1989).

Tubiana, M., Dutreix, J., and Wambersie, A., *Introduction to Radiobiology,* Taylor & Francis, London (1990).

Wambersie, A., "Fast Neutron Therapy at the End of 1988 – a Survey of the Clinical Data," *Strahlenth. Onk.* **166**, 52-60 (1990).

Wambersie, A., Barendsen, G.W., and Breteau, N., "Overview and Prospects of the Application of Fast Neutrons in Cancer Therapy," *J. Eur. Radiother.* **5**, 248-264 (1984).

Wambersie, A. and Battermann, J.J., "Review and Evolution of Clinical Results in the EORTC Heavy-particle Therapy Group," *Strahlenth. Onk.* **161**, 746-755 (1985).

Wambersie, A., Bewley, D.K., and Lalanne, C.M., "Prospects for the Application of Fast Neutrons in Cancer Therapy. Radiobiological Bases and Survey of the Clinical Data," *Bull. Cancer* (Paris) **73**, 546-561 (1986).

Wells, G., Koh, Wui-jin, Pelton, J., Russell, K., Griffin, B., Laramore, G., Griffin, T., Parker, R., Peters, L.J., Davis, L., and Pajak, T.F., "Fast Neutron Teletherapy in Advanced Epidermoid Head and Neck Cancer," *Am. J. Clin. Oncol (CCT)* **12**, 295-300 (1989).

Withers, H.R., and Peters, L.J., "The Application of RBE Values to Clinical Trials of High-LET Radiations," In: *High-LET Radiations in Clinical Radiotherapy*, G.W. Barendsen, J.J. Broerse, K. Breur (eds.), pp. 257-261, Pergamon Press, Oxford (1979).

3 Protocols for the Determination of Absorbed Dose

3.1 Introduction

The response of biological tissues reflects both non-stochastic quantitative energy deposition, the absorbed dose, as well as the stochastic qualitative individual energy deposition (microdosimetry). The quantitative aspects concern the values of kerma and absorbed dose, while qualitative aspects are related to microdosimetric quantities such as linear energy transfer, LET, and lineal energy, y.

Exposure conditions can modify the biological effects appreciably, which can be exemplified for the irradiation of cultured cells in monolayer with D-T neutrons (see Figure 9). For the same kerma in soft tissue determined under charged particle equilibrium conditions, the energy deposition in the cells varies both quantitatively and qualitatively when different materials are used to establish equilibrium of secondary charged particles (Broerse and Zoetelief, 1978). With neutron radiation the absorbed dose is deposited primarily by protons, alpha particles and recoil nuclei of carbon, nitrogen and oxygen. For any given neutron energy, the maximum range of the recoil protons is about 20 times that of alpha particles and 200 times that of heavy recoils (ICRU, 1977). While replacement of a layer of tissue equivalent plastic by carbon results in a reduction of absorbed dose, the remaining alpha particles and heavy recoils have a higher LET and thus a larger relative biological effectiveness (RBE). The biological consequences of the disturbance of secondary charged particle equilibrium at interfaces have been investigated with D-T neutrons (Broerse et al., 1968) and d(16)Be neutrons (Bewley et al., 1974). It will be of fundamental and practical interest to extend these studies to higher neutron energies.

The biological effects of neutron radiation depend on neutron energy with a general tendency of highest RBE values at energies around 1 MeV and a gradual decrease with increasing neutron energy. In view of the steep dose-effect relations for tumor response and normal tissue damage, the absorbed dose at relevant points in the patient should be delivered with high precision. To compare the clinical results of different neutron radiotherapy centers, the absolute absorbed dose should also be determined with good accuracy. Recently, an accuracy requirement of ± 3.5% was proposed (Mijnheer, 1988) for the total uncertainty (1σ) in the absorbed dose delivery to the dose specification point in a patient.

In order to determine whether the required value for the total uncertainty is a realistic value in clinical practice, the sequence of dosimetry procedures to deliver the absorbed dose to the patient must be analyzed (see Figure 10).

Standardization of clinical dosimetry procedures can be achieved using common dosimetry protocols. In these protocols guidelines are formulated for clinical dosimetry procedures while, in addition, recommendations are given for a number of physical quantities and correction and conversion factors. In the USA and Europe, parallel efforts by the American Association of Physicists in Medicine (AAPM) and the European Clinical Neutron Dosimetry Group (ECNEU), respectively, have resulted in separate protocols for neutron beam dosimetry (AAPM, 1980; Broerse et al., 1981). Differences between the two protocols concerned the use of physical parameters and the choice of the phantom material. The Americans recommended the use of TE liquid while the Europeans preferred water as phantom material. Both the European
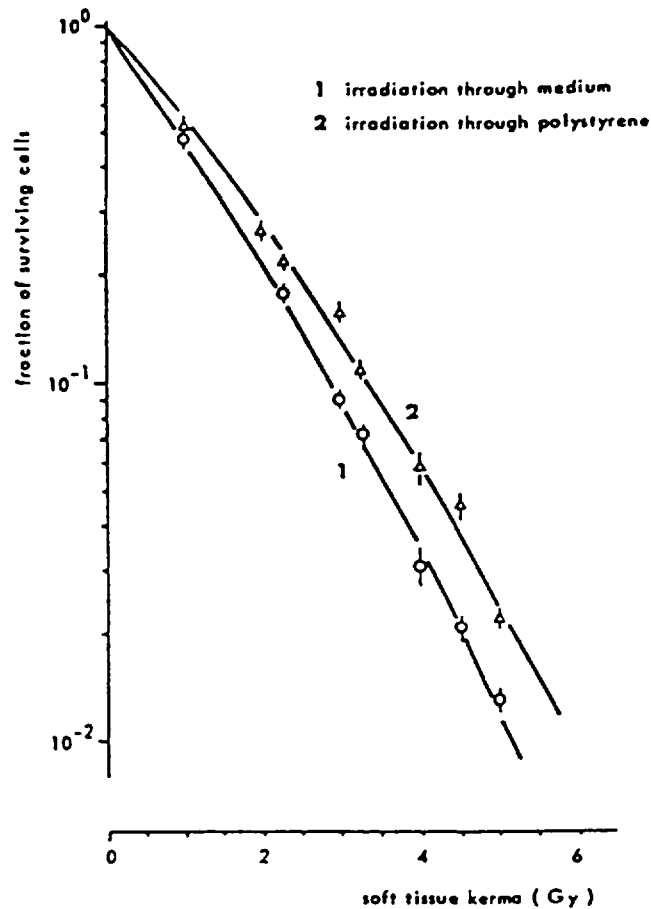
Figure 9: Survival curves of cultured cells irradiated with D-T neutrons through the medium (curve 1) or through the polystyrene bottom of the culture flasks (curve 2).

and the American groups recommend the use of TE ionization chambers constructed of A-150 plastic and flushed with methane-based TE gas. Up to neutron energies of 15 MeV the dosimetric parameters are known with an acceptable degree of accuracy. The absorbed dose values determined with an IC-17 chamber as derived according to both protocols differ by 3.4% for D-T neutrons and by 2.5% for d(15)Be neutrons (Mijnheer, 1987).

With the advent of a new phase of American and European clinical trials with cyclotron-produced high-energy neutrons beams, it became clear that a consensus was required with respect to dose specification. The earlier protocols for clinical neutron dosimetry were updated (Mijnheer et al., 1987; ICRU, 1989) to achieve better uniformity. The revised recommendations mainly concern numerical values for the physical constants and the use of the reference phantom material. Other aspects of the protocols such as the determination of the photon component of the total absorbed dose, corrections for the readings of the ionization chamber for temperature and pressure, gas flow rate, leakage current, polarity and humidity have not been revised. ICRU Report 45 (1989) has been used as the main source of reference for the following sections.
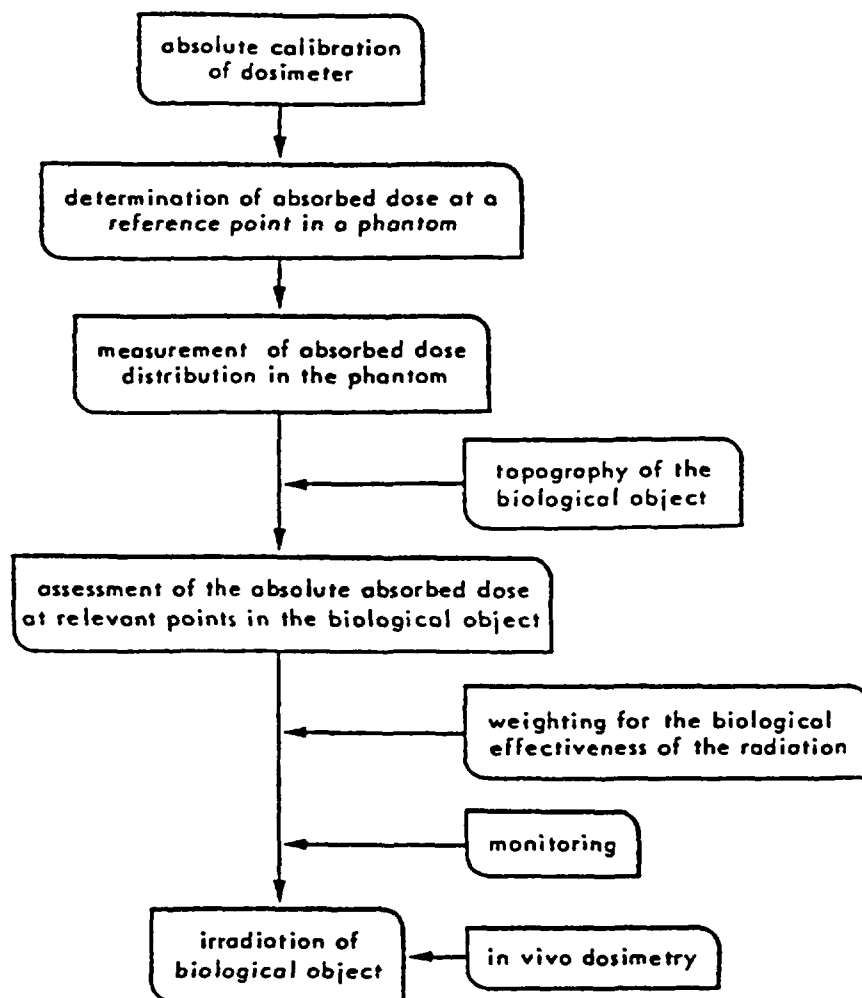
Figure 10: Sequence of dosimetry procedures to deliver the absorbed dose to the biological object.

3.2 Reference Phantom Material

The choice of material for a reference phantom is dictated by the principle that it should be matched to muscle tissue so as to have the same or very similar neutron absorption and scattering properties. According to ICRP Report 23 (1975), muscle, as well as other tissues such as liver and kidney, has densities varying between 1.03 and 1.05 g cm^{-3}. An ideal phantom material therefore, would be a muscle tissue-equivalent liquid or solid with a density of 1.04 g cm^{-3}. The fat-free, muscle-equivalent liquid of Frigerio *et al.* (1972) has been used as a standard TE liquid medium for reference phantoms. This liquid mixture is exactly equivalent to ICRU muscle tissue, and it also contains the correct amounts of the trace elements found in muscle tissue. Its density, however, is 1.07 g cm^{-3} which compares well with that of adipose-free muscle but is higher than that of muscle. In the majority of applications, it is not necessary to reproduce in a phantom the trace elements present in tissue.

37

As in the case of photon beams, water can also be used as the reference phantom material for purposes of clinical tissue-absorbed dose determination. It has been shown that central axis percentage depth-dose curves in water almost coincide with those in a muscle-equivalent liquid of density 1.04 g cm^{-3}. Water has been found to be valid as a suitable medium for the low- as well as the high-energy therapeutic neutron beams. The lower density of water compared with the average density of muscle is apparently compensated by the difference in composition, i.e., the higher hydrogen content of water. The difference in tissue absorbed-dose values measured in water and in TE liquid of density 1.07 g cm^{-3} is acceptable for clinical practice at low-neutron energies, i.e., it is smaller than 1% at depths between 2 and 12 cm for D-T and d(15)Be neutrons. For higher neutron energies, differences of several per cent can occur. It should be noted that to obtain absorbed-dose distributions in irradiated patients, correction factors are needed for all phantom materials to account for differences in atomic composition and density between the phantom and the irradiated volume in the patient. Based on these conclusions, it is recommended that water should be used as the reference phantom material (ICRU, 1989).

3.3 Reference Dosimeter Material

The requirement of tissue equivalence is even more stringent for the dosimeter material than for the reference phantom. Homogeneous ionization chambers are used almost exclusively in clinical neutron dosimetry for two reasons: first, because the requirement for small cavities compared to the ranges of all secondary charged particles is difficult to achieve for chambers yielding adequate ionization current for reliable measurement; and second, because cavity-chamber data applicable to neutron dosimetry with nonhomogeneous chambers are sparse. Chamber homogeneity is achieved for neutron dosimetry by using wall, gas, and insulator materials that have about the same energy transfer coefficient for the primary radiation and the same stopping power for the secondary particles.

The wall material commonly used and recommended for clinical neutron dosimetry is a tissue-equivalent plastic designated A-150, and the gas is a methane-based TE (tissue-equivalent) gas mixture. The gas contains 64.4% methane, 32.4% carbon dioxide, and 3.2% nitrogen by partial pressures. Hydrogenous insulator materials suitable for use in ionization chambers are amber, nylon, polyethylene, polymethylmethacrylate, and polystyrene. If insulators could substantially contribute to the production of secondary particles in the gas volume, care must be exercised to use an insulator with a composition similar to A-150 plastic. Further information on A-150 plastic, the gas, and other tissue-like materials is given in the appendices of ICRU Report 26 (1977) and ICRU Report 44 (1989). The hydrogen content of ICRU muscle tissue (striated) differs from that in ICRU soft tissue, (see Table X), requiring a 1% different kerma correction factor in high-energy neutron beams for muscle tissue compared to soft tissue (see Table XI).

Because a vast amount of clinical information is already based on it, it is recommended that ICRU muscle tissue (striated) be taken as the reference tissue. The principal compromise made when using A-150 plastic is the substitution of carbon for much of the oxygen required to match muscle tissue. The methane-based TE gas mixture used with this plastic is also deficient in oxygen, but to a lesser extent. This deficiency, and the concomitant excess of carbon, generally results in an increase of

Table X: Elemental composition of several solids, liquids, and gases similar to tissue.

Substance	Percent Elemental Mass					Reference
	H	C	N	O	Other	
Standards						
standard man	10.0	18.0	3.0	65.0	1.5 Ca, 1.0 P, 0.8 S+ K+Ca	ICRP, 1959
muscle(striated)	10.2	12.3	3.5	72.0	1.1 Na+Mg+P+S+ Na+Mg+K+Ca+Cl	ICRU, 1964
muscle(skeletal)	10.2	14.3	3.4	71.0	0.1 Na, 0.2 P, 0.3 S, 0.1 Cl, 0.4 K	ICRU, 1989
Solids						
A-150 plastic	10.1	77.6	3.5	5.3	1.8 C, 1.7 F	Smathers *et al.*, 1975
polymide, nylon Zytel	10.4	64.8	10.0	14.8		ICRU, 1977
polymethyl methacrylate	8.0	60.0		32.0		$(C_2H_8O_2)_n$
Liquids						
water	11.2	–	–	88.8		
muscle equivalent	10.2	12.0	3.6	74.2		Goodman, 1969
Gases						
air	–	–	75.5	23.2	1.3 Ar	ICRU, 1984
muscle equivalent -methane	10.2	45.6	3.5	40.7		Rossi & Failla, 1956
muscle equivalent -propane	10.3	56.9	3.5	29.3		Srdoc, 1970

Table XI: Kerma, K_m, in different materials as a percentage of kerma, K_t, in ICRU muscle (from Awschalom *et al.*, 1983a).

NEUTRON SOURCE				
Material	p(65)Be	p(41)Be	d(16)Be	D-T
Soft tissue (ICRU)	99 ± 2	99 ± 2	99 ± 2	99 ± 2
Whole blood	98 ± 2	98 ± 2	98 ± 2	98 ± 2
Fat (adipose)	115 ± 5	116 ± 5	113 ± 5	113 ± 6
A-150 plastic	108 ± 4	107 ± 3	102 ± 2	104 ± 5
Water	104 ± 2	105 ± 2	108 ± 2	106 ± 2

several per cent in the energy released by neutron interactions in the plastic, relative to that released in muscle tissue (see Table XI). For neutron energies below ~ 10 MeV additional fluctuations of several per cent at various neutron energies also result from significant disparate resonances in the interaction cross sections of oxygen and carbon.

3.4   Principles of Mixed Neutron-Photon Beam Dosimetry

In practical situations neutron radiation is always accompanied by a fluence of photons. These photons may be generated as part of the neutron production process, or as a result of interactions in the absorbing medium in which the absorbed dose is to be determined or interactions in the target, collimator, or other irradiated structures. In an extended medium the relative contributions to the absorbed dose from neutrons and photons may vary, as may the neutron and photon spectra. The simplest useful description of the mixed field is a statement of the separate absorbed doses due to the two components. These may have to be determined where neither the neutron nor the photon spectra are known at the points of interest.

In general, a dose measurement then requires the use of two dosimeters, ideally a photon dosimeter which is insensitive to neutrons and a neutron dosimeter which is insensitive to photons. However, dosimeters for photons (*e.g.*, ionization chambers, Geiger-Müller counters, photographic emulsions, thermoluminescent materials) are also sensitive to neutrons. There are neutron instruments which are virtually insensitive to photons (*e.g.*, the precision long counter, pulse fission counters, activation methods), but they determine the neutron fluence, and deducing the absorbed dose with these devices requires a fairly detailed knowledge of the neutron spectrum.

In most mixed-field situations two dosimeters with different sensitivities to the two types of radiation are commonly used to evaluate the separate absorbed doses of neutrons and photons. One instrument (T) is usually constructed to have approximately the same sensitivity to neutrons as photons, whereas the construction of the second instrument (U) results in a lower sensitivity to neutrons than photons. Thus, for the same mixed field, the quotients of the readings of the dosimeters by their responses (*i.e.*, the readings per unit absorbed dose) to the gamma rays used for calibration, D'_T and D'_U, are given by:

$$D'_T = k_T D_n + h_T D_\gamma \tag{1}$$

$$D'_U = k_U D_n + h_U D_\gamma \tag{2}$$

where D_n and D_γ are the absorbed doses in tissue of neutrons and of photons in the mixed field, k_T and k_U are the ratios of the responses of each dosimeter to neutrons to its response to the gamma rays used for calibration, and h_T and h_U are the ratios of the responses of each dosimeter to the photons in the mixed field to its response to the gamma rays used for calibration, respectively.

It is generally assumed that k_T ranges from 0.95 to 1.00 for TE ionization chambers and that h_T and h_U are equal to 1. The accuracy with which the neutron absorbed dose can be determined is, in general, greatest when, as the second instrument, a photon dosimeter with the smallest possible k_U is used (ICRU, 1977).

Among the nonhydrogenous ionization chambers to be used as a neutron-insensitive device, the Mg-Ar and Al-Ar chambers are preferable in comparison with C-CO$_2$ chambers. A dosimeter which has a particularly low k_U value is a small Geiger-Müller

counter used with a photon-energy compensating filter (see ICRU, 1977 and 1989b for details). For higher-energy neutron beams, and a commercially-available counter (ZP-1100), k_U/k_T values, of 3.7 ± 1.0 % for p(45)Be, 4.1 ± 0.4 % for d(50)Be, and 6.1 ± 0.9 % for p(66)Be neutron beams have been determined by Pihet *et al.* (1982). GM counters with their energy-compensating filters for photons have a high thermal neutron response and should be shielded by a thermal neutron absorber, *e.g.*, ^{6}Li metal or ^{6}LiF powder, which does not emit prompt gamma radiation in the neutron capture process.

3.5 Dosimetry With TE Ionization Chambers

In practice, clinical neutron dosimetry is based on measurements made with nearly homogeneous TE ionization chambers, because these instruments are more accurate and convenient than other methods. These TE dosimeters are used either free-in-air to characterize the neutron beam, or inserted into phantoms made of tissue-simulating materials to determine absorbed dose in patients.

The status of ionization chambers and their use for neutron dosimetry has been reviewed by Broerse (1980), who have recommended that a common type of TE ionization chamber be used as a reference instrument.

The measurement of absorbed dose by means of an ionization chamber is based on the Bragg-Gray relation:

$$D = \frac{Q}{m} \cdot \frac{W}{e} \cdot S_{m,g} \tag{3}$$

where D is the absorbed dose in the wall surrounding a cavity, Q is the charge of one sign produced within the cavity, m is the mass of the cavity gas, W is the average energy expended per ion pair formed in the gas, e is the electronic charge, and $S_{m,g}$ is the mass stopping-power ratio for the wall material, m, and the gas, g of the chamber for the charged particles liberated in the wall. It is assumed that the dimensions of the cavity are small compared with the range of the charged particles that impart the absorbed dose and that the cavity does not disturb either the neutron or photon fluence, or the secondary particle fluence.

The application of the Bragg-Gray relation to neutron dosimetry with tissue-equivalent ionization chambers is subject to a number of corrections as well as spectral averaging of physical quantities. In the practical situation, equation (3) can, therefore, be given in the form:

$$D = \frac{Q_n}{m} \cdot \frac{W_n}{e} \cdot (r_{m,g})_n \cdot d_T \cdot \frac{1}{1 + \delta} \tag{4}$$

where W_n is a mean W value to be applied for a specific neutron beam and is an average value for a mixture of secondaries. W_n has to be evaluated taking into account all secondary charged particles, having different mass and energy, originating from neutron interactions with the wall or the cavity gas, and producing charge in the cavity.

$(r_{m,g})_n$ is the gas-to-wall absorbed-dose conversion factor. If the atomic composition of wall and gas are the same, and assuming that the density correction to stopping power can be neglected, $(r_{m,g})_n$ equals $S_{m,g}$ and will be unity for all charged particles. Because the atomic composition of wall and gas are generally not the same, $S_{m,g}$ must be averaged over all secondary charged particles produced by neutron in-

teractions in the wall. In most neutron beams, not only secondary particles generated in the wall produce ionization, but the gas cavity also contributes to the secondary particle spectrum. $S_{m,g}$, which applies when the gas cavity of the ionization chamber is a Bragg-Gray cavity, is therefore replaced by $(r_{m,g})_n$ in neutron dosimetry.

d_T is the displacement correction factor. This factor accounts for the difference in absorption and scattering when the ionization chamber replaces phantom material. Due to the ionization chamber, the neutron energy fluence is perturbed and the charge collected must be multiplied by d_T, to yield the undisturbed total absorbed dose of the geometric center of the chamber.

δ corrects for the difference in response of the TE chamber for neutrons and photons in the neutron beam.

The total absorbed dose, $D_n + D_\gamma$, the sum of the neutron and photon absorbed doses to ICRU muscle tissue, can now be given by:

$$D_n + D_\gamma = D \cdot (K_t/K_m)_n \tag{5}$$

where $(K_t/K_m)_n$ is the ratio of the kerma in the reference tissue (ICRU muscle tissue) to that in the dosimeter wall material (A-150 plastic). It should be realized, however, that this relation is only valid when $D_\gamma \ll D_n$.

The total absorbed dose may then be evaluated for the charge produced in the TE chamber in a neutron beam:

$$D_n + D_\gamma = \frac{Q_n}{m} \cdot \frac{W_n}{e} \cdot (r_{m,g})_n \cdot (K_t/K_m)_n \cdot d_T \cdot \frac{1}{1 + \delta} \tag{6}$$

Several methods are available to calibrate TE ionization chambers, *i.e.*, to determine the mass of the gas in the chamber and the absolute value of the energy expended within the cavity. Until now it has been recommended that the chamber be calibrated in a photon field relative to a secondary standard exposure chamber which has a calibration factor traceable to a national standards laboratory. However, one might calibrate a TE ionization chamber in a neutron beam if the kerma or absorbed dose, under the calibration conditions, is well-known. Standards laboratories are presently developing methods for providing calibrations in terms of such quantities. If the TE ionization chamber is calibrated in a reference neutron field with well-known absorbed-dose components, then the overall uncertainty in a total absorbed-dose measurement in an unknown neutron field will be smaller than when a photon calibration is applied (Mijnheer and Williams, 1984). Details concerning the photon calibration of TE ionization chambers can be found elsewhere (ICRU, 1989b).

3.6 Physical Parameters for Dosimetry With TE Ionization Chambers

The overall uncertainty in the assessment of absorbed dose from TE ionization chamber measurements in a neutron beam is much larger than that from measurements in photon and electron beams, which is less than 1% (see Table XII). Because of continuing efforts to improve the data base of neutron dosimetry, recommended values for the physical parameters applied in equation (6), may differ from those given in ICRU Report 26 (1977) and from those given in the protocols cited previously. They may also be subject to future changes. It is anticipated that the adoption of a common set of basic physical parameters will achieve greater consistency in clinical neutron dosimetry. The parameters discussed below will be $(r_{m,g})_n$, W_n, $(K_t/K_m)_n$ and d_T.

Table XII: Estimated uncertainties (one standard deviation) in the determination of the total absorbed dose in a phantom irradiated by a p(65)Be neutron beam using a TE ionization chamber having an air-kerma calibration factor (ICRU, 1989b).

SOURCE	RELATIVE UNCERTAINTY (%)
Electrometer reading	0.1
Reading correcting factor	0.2
Air-kerma calibration factor	1.0
Absorption and scattering correction factor	0.2
Ratio of photon mass energy absorption coefficients	0.5
Displacement correction factor	0.3
Ratio of average energies required to create an ion pair for A-150/TE-gas chamber	2.0
Ratio of gas-to-wall absorbed dose conversion factor and ratio of mean restricted collision mass stopping powers	2.0
Ratio of neutron kerma	3.5
Overall uncertainty	4.6*

*A lower value of 3.4% is valid for a d(16)Be beam where the uncertainty in the ratio of neutron kerma, is about 1.5%.

3.6.1 Gas-to-Wall Absorbed Dose Conversion Factor

Only limited information is available for the gas-to-wall absorbed dose conversion factor for neutrons, $(r_{m,g})_n$, which was formerly called the effective stopping-power ratio. ICRU Report 26 (1977) assumed $(r_{m,g})_n = 1$ to be a valid approximation for most neutron energy spectra. Its calculation is complicated due to the differences in type and spectra of secondary particles. Various groups have calculated $(r_{m,g})_n$ at specific neutron energies and for some cavity sizes (ICRU, 1989b) resulting in values between 0.98 and 1.06. The deviation from unity is caused by the difference in both stopping power and atomic composition between A-150 plastic and TE gas. Because the accuracy of calculated values of $(r_{m,g})_n$ and $S_{m,g}$ is limited by the lack of adequate stopping-power data for the gas and solid phases and due to the neutron energy dependence of $(r_{m,g})_n$, a value of $(r_{m,g})_n/S_{m,g} = 1.00 \pm 0.02$ is recommended for the TE ionization chambers and neutron energies employed for neutron therapy (ICRU, 1989b).

3.6.2 Energy Required to Produce an Ion Pair

Values of W_n and of W_n/W_c, where W_c is for ^{60}Co gamma rays, in the methane-based TE gas have been published by Goodman and Coyne (1980) for neutrons with energies up to 20 MeV. This reference states that W_n is almost constant at 31.1 eV for neutron spectra with mean energies greater than 5 MeV and that this is probably true for neutron energies somewhat higher than 20 MeV. In principle, the W_n values calculated by these authors are only valid for chambers having diameters that are very large compared with the range of the recoil particles because TE gas kerma, instead of absorbed dose to TE gas, was used in their calculations. For the methane-based TE gas and the neutron spectra typically employed for therapy applications, a value

$W_n/W_c = 1.06 \pm 0.02$, for which the value $W_c = 29.3$ eV was used, was recommended by Goodman and Coyne (1980). The American protocol (AAPM, 1980) cites current practice in the United States, but makes no recommendation as to the value to be adopted. The European protocol (Broerse *et al.*, 1981) recommends that $W_n/W_c = 1.06$ be used for most neutron radiotherapy beams. A value of $W_n/W_c = 1.05$ was recommended in ICRU Report 26 (1977) with an uncertainty of $\pm 5\%$ for neutron energies above 1 MeV and an increased systematic uncertainty at lower energies. The kerma weighted energy fluence spectrum W_n/W_c should be calculated from the consistent set of data of Goodman and Coyne (1980) for neutron beams with energies up to about 15 MeV, if the neutron energy spectrum at the reference point is available (see Figure 11). For relative kerma spectra from a collimated D-T neutron beam, W_n/W_c values varying between 1.063 at the surface and 1.068 at 10 cm depth outside the penumbra have been calculated. This indicates that position-independent W_n/W_c values can be applied for the determination of isodose curves. For neutron energies higher than about 15 MeV, or, if no spectra data are available, a value of $W_n/W_c = 1.06 \pm 0.02$ should be adopted (ICRU, 1989b).

3.7 Neutron Kerma Ratio

The ratio of the kerma in the tissue of interest to the kerma in the dosimeter wall material (A-150 plastic), $(K_t/K_m)_n$, is needed to convert the neutron absorbed dose measured by the dosimeter to that which would be produced in tissue. Since the tissue type in the clinical situation is often not well-defined, it has become customary to assume that the composition of ICRU muscle tissue (Table X) is sufficiently representative of the actual tissue(s) to be irradiated with fast neutrons. The neutron kerma ratios for ICRU muscle tissue relative to A-150 plastic which have been used in the past by the United States neutron therapy groups range from 0.95 to 0.96 (AAPM, 1980).

Appendix A of ICRU Report 26 (1977) gives the kerma factors for these materials for neutron energies up to 30 MeV. This tabulation has been updated by Caswell *et al.* (1980, 1982). Further evaluations of kerma factors have recently been performed by Howerton (1991), Brenner (1991), and White *et al.* (1992) . The most recent information on kerma ratios is summarized in Figures 12 and 13.

For neutron beams with a broad energy spectrum, spectrum-weighted mean kerma factors must be used. Hence, an attempt should be made to obtain information on the radiation spectrum at the point of interest. The neutron kerma factor ratio can be calculated for the neutron energy spectrum at the reference point on the basis of the updated set of kerma values. Uncertainties in kerma factors for tissue and tissue-like materials increase with energy from about 1% at low neutron energies, to > 20% in nonhydrogenous materials at the higher energies employed for neutron therapy. Because the kerma factor for tissue and tissue substitutes is dominated by high energy kerma factor which is known to at least 1% accuracy, the kerma ratio is less dependent on neutron energy. Until more reliable data on spectra and kerma factors for neutron energies greater than about 15 MeV become available, it was recommended (ICRU, 1989b) that the ratio of kerma in ICRU muscle to A-150 plastic be taken as 0.95 for the high energy beams. More information on kerma factor ratios is given in Chapter 4.
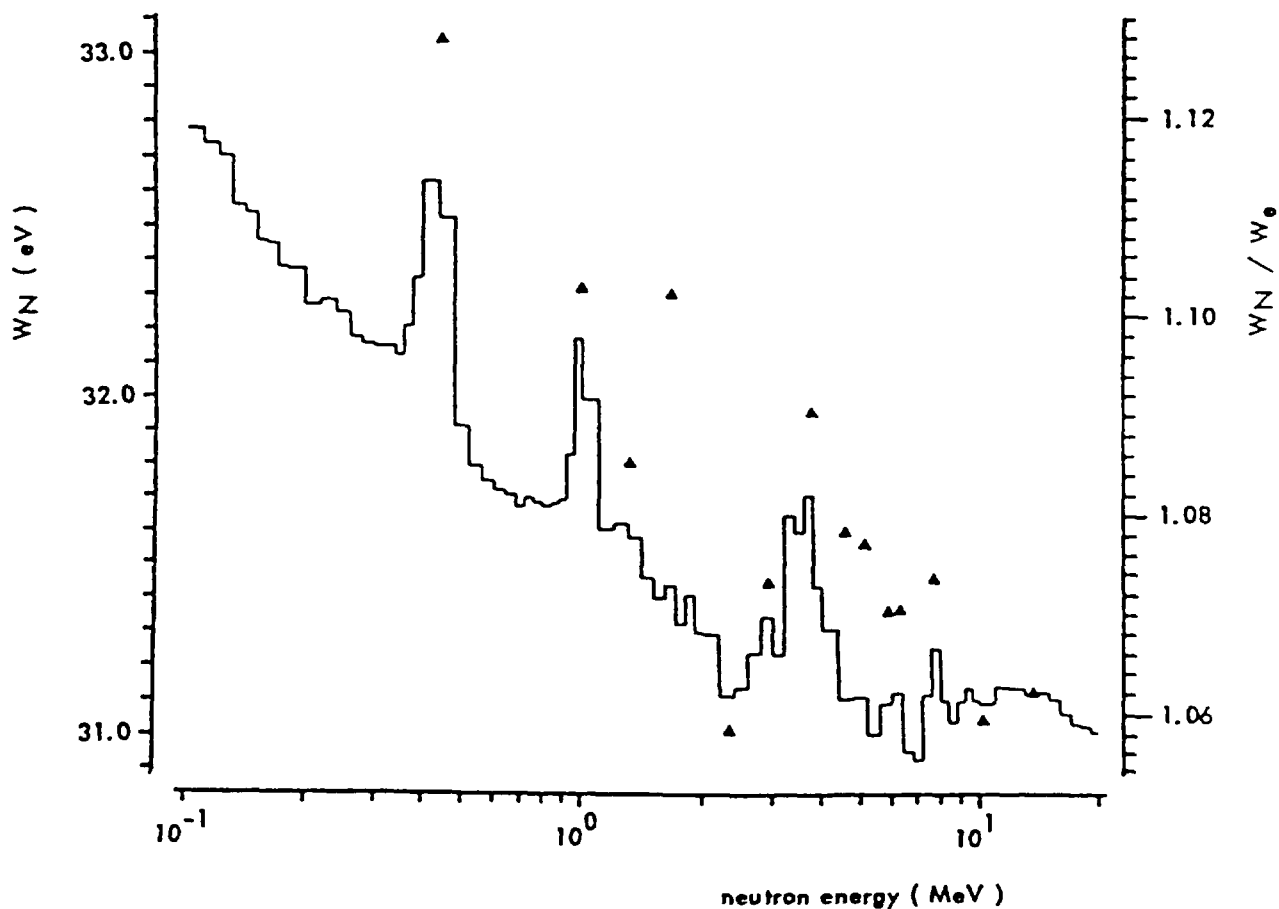
Figure 11: Values for W_n calculated for methane-based tissue equivalent gas by Goodman and Coyne (1980). The triangular points shown on the graph are W_n values evaluated at discrete energies of prominent resonances, rather than the values averaged over energy bins shown by the solid lines.
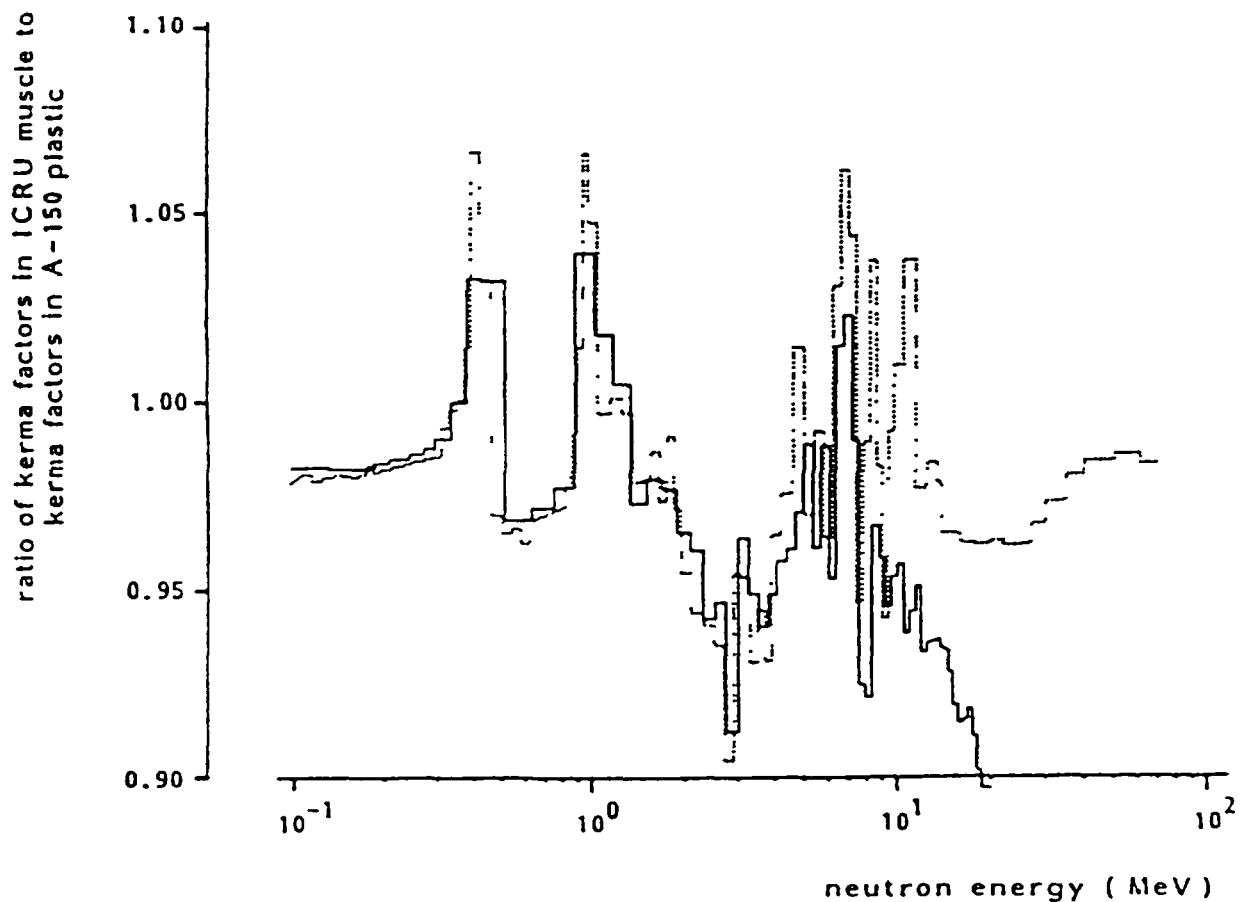
Figure 12 Ratio of kerma in ICRU muscle tissue to kerma in A-150 as a function of neutron energy on a logarithmic scale. The solid line represents the calculations of Howerton (1991), the dashed line is based on the calculations of Caswell *et al* (1980) up to 15 MeV, and on calculations of Brenner (1991) for the energy range 15-70 MeV

3.7.1 Displacement Correction

The displacement correction accounts for the reduced absorption and scattering of the radiation sensed by an ionization chamber due to the displacement of phantom material by the gas cavity of the chamber. This correction can take the form of a multiplicative factor, d_T, which adjusts the measured ionization to the value that would be obtained if the cavity were filled with phantom material, or it can be expressed by stating the position of the effective measuring point as a certain fraction of the radius of the gas cavity upstream of the chamber's geometrical center. The American protocol (AAPM, 1980) uses the multiplicative-factor method and recommends for all clinical neutron beams a factor of 0.970 for the 1 cm^3 spherical chamber and 0.989 for the 0.1 cm^3 thimble type chamber, based on the measurements of Shapiro *et al.* (1976). These factors can be applied only to the descending portion of the depth-dose curve, *i.e.*, where the measurements show that the factors are not dependent on neutron beam field size. The European protocol (Broerse *et al.*, 1981) also recommends use of multiplicative displacement correction factors. Their recommendations are based on the measurements of Zoetelief *et al.* (1980a, b) for spherical TE ionization cham-
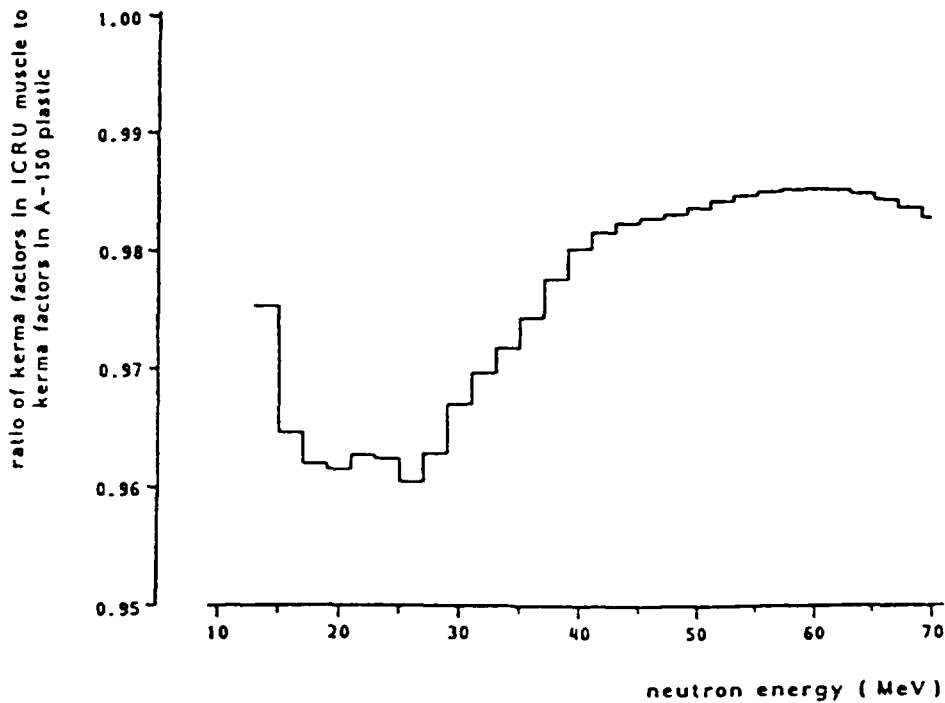
Figure 13: Ratio of kerma in ICRU muscle tissue to kerma in A-150 plastic as a function of neutron energy on a linear scale (Brenner, 1991).

bers in a water phantom (see Table XIII). These measurements showed no change in the factors with depth in the phantom. For a 1 cm^3 spherical ionization chamber, the data of Zoetelief et $al.$ (1980a,b) would result in a factor $d_T = 0.984 \pm 0.004$ for d(50)Be neutrons. For a chamber of the same dimension Awschalom et $al.$ (1983b) derived a value of 0.970 ± 0.005 for p(66)Be neutrons, which agreed very well with the value obtained in a d(35)Be neutron beam by Shapiro et $al.$ (1976), but is lower than the value given by Zoetelief et $al.$ (1980a,b). For a 0.5 cm^3 thimble type of ionization chamber the results of Awschalom et $al.$ (1983b) are equal to, or within the experimental uncertainties of, data obtained by other methods.

Because all of these groups used different techniques to determine d_T, each with different uncertainty, the ICRU (1989b) recommended values for the displacement factors for neutron therapy beams as the unweighted average of all results yielding 0.978 ± 0.004 for a 1.0 cm^3 spherical chamber; 0.986 ± 0.003 for a 0.5 cm^3 thimble chamber; and 0.993 ± 0.002 for a 0.1 cm^3 thimble chamber. The systematic uncertainty in d_T due to the somewhat different data can, therefore, be minimized by using small ionization chambers.

3.8 Results of Neutron Dosimetry Intercomparisons

Dosimetry intercomparisons can be divided into two groups: (1) studies primarily intended to compare dosimetry methods using similar or different techniques and (2)

Table XIII: Displacement correction factors, d_T, of spherical ionization chambers (with radius r in mm) for measurements in phantoms with different types of radiation (Zoetelief et al., 1981).

TYPE OF RADIATION	d_T
150, 200 and 300 kV X rays	$1.000 \pm 0.05.10^{-2} \cdot r$
^{137}Cs γ rays	$1 - (0.22 \pm 0.05).10^{-2} \cdot r$
^{60}Co γ rays	$1 - (0.37 \pm 0.04).10^{-2} \cdot r$
Fission neutrons ($\bar{E}_n = 1$ MeV)	$1.000 \pm 0.1 \cdot 10^{-2} \cdot r$
d(2.3)D neutrons ($E_n = 5.3$ MeV)	$1 - (0.25 \pm 0.09) \cdot 10^{-2} \cdot r$
d(0.25)T neutrons ($E_n = 14.2$ MeV)	$1 - (0.25 \pm 0.06) \cdot 10^{-2} \cdot r$
d(0.5)T neutrons ($E_n = 14.8$ MeV)	$1 - (0.25 \pm 0.06) \cdot 10^{-2} \cdot r$
d(50)Be neutrons ($\bar{E} = 21$ MeV)	$1 - (0.21 \pm 0.05) \cdot 10^{-2} \cdot r$

intercomparisons of dosimetry systems on which clinical dosimetry has been based. The first type of intercomparison can be performed in neutron beams used in either laboratories or clinics. During the International Neutron Dosimetry Intercomparison Project, ENDIP-1 (Broerse et al., 1978), all participants took their dosimetry systems to a specific experimental site. Both intercomparisons were, therefore, an intercomparison of instrumentation and methods under laboratory conditions with neutron energies and absorbed-dose rates which differed from those of therapy units. In clinically applied neutron beams, absorbed-dose values, determined with a TE ionization chamber in combination with a neutron insensitive device and derived according to a procedure given in a protocol, have also been compared with values obtained from other methods, e.g., calorimetry or fluence measurements. In the second group of intercomparisons, institutions involved in cooperative clinical trials intercompared their reference dosimetry systems in various therapy beams. A link between both groups of intercomparisons was made in the NPL neutron dosimetry intercomparison (Lewis, 1985), where standards laboratories, the ENDIP team, and several radiotherapy institutes participated.

The results of both intercomparisons were similar. The uncertainty (one standard deviation) of the measured total absorbed dose to ICRU muscle tissue, was 7 to 8%. The values reported for the relatively low gamma-ray contribution to the absorbed dose varied by more than 50%. These variations would not be acceptable for radiotherapy since it is generally necessary to know the absorbed dose at an arbitrary point in the target volume in a patient with an overall uncertainty of 5% and at the dose specification point with even higher accuracy. Analysis of the results showed that the differences could be attributed to the use of different dosimetry systems, physical parameters, and measurement procedures. Measurements performed with Mg chambers of the same type have also shown appreciable variations (Zoetelief et al., 1986).

McDonald et al. (1981a,b) have compared the value of the absorbed dose to A-150 plastic, determined with TE ionization chambers, to that measured with an A-150 plastic calorimeter in an A-150 plastic phantom in various neutron therapy beams. The results agreed within 2%. A difference of about 2% is obtained if either the American or European protocol for neutron dosimetry for external beam therapy

for a D-T beam is applied. Caumes *et al.* (1984) observed in a p(34)Be beam a difference of 1.4% between the absorbed dose to A-150 plastic measured with an A-150 plastic calorimeter versus an A-150 plastic ionization chamber applying the European protocol. A further intercomparison in a d(13.4)Be beam showed a difference of about 2% (Brede *et al.*, 1988).

These comparisons lend confidence to the absorbed-dose calculation procedures and data employed as outlined in the protocols. It should be noted, however, that the absorbed dose in tissue will have a larger uncertainty due to the application of the kerma ratio. The results of other intercomparisons, including those performed with fluence measuring devices and proportional counters are summarized in ICRU Report 45 (1989).

In the second group of intercomparisons carried out among a limited number of institutions, using TE ionization chambers, the observed differences were generally smaller than during the previous intercomparisons. The variations among data from participants in the dosimetry intercomparisons in the United States were smaller than in the results obtained among the European groups (Broerse *et al.*, 1979) and in the intercomparisons carried out between American and Japanese groups (Ito, 1978). These larger differences were due partly to the use of various types of TE ionization chambers in Europe and Japan, whereas all American groups adopted a common type of chamber. Differences in the photon calibration procedure may result in an additional deviation of about 5% in the measurement of total absorbed dose in a neutron beam (Williams *et al.*, 1981).

It was concluded from these intercomparisons that a protocol was needed in which recommendations are given for the measurement procedure including dosimeter calibration. Such a protocol should, in addition, recommend a consistent set of values for the physical parameters used to convert the dosimeter reading into an absorbed dose value. The introduction of both the American and the European protocol for neutron dosimetry for external beam therapy has considerably reduced variations in absorbed-dose determination between different groups. This has been demonstrated, for instance, in the more recent ENDIP-2 intercomparison (Zoetelief and Schraube, 1985), where a measuring team visited a number of institutions and compared their absorbed-dose measurements, using the two-dosimeter method, with the values stated by the institution. A maximum deviation of about 2% was observed between local and ENDIP-2 photon calibration factors, which is considerably smaller than the spread observed during the ENDIP-1 intercomparison. The measurements in the neutron beam showed a deviation of less than 3% between the total absorbed-dose values measured by the visiting team and the values stated by the institution, again much smaller than observed earlier. A similar result was obtained during the NPL intercomparison (Lewis, 1985). The adoption of a secondary standard or reference dosimeter and the installation of neutron calibration facilities for such an instrument by national standards laboratories would be the next step in the reduction of systematic errors in clinical neutron dosimetry.

Small-scale intercomparisons between centers participating in collaborative trials will remain important even after the introduction of a common protocol, a reference type dosimeter, and calibration in a neutron beam. These intercomparisons will be useful not only for groups entering the field but also for groups currently engaged in neutron therapy. They will serve as an independent check on the dosimetry chain from the standardizing laboratory to absorbed dose delivered within a hospital. Preferably, these intercomparisons should not be restricted to the absorbed-dose measurement

at the reference point in the phantom under reference conditions. Intercomparison of the whole procedure of treatment of a specific tumor may also reveal other systematic uncertainties, e.g., in dose planning by computer, output determination under treatment conditions, and dose specification for reporting.

3.9 Recommendations for Future Work in Dosimetry

Although we have to be more modest about the applicability of fast neutrons for radiotherapy than we originally anticipated, there is a future for high energy neutron beams. In addition, the increasing interest in proton beams should be stated because of the great potential of these particles for beam definition. Possible clinical advantages of protons are based only on their physical properties. When cyclotrons are constructed for proton therapy, an additional beamline and a beryllium target could be installed as well, to provide a high energy neutron beam with the specific biological advantages of high-LET radiation.

The dosimetry requirements for these high-energy neutron beams were covered by Caswell et al. (1988). New data on total cross sections for carbon have become available. Accurate kerma factors, however, are needed for the neutron energy range up to 20-60 MeV. The instruments to be used for quantitative and qualitative determination of the energy deposition should include the following: tissue-equivalent ionization chambers, non-hydrogenous chambers, preferably Mg-Ar and Al-Ar, Geiger-Müller counters, TE proportional counters, and calorimeters. As described by McDonald and Cummings (1988), the last instrument can now be confined to relatively small dimensions.

Concerning the need for nuclear and atomic data for neutron radiotherapy, the following recommendations (Mijnheer, 1988) have been formulated:

1. More accurate neutron cross section data for the elements in tissue and ionization chamber wall materials are needed to reduce the uncertainty in the kerma factor ratio.

2. Additional information is required on W_n/W_c and $(r_{m,g})_n$ if a photon calibration of an ionization chamber is applied.

3. More data are required to assess the perturbation of the absorbed dose distribution behind bone, fatty tissue and brain, particularly for the higher neutron energy beams.

4. Better knowledge of dose distributions at interfaces between tissues or organs of different density or composition is required.

5. More data are needed to quantify the effect of air cavities on dose distributions.

Furthermore, a strong plea should be made for the continuation of small scale intercomparisons, including the determination of absorbed dose and radiation quality. For this purpose, neutron dosimeters, proportional counters and biological dosimeters could be used. Such intercomparisons will be essential when new institutions apply neutron beams for radiotherapy.

Within Europe the physicists involved in high-LET therapy have formalized their cooperation in the European Clinical Heavy Particle Dosimetry Group: ECHED, which is the successor of ECNEU. European scientists active on dosimetry for radi-

ation protection are cooperating within the European Radiation Dosimetry Group: EURADOS (Broerse and Dennis, 1990). The activities of the latter group cover the following subjects: skin dosimetry and surface contamination monitoring, numerical dosimetry, basic physical data and characteristics of radiation protection instrumentation, assessment of internal dose, radiation spectrometry in working environments, development of individual dosimeters and criticality accident dosimetry. The activities performed within the different EURADOS working groups are financially supported by the Commission of the European Communities (CEC). The collection and evaluation of basic data for neutron dosimetry and the implementation of new dosimetry techniques are included in the objectives of ECHED and EURADOS.

References

American Association of Physicists in Medicine, *Protocol for Neutron Beam Dosimetry*, Report 7, Task Group 18, Fast Neutron Beam Dosimetry Physics Radiation Therapy Committee (American Association of Physicists in Medicine, New York) (1980).

Awschalom, M., Rosenberg, I., and Mravca, A., "Kermas for Various Substances Averaged Over the Energy Spectra of Fast Neutron Therapy Beams: A Study in Uncertainties," *Med. Phys.* **10**, 395-409 (1983a).

Awschalom, M., Rosenberg, I., and Ten Haken, R.K., "A New Look at Displacement Factor and Point of Measurement Corrections in Ionization Chamber Dosimetry," *Med. Phys.* **10**, 307 (1983b).

Bewley, D.K., McNally, N.J., and Page, B.C., "Effects of the Secondary Charged Particle Spectrum on Cellular Response to Fast Neutrons," *Radiat. Res.* **58**, 111-121 (1974).

Brede, H.J., Schlegel-Bickmann, D., Dietze, G., Daures-Caumes, J., and Ostrowsky, A., "Determination of Absorbed Dose Within an A150 Plastic Phantom for a d(13.5 MeV)+Be Neutron Source," *Phys. Med. Biol.* **33**, 413-426 (1988).

Brenner, D., Private Communication (1991).

Broerse, J.J., Barendsen, G.W., and Kersen G.R. van, "Survival of Cultured Human Cells After Irradiation with Fast Neutrons of Different Energies in Hypoxic and Oxygenated Conditions," *Int. J. Radiat. Biol.* **13**, 559-572 (1968).

Broerse, J.J. and Zoetelief, J., "Dosimetric Aspects of Fast Neutron Irradiations of Cells Cultured in Monolayer," *Int. J. Radiat. Biol.* **33**, 383-385 (1978).

Broerse, J.J., Burger, G., and Coppola, M. (eds.), *A European Neutron Dosimetry Intercomparison Project (ENDIP). Results and Evaluation,* Publication EUR-6004 of the Commission of the European Communities, Brussels-Luxembourg, (1978).

Broerse, J.J., Mijnheer, B.J., Eenmaa, J., and Wootton, P., "Dosimetry Intercomparisons and Protocols for Therapeutic Applications of Fast Neutron Beams," In: *High-LET Radiations in Clinical Radiotherapy,* G.W. Barendsen, J.J. Broerse, and K. Breur (eds.), pp. 117-123, Pergamon Press, Oxford (1979).

Broerse, J.J. (ed.), *Ion Chambers for Neutron Dosimetry*, EUR-6782, Harwood Academic Publishers, London (1980).

Broerse, J.J., Mijnheer, B.J., and Williams, J.R., "European Protocol for Neutron Dosimetry for External Beam Therapy," *Brit. J. Radiol.* **54**, 882-898 (1981).

Broerse, J.J. and Dennis, J.A., "Dosimetric Aspects of Exposure of the Population to Ionizing Radiation," *Int. J. Radiat. Biol.* **57**, 633-645 (1990).

Caswell, R.S., Coyne, J.J., and Randolph, M.L., "'Kerma Factors for Neutron Energies Below 30 MeV," *Radiat. Res.* **82**, 217-254 (1980).

Caswell, R.S., Coyne, J.J., and Randolph, M.L., "Kerma Factors of Elements and Compounds for Neutron Energies Below 30 MeV," *Int. J. Appl. Radiat. Isot.* **33**, 1227 (1982).

Caswell, R.S., Coyne, J.J., Gerstenberg, H.M., and Axton, E.J., "Basic Data Necessary for Neutron Dosimetry," *Radiat. Prot. Dosimetry*, **23**, 11-17 (1988).

Caumes, J., Ostrowsky, A., Steinschaden, K., Mancaux, M., Cance, M., Simoen, J.P., Sabattier, R. and Breteau, N., "Direct Calibration of Ionization Chambers with a TE Calorimeter at the Orléans Cyclotron Neutron Facility," *Strahlenth. Onk.* **160**, 127 (1984).

Frigerio, N.A., Coley, R.F., and Sampson, M.J., "Depth Dose Determinations. I. Tissue-equivalent Liquids for Standard Man and Muscle," *Phys. Med. Biol.* **17**, 792 (1972).

Goodman, L.J., "A Modified Tissue Equivalent Liquid," *Health Phys.* **16**, 763 (1969).

Goodman, L.J. and Coyne, J.J., "W_n and Neutron Kerma for Methane-based Tissue Equvialent Gas," *Radiat. Res.* **82**, 13-26 (1980).

Howerton, R.J., *Calculated Neutron Kerma Factors Based on the LLNL ENDL Data File*, UCRL-50400, Vol. 27, Rev. 1 (1991).

ICRP59 International Commission on Radiological Protection, *Report of Committee II on Permissible Dose for Internal Radiation*, ICRP Publication 2 (Pergamon Press, New York) (1959).

International Commission on Radiological Protection, *Reference Man: Anatomical, Physiological, & Metabolic Characteristics*, ICRP Report 23, (Pergamon Press, Oxford) (1975).

International Commission on Radiation Units and Measurements, *Physical Aspects of Radiation*, ICRU Report 10b, published as National Bureau of Standards Handbook 85 (International Commission on Radiation Units and Measurements, Bethesda, MD) (1964).

International Commission on Radiation Units and Measurements, *Neutron Dosimetry for Biology and Medicine*, Report 26 (International Commission on Radiation Units and Measurements, Washington, DC) (1977).

International Commission on Radiation Units and Measurements, *An International Neutron Dosimetry Intercomparison,* Report 27 (International Commission on Radiation Units and Measurements, Washington, DC) (1978).

International Commission on Radiation Units and Measurements, *Stopping Powers for Electron Beams with Energies Between 1 and 50,* Report 37 (International Commission on Radiation Units and Measurements, Bethesda, MD) (1984).

International Commission on Radiation Units and Measurements, *Tissue Substitutes in Radiation Dosimetry and Measurement,* Report 44 (International Commission on Radiation Units and Measurements, Bethesda, MD) (1989a).

International Commission on Radiation Units and Measurements, *Clinical Neutron Dosimetry. Part I.: Determination of Absorbed Dose in a Patient Treated by External Beams of Fast Neutrons,* Report 45 (International Commission on Radiation Units and Measurements, Bethesda, MD) (1989b).

Ito, A., "Neutron Dosimetry Intercomparison between Japan (Univ. of Tokyo) and USA," In: *Proc. Third Symposium on Neutron Dosimetry in Biology and Medicine,* EUR 5848, G. Burger and H.G. Ebert (eds.) (Commission of the European Communities, Brussels, Luxembourg) (1978).

Lewis, V.E., *Neutron Dosimetry Intercomparison at the National Physical Laboratory,* NPL Report RS (EXT) 79 (National Physical Laboratory, Teddington, Middlesex, UK) (1985).

McDonald, J.C., Ma, I.-C., Ling, J., Eenmaa, J., Awschalom, M., Smathers, J.B., Graves, R., August, L.S., and Shapiro, P., "Calorimetric and Ionimetric Dosimetry Intercomparisons. I. US Neutron Radiotherapy Centers," *Med. Phys.* **8**, 39 (1981a).

McDonald, J.C., MA., I.-C., Mijnheer, B.J., and Zoetelief, J., "Calometric and Ionometric Dosimetry Intercomparisons. II: d+T Neutron Source at the Antoni van Leeuwenhoek Hospital," *Med. Phys.* **8**, 44 (1981b).

McDonald, J.C. and Cummings, F.M., "Calorimetric Measurements of Carbon and A-150 Plastic Kerma Factors for 14.6 MeV Neutrons," *Radiat. Prot. Dosimetry* **23**, 31-33 (1988).

Mijnheer, B.J. and Williams, J.R. "Calibration Procedures of Tissue-equivalent Ionization Chambers Used in Neutron Dosimetry," In: *Advances in Dosimetry for Fast Neutrons and Heavy Charged Particles for Therapy Applications,* pp. 127-139 (International Atomic Energy Agency, Vienna) (1984).

Mijnheer, B.J., "Protocols for the Determination of Absorbed Dose in Patients Irradiated by Beams of Nuclear Particles in Radiotherapy Procedures," In: *Proc. of an Advisory Group Meeting, Rijswijk,* pp. 141-154 (International Atomic Energy Agency, Vienna) (1987).

Mijnheer, B.J., Wootton, P., Williams, J.R., Eenmaa, J., and Parnell, C.J., "Uniformity in Dosimetry Protocols for Therapeutic Applications of Fast Neutron Beams," *Med. Phys.* **14**, 1020-1026 (1987).

Mijnheer, B.J., "Clinical Dosimetry of High Energy Neutron Beams: Future Developments," *Radiat. Prot. Dosimetry* **23**, 373-380 (1988).

Pihet, P., Meulders, J.P., Octave-Prignot, M., Vynckier, S., and Wambersie, A., "Gamma Contribution to the Total Absorbed Dose in the d(50)-Be and p(65)-Be Therapeutic Neutron Beams at 'Cyclone'," *J. Eur. Radiother.* **3**, 121 (1982).

Rossi, H.H. and Failla, G., "Tissue-equivalent Ionization Chambers," *Nucleonics* **14**, 32 (1956).

Shapiro, P., Attix, F.H., August, L.S., Theus, R.B., and Rogers, C.C., "Displacement Correction Factor for Fast-neutron Dosimetry in a Tissue-equivalent Phantom," *Med. Phys.* **3**, 87-90 (1976).

Smathers, J.B., Otte, V.A., Smith, A.R., Almond, P.R., Attix, F.H., Spokas, J.J., Quam, W.M., and Goodman, L.J., "Composition of A-150 Tissue Equivalent Plastic," *Med. Phys.* **4**, 74 (1975).

Srdoc, D., "Experimental Technique of Measurement of Microscopic Energy Depositions in Irradiated Matter Using Rossi Counters," *Radiat. Res.* **43**, 302 (1970).

White, R.M., Broerse, J.J., DeLuca, P.M. Jr., Dietze, G., Haight, R.C., Kawashima, K., Menzel, H.G., Olsson, N., and Wambersie, A., "Status of Nuclear Data for Use in Neutron Therapy", *Rad. Prot. Dos.* **44**, 11 (1992).

Williams, J.R., Mijnheer, J., Rassow, J., Meissner, P., and Hensley, F., "A Small Scale Neutron Dosimetry Intercomparison Between Essen, Amsterdam and Edinburgh," *Strahlenth. Onk.* **157**, 245 (1981).

Zoetelief, J., Engels, A.C., and Broerse, J.J., "Effective Measuring Point of Ion Chambers for Photon Dosimetry in Phantoms," *Brit. J. Radiol.* **53**, 580-583 (1980a).[2ex] Zoetelief, J., Engels, A.C., Broerse, J.J., and Mijnheer, B.J., "Effect of Finite Size of Ion Chambers Used for Neutron Dosimetry," *Phys. Med. Biol.* **25**, 1121-1131 (1980b).

Zoetelief, J., Engels, A.C., and Broerse, J.J., "Displacement Corrections for Spherical Ion Chambers in Phantoms Irradiated With Neutron and Photon Beams," In: *Biomedical Dosimetry: Physical Aspects, Instrumentation, Calibration*, pp. 125-138 (International Atomic Energy Agency and The World Health Organization, Vienna) (1981).

Zoetelief, J. and Schraube, H., "Experimental Procedures for the On-site Neutron Dosimetry Intercomparison," In: *Proc. Fifth Symp. on Neutron Dosimetry*, Schraube, H., Burger, G., and Booz, J. (eds.), ENDIP-2, pp. 1179-1190, Eur 9762 (Commission of the European Communities, Luxembourg) (1985).

Zoetelief, J., Schlegel-Bickmann, D., Schraube, H. and Dietze, G., "Characteristics of Mg/Ar Ionization Chambers Used as Gamma-ray Dosimeters in Mixed Neutron-photon Fields," *Phys. Med. Biol.* **31**, 1339-1351 (1986).

4 ^{9}Be(p,n) Neutron Source Reaction for Radiotherapy

4.1 Introduction

The data needs for neutron source reactions have been discussed by Chaudri (1987) and the neutron energy spectra have been treated by Bewley (1987). The general characteristics which make a source and its resulting neutron beam properties suitable for cancer therapy are outlined in a review paper by Cross (1978).

Of the seventeen centers throughout the world that are routinely applying fast neutron therapy, the majority of new facilities use the $^9Be(p,n)$ reaction as the source of high energy neutrons. There are several reasons for this choice with the most important being that high-energy protons give a much harder spectrum of neutrons than for deuterons of the same energy and the low-energy neutron tail of the $^9Be(p,n)$ reaction can be significantly suppressed with filters. Therefore, this section concentrates exclusively on the high-energy ($E_p \geq 20$ MeV) $^9Be(p,n)$ reaction, with emphasis on the microscopic (thin-target) nature of the reaction cross section and its connection to the nuclear structure of the reaction residual ^9B. Note: The reaction $^9Be(p,n)$ for an incident proton energy of 60 MeV is commonly represented as p(60)Be in medical physics literature.

In the following sections, a description of the high-energy shape of the $^9Be(p,n)$ neutron emission spectrum will be given from a nuclear structure standpoint. The microscopic data which have been measured will be discussed along with the difficulties encountered in attempting to carry out an evaluation of $^9Be(p,n)$ with currently available thin-target data. A description of the minimum microscopic measurements needed for an acceptable evaluation of this reaction is then given along with the procedure for calculating thick-target yields. A characterization of thick-target yields is presented as well as a discussion of how microscopic differential cross sections could improve our knowledge of these yields.

4.2 Physics of the ^{9}Be(p,n) Reaction

The (p,n) reaction has been known for many years to exhibit a complex spectrum in the emerging neutrons at essentially all proton energies. However, for certain reactions, e.g., ^9Be, at or near 0° and at proton energies greater than 20 MeV, certain features emerge at the highest neutron emission energies. These features have simple explanations as well as important ramifications for the production of high energy neutrons. To understand why the high-energy neutron spectrum for $^9Be(p,n)$ reaction behaves the way it does, it is useful to begin with an analogous reaction. Consider the reaction $^{13}C(p,n)^{13}N$, i.e., the (p,n) reaction leading from the ground state of ^{13}C to the ground state of ^{13}N. This reaction joins two nuclear states that are mirrors of each other. This is something like having a collection of spinning tops, some of them up and some of them down. Reversing the spins gives back the same system, except for a mirror reflection. Hence the term mirror nuclei, although the spins in this case are called isospin and this reversal represents charge-exchange.

The $^{13}C(p,n)^{13}N$ reaction is a very close analog of the inverse decay process $^{13}N \rightarrow {}^{13}C + e^+ + \nu$, i.e., the so-called superallowed beta decay of ^{13}N. There are two parts to this interaction, namely the Fermi part and the Gamow-Teller part. The operator producing the mirror transition described above, i.e., the charge exchange,
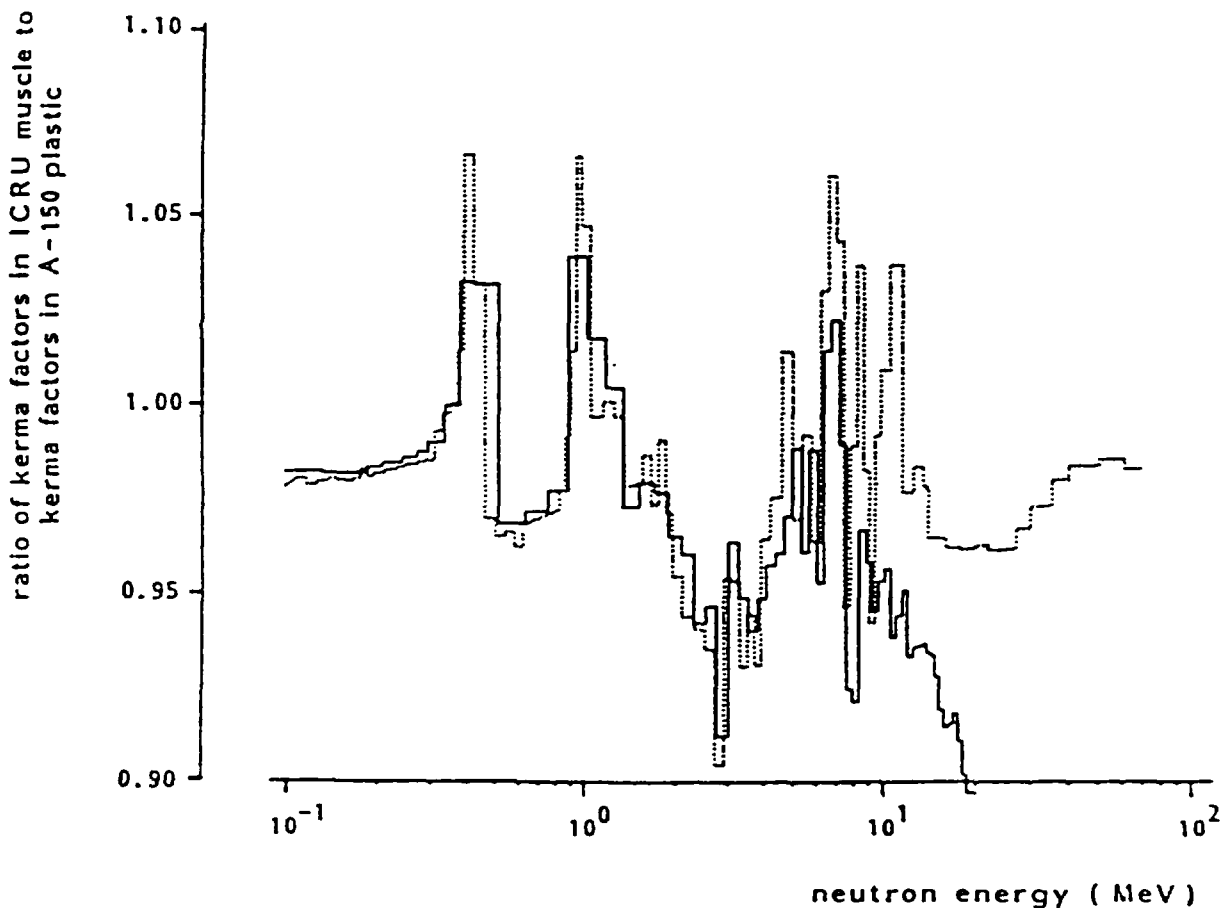
Figure 12: Ratio of kerma in ICRU muscle tissue to kerma in A-150 as a function of neutron energy on a logarithmic scale. The solid line represents the calculations of Howerton (1991), the dashed line is based on the calculations of Caswell *et al.* (1980) up to 15 MeV, and on calculations of Brenner (1991) for the energy range 15-70 MeV.

is the Fermi part of the interaction and, whenever such a transition is possible, the probability for the reaction is particularly strong, either in beta-decay or in a nuclear reaction like (p,n). Similar to the Fermi part of the interaction, the Gamow-Teller part can also lead to a strong transition. In this case, flipping the isospin (charge), and, in addition, the intrinsic spin, gives back the same nucleus, except mirrored in *both* charge and spin space. ^{13}C and ^{13}N can be related in precisely this way and thus both the decay of ^{13}N and the inverse reaction $^{13}C(p,n)^{13}N$ will be very strong due to the double possibility of going either via pure charge exchange or charge exchange plus spin flip.

In the $^{9}Be(p,n)^{9}B$ reaction, the same considerations obviously apply in going to the ground state. Just as in the ^{13}C reaction, excited states in ^{9}B can be accessed via the Gamow-Teller interaction but, in the ^{9}Be case, the inverse beta decay is unobservable because ^{9}B is particle unstable. We are confident that if it could be observed, it would be just as strong as the decay of ^{13}N. Like $^{13}C(p,n)$ and $^{9}Be(p,n)$ reactions, $^{7}Li(p,n)$ is another reaction in which the Fermi and Gamow-Teller transitions predominately affect the high-energy 0° neutron emission spectrum. ^{9}Be is the preferred target because of the difficulty involved in preparing a ^{7}Li target and the expense involved in making a ^{13}C target.
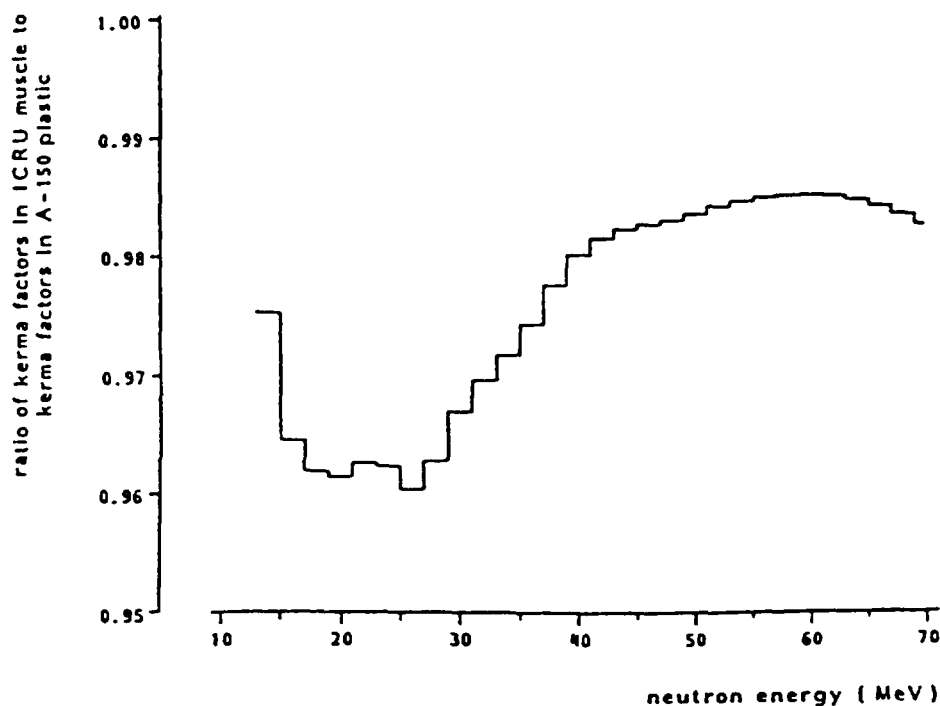
Figure 13: Ratio of kerma in ICRU muscle tissue to kerma in A-150 plastic as a function of neutron energy on a linear scale (Brenner, 1991).

In Figure 14, the very strong (p,n) reaction can be clearly seen in the neutron emission spectra at and near 0° to the ground state and the first few excited states of ^9B resulting from the $^9Be(p,n)^9B$ reaction at an incident proton energy of 135 MeV (Pugh, 1985). The data in this figure show that both the Fermi and Gamow-Teller interactions play crucial roles in the high-energy neutron production from the $^9Be(p,n)^9B$ reaction through both the dramatic forward-peaking of the high-energy part of the spectrum and how greatly it decreases with angle. From kinematics, the peaks at 9° and 12° should be shifted down in energy by 0.4 and 0.75 MeV, respectively, but their energy scales have been adjusted to correspond to the 0° peak for clarity.   Figure 15 shows the same information as Figure 14, but only for the first and higher excited states and on a scale which shows what happens to the relatively flat continuum behind the clearly-resolved excited states as a function of angle from 0° to 12°.

The energy levels (excited states) for ^9B are shown in Figure 16 and are taken from the latest compilation of Ajzenberg-Selove (1984).   The parentheses in Figure 16 indicate uncertainty in the assigned energy or spin and parity. The correspondence of states in ^9B with states in the mirror nucleus ^9Be is very good. Based on the ^9Be energy levels, the spins and parities of the ^9B levels at 1.6, 2.788, and 4.8 MeV are probably $1/2^+$, $5/2^+$, and $(3/2)^+$, respectively. Around 2.75 MeV, there is evidence for an additional broad state of width greater than 1 MeV. This is based on the broad $1/2^-$ state seen in ^9Be and the recent work of Pugh (1985) who observed a very broad state (width of 3.1 MeV) at 2.75 MeV in the analysis of $^9Be(p,n)^9B$
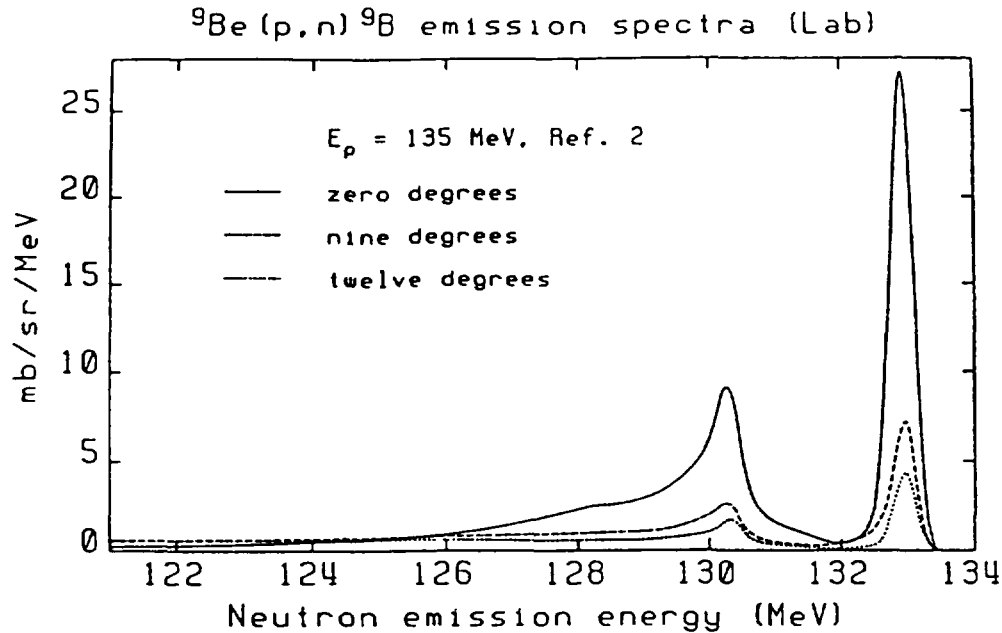
Figure 14: Measurement of the $^9Be(p,n)^9B$ neutron emission spectra for 135 MeV incident protons at angles of 0, 9, and 12 degrees from Pugh (1985). The data in this figure show that both the Fermi and Gamow-Teller interactions play crucial roles in the high-energy neutron production from the $^9Be(p,n)^9B$ reaction through both the dramatic forward-peaking of the high-energy part of the spectrum and how greatly it decreases with angle. The energy scales of the 9° and 12° spectra have been adjusted to correspond to the 0° peak for clarity.

data at $E_p = 135$ MeV. His analysis is shown in Figure 17 and illustrates why the structure of the reaction residual, ^9B, is important in the production of high energy neutrons at 0°. The relatively flat continuum of neutrons seen in Figure 14 extends downward to a few MeV and represents reactions to the higher (continuum) levels of ^9B. For energetic protons incident on ^9Be, there are other reactions which can lead to the production of neutrons. However, these reactions involve 3-body (or more) final states. As a result, the neutrons from these reactions will only contribute to the low-energy tail of the emission spectrum.

4.3 Cross Section Data for the ^{9}Be(p,n) Reaction

Allab (1984) completed an extensive survey of measurements of neutron energy spectra and angular distributions from the $^9Be(p,n)$ reaction for fast neutron radiotherapy. It follows the earlier work of Cross (1978). A scan of the literature since that time has uncovered only one new double-differential, high-energy cross section measurement (Pugh, 1985). Microscopic (or thin-target) angular distribution measurements (Bentley, 1972; Clough, 1970; Goodman, 1980; Pugh, 1985) of the $^9Be(p,n)^9B$ reaction to the ground state of ^9B are shown in Figure 18 in the center-of-mass frame. The experimental data have been smoothed and plotted as lines on the same scale for comparison purposes.   As a general trend, the angular distributions become more forward-peaked for higher incident proton energies. The differences in the 0° cross sections at 120 and 135 MeV are large and may be indicative of difficulties in
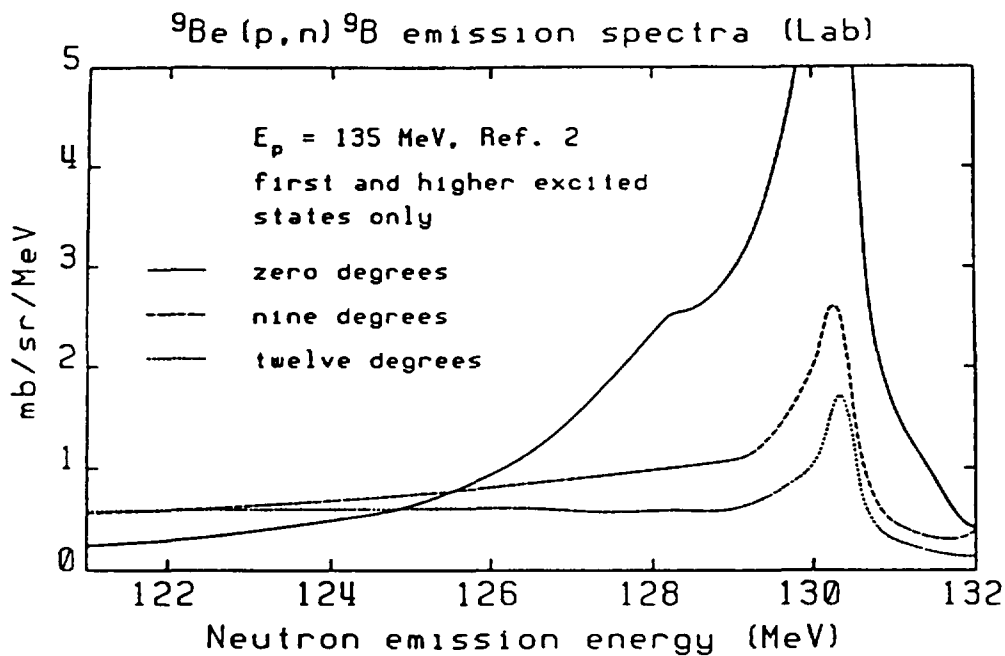
Figure 15: The same data as in Figure 14 but only for the first and higher excited states and on a scale which shows what happens to the (essentially) flat high-energy continuum behind the clearly resolved excited states as a function of angle 0° to 12°.
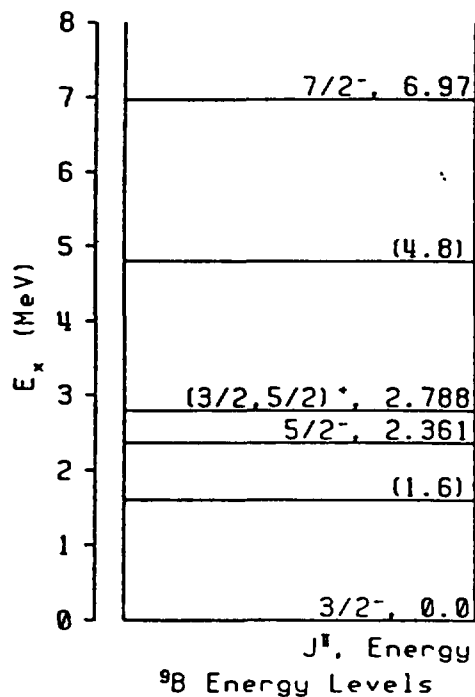
Figure 16: The energy levels (excited states) for ^9B taken from the latest compilation of Ajzenberg-Selove (1984). The parentheses indicate uncertainty in the assigned energy or spin and parity. The correspondence of states in ^9B with states in the mirror ^9Be is very good. Based on the ^9Be energy levels, the spins and parities of the ^9B at 1.6, 2.788, and 4.8 MeV are probably $1/2^+$, $5/2^+$, and $(3/2)^+$, respectively. Around 2.75 MeV, there is evidence for an additional broad state of width greater than 1 MeV.

$^9Be(p,n)\,^9B$ emission spectra (Lab)
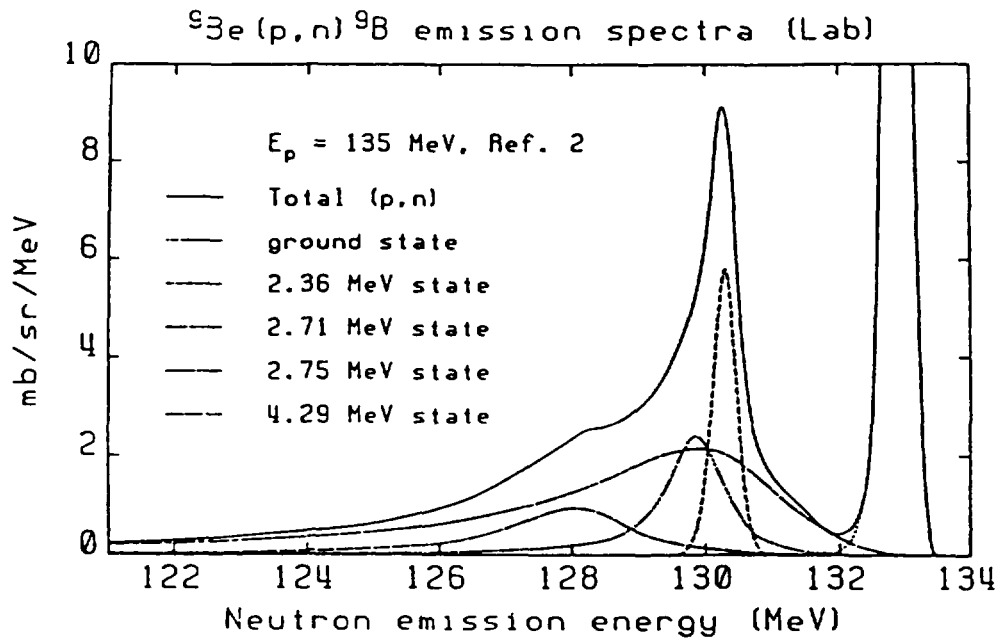
Figure 17: Analysis of the ground state and first few excited states of ^9B from the recent $^9Be(p,n)^9B$ work of Pugh (1985). His analysis illustrates why the structure of the reaction residual, ^9B is important in the production of high energy neutrons at $0°$.

$^9Be(p,n)\,^9B$ g.s. angular distributions
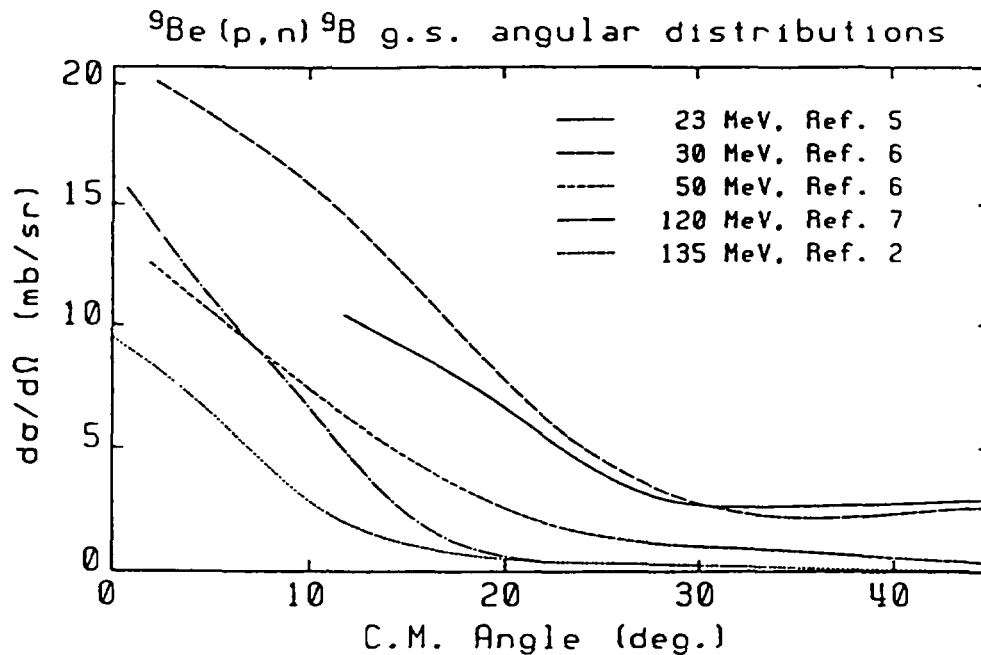
Figure 18: Microscopic (or thin-target) angular distribution measurements of the $^9Be(p,n)^9B$ reaction to the ground state of ^9B are plotted in the center-of-mass frame. The experimental data have been smoothed and plotted as lines on the same scale for comparison purposes. As a general trend, the angular distributions become more forward-peaked for higher incident proton energies. The differences in the $0°$ cross sections at 120 and 135 MeV are large and may be indicative of the uncertainties in one or both measurements at these high energies.

one or both measurements at these energies. There are significant differences (not shown in this paper) in systematics of all of these measurements between the ratios of cross sections to the ground state and first excited state (2.36 MeV) with increasing incident proton energy. The high-energy end of the emission spectra from the $^9Be(p,n)^9B$ reaction at 0° in the laboratory frame are compared in Figure 19 for proton energies of 30, 50, and 135 MeV. In this figure the energy scales have been adjusted so that the high energy peaks all coincide. The laboratory energy of a point on a specific emission spectrum is obtained by [E_p + Q + the value on the x-axis] (Q = -1.85 MeV for $^9Be(p,n)^9B$). The cross section to the ground state is obtained by integrating the area under the ground-state peak. The values given in Figure 19 are taken from the respective references and indicate the expected trend in the cross section. Because the data of Pugh (1985) were presented graphically as counts vs. excitation energy (in ^9B), we used their 0° center-of-mass cross section value (9.52 mb/sr) and a digitizing program to convert their data to mb·sr^{-1}·M The difference in resolution between these measurements is obvious. This figure demonstrates the importance of carefully determining and specifying the resolution function in this kind of measurement if a data evaluator is to provide interpolated results at energies other than those given here. Also critical to this process is the necessity of the experimenter to understand the efficiency, as a function of neutron energy, of the neutron detector used to measure neutrons at these high energies. Not shown in Figure 19 is a neutron energy spectrum measured at 0° for E_p = 39.3 MeV by Jungerman (1971). His work also included measurements for E_p = 29.4 and 50.6 MeV. The ground state cross sections from his work at 0° were revised by Romero (1976) as follows: E_p = 29.4
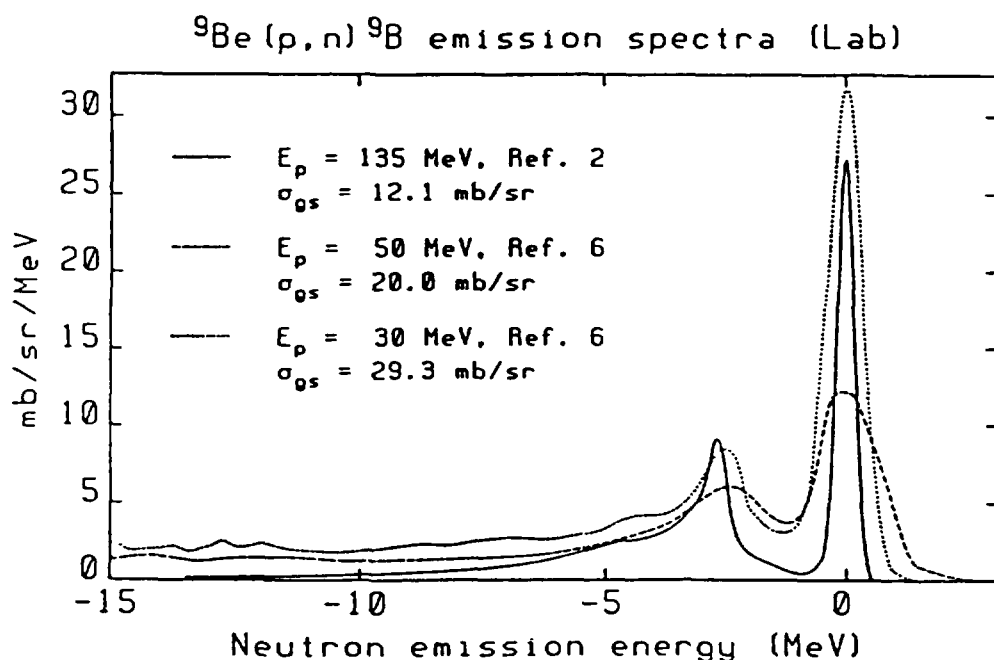
Figure 19: Comparison of the neutron emission spectra from the $^9Be(p,n)^9B$ reaction at 0° in the laboratory frame for proton energies of 30, 50, and 135 MeV. In this figure the energy scales have been adjusted so that the high energy peaks coincide. The cross sections to the ground states are obtained by integrating the area under the ground-state peaks. Note that the measurements were made with different resolutions.

MeV, $\sigma_{g.s.} = 30.0\pm3.0$ mb/sr (-9.6%); $E_p = 39.2$ MeV, $\sigma_{g.s} = 28.8\pm3.0$ mb/sr (-8.6%); and $E_p = 50.6$ MeV, $\sigma_{g.s.} = 24.5\pm2.6$ mb/sr (-2.8%). The numbers in parentheses indicate the percent change in the values from Jungerman (1971). The data shown in Figures 14, 18, and 19 and contained in Pugh (1985), Bentley (1972), Clough (1970), Goodman (1980), Batty (1969), Jungerman (1971), and Romero (1976) comprise all the microscopic (thin-target) data known to us and are not adequate to perform an acceptable evaluation of the $^9Be(p,n)$ reaction.

4.4   Data Needed for Evaluation of the ^{9}Be(p,n) Reaction

For both technical and economic reasons, an experimental database needs to be established for the $^9Be(p,n)$ reaction which is sufficient to carry out an evaluation that will allow the accurate calculation of thick-target yields for any target thickness both on- and off-axis. Unfortunately, medical accelerator facilities are frequently not suitable for these kinds of measurements because the optimal path length from source to patient ($\sim$1.25 meters) is too short to provide the needed energy resolution for time-of-flight techniques. One facility possessing the capability for these kinds of measurements is the Indiana University Cyclotron Facility (IUCF). The work of Pugh (1985) shown in Figures 14, 15, 17, 18, and 19 represents exactly the kind of double-differential measurements required for the present problem. A recent work by Trabandt (1989) also performed at IUCF measured double-differential cross sections for the ^{7}Li(p,n) and ^{13}C(p,n) reactions, as well as the (p,n) reactions on many other targets, at incident proton energies of 80.5 and 160.3 MeV at up to 11 emission angles from $0°$ to $144°$. Because of the experimental capabilities at IUCF, including flight paths to 60 meters, energy resolutions of $\sim$1 MeV at forward angles and a few MeV in the backward angles were obtained. It is unfortunate for the present purposes that ^9Be was not included in these measurements.

At least four facilities around the world are presently using p(60, 62, or 66)Be for neuton therapy purposes. To carry out an adequate evaluation of the $^9Be(p,n)$ reaction so that thick-target yields can be reliably calculated, double-differential cross section measurements are needed at incident proton energies of 25, 50, 75, and 100 MeV, and at a minimum of six angles from 0 to $50°$ and one back angle for each of these energies. While the thick-target yield is a two-dimensional problem, the most important computations needed is in the forward direction. The measurements are needed at the energies specified so that the systematics of the reaction with energy can be reasonably established. The 6 angles are required so that systematics of the angular dependence of the spectrum can be established. The determination of the entire neutron emission spectrum at a particular forward angle requires a large dynamic range for the neutron detector. However, for a given incident energy and angle, it is critical to obtain the correct shape and magnitude of the spectrum to as low a neutron emission energy as possible. New techniques now allow neutron detectors to span most of the dynamic range necessary for these measurements. If such measurements are to be carried out, it is essential that during the experiment at least one thick-target measurement be made at $0°$ for each incident proton energy using the same detector arrangement as in the thin-target measurements. This measurement would circumvent many resolution difficulties, etc., and would provide an excellent benchmark for testing the calculation of thick-target yields from microscopic differential cross sections as described in the following section.

4.5   Procedure for Calculating Thick-Target Yields

In this section, a discussion of the procedure for making thick-target yield calculations is presented. Because the source-to-patient distance is $\sim$1 meter and the area of the patient to be irradiated may exceed 10×10 cm^2, a two-dimensional calculation is needed. For simplicity, we will consider the procedure for a one-dimensional calculation, which can then be extended to two dimensions in a straightforward manner.

The thick-target yield of neutrons produced when a beam of protons is incident upon a slab of Be can be simulated using one-dimensional Monte Carlo particle-tracking techniques. The Be is assumed to be thick to protons and (relatively) thin to neutrons and is initially divided into equally spaced zones which are picked thin enough to allow accurate dE/dx determination. Tracking is initiated by selecting a proton with a specific incident energy. Three distances are then calculated: *a)* the maximum distance that the proton can travel before dE/dx losses take the proton below some minimum energy (using stopping powers and media density), *b)* the distance to the next zone (as specified in problem input), and *c)* the distance to a nuclear collision (determined by a random number between 0 and 1 and the total proton *nuclear* cross section). If the shortest distance is *a*, the tracking of this proton is stopped and a new proton at the specified incident energy is tracked through the Be. If *b* or *c* is the shortest distance, the proton's new energy is calculated taking into account the dE/dx loss over the distance. For this new energy, the cross section for producing a neutron, *i.e.*, (p,n), is divided by the total proton cross section. This ratio is compared to a random number between 0 and 1 to determine whether a neutron is produced. If it is not, the tracking of the proton continues. Otherwise, using a random number between 0 and 1 and the angular dependence of the (p,n) reaction, the angle at which the neutron is produced is determined. Since a one-dimensional problem has been assumed, if the angle is not within some predetermined small forward angle, the neutron is considered to be taken out of the forward beam. If the angle is within the small-angle limit, the energy of the neutron is calculated for the given angle but then the neutron is assumed to travel in the forward direction. The neutron is then tracked until there is a reaction which removes the neutron or the neutron escapes from the Be and is tallied.

In the foregoing discussion, several issues become clear. First, the total nuclear proton cross section is needed, but at these energies a reasonable approximation can be obtained from a proton optical model. Also, it is assumed that all other reactions from p+^{9}Be are not important in producing high-energy neutrons, but they most certainly will be important in producing neutrons in the low-energy tail. Having good high-energy (p,n) data will allow the accurate calculation of the higher-energy portion of the thick-target yields. In therapy applications, it is assumed that the low-energy tail will be largely removed by filters before the collimator. Recent measurements of the high-energy n+^{9}Be total cross section from 5 to 550 MeV have been carried out at the Los Alamos National Laboratory (Finlay, 1991). These data are essential for determining the attenuation of the neutrons produced by the $^9Be(p,n)$ reaction in the target. It should be noted that experimental data do not exist above 20 MeV to track secondary neutrons produced by the ^9Be(n,2n) reaction and this is important to the extent that the Be target is not "thin" to neutrons. After thick-target yields are calculated, they can be compared with a number of published thick-target measurements (see Allab, 1984, and references contained therein).
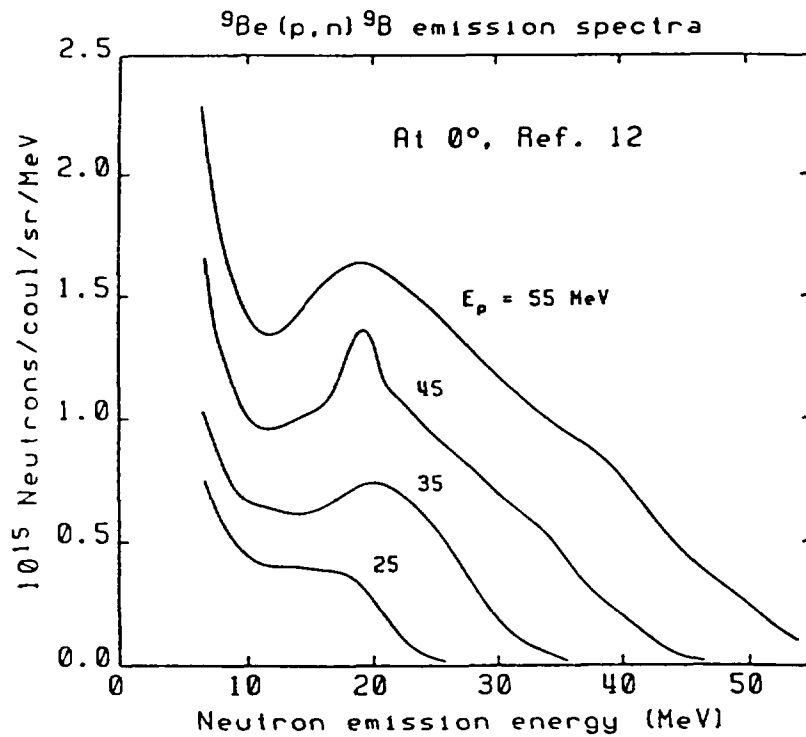
Figure 20: Representative $^9Be(p, n)$ thick-target emission spectra from the work of Johnsen (1977) at 0° for $E_p = 25, 35, 45,$ and 55 MeV. These data show a large low-energy component and a higher-energy component peaking at ~20 MeV.
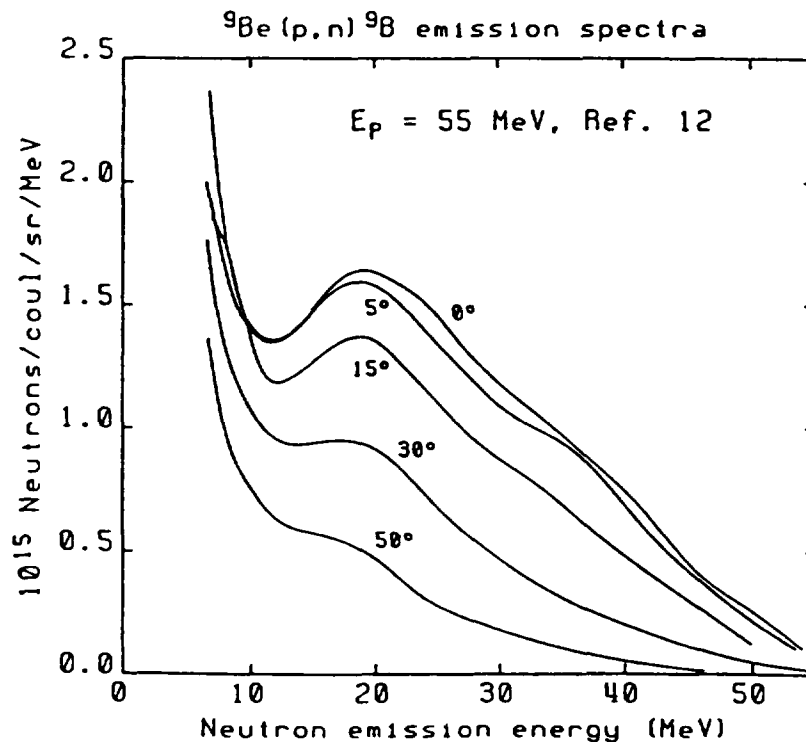
Figure 21: Representative $^9Be(p, n)$ thick-target emission spectra from Johnsen (1977) for a fixed proton energy of 55 MeV at angles ranging from 0° to 50°. The large low-energy component is evident at all angles and the peaking at ~20 MeV seen in Figure 20 and forward angles becomes less pronounced at larger angles.

64

4.6   Thick-Target Yield Characterization

Representative $^9Be(p,n)$ thick-target emission spectra from the work of Johnsen (1977) at $0°$ for E_p = 25, 35, 45, and 55 MeV are shown in Figure 20. These data show a large low-energy component along with a high-energy component peaking at $\sim$20 MeV.   Also from Johnsen (1977) and for a fixed proton energy of 55 MeV, neutron emission spectra are shown in Figure 21 at angles ranging from $0°$ to $50°$. In this figure, the large, low-energy component is evident at all angles and the peaking at $\sim$20 MeV seen in Figure 20 at $0°$ becomes less pronounced at larger angles. Considering what is known from thin-target yields, and from the fact that the protons are continually slowing down in the thick targets due to dE/dx loss, one may qualitatively understand the gross structure of these curves. A measurement of the microscopic cross sections of $^9Be(p,n)$ as discussed earlier, when coupled with a complete evaluation, and the Monte Carlo method described in the preceeding section, would allow the calculation of the thick-target yield for any reasonable thickness. This approach would greatly simplify the target design for hospital-based cyclotrons and improve the characterization of the resulting neutron beam for use in neutron radiotherapy.

References

Ajzenberg-Selove, F., "Energy Levels of Light Nuclei A = 5-10," *Nucl. Phys. A* **413**, 124 (1984).

Allab, M., "A Survey of Neutron Energy Spectra and Angular Distributions of the $^9Be(p,n)^9B$ Reaction for Fast Neutron Radiotherapy," IAEA Report INDC(NDS)-153/L (1984).

Batty, C.J., Bonner, B.E., Kilvington, A.I., Tschalär, C., Williams, L.E., and Clough, A.S. "Intermediate Energy Neutron Sources," *Nucl. Instr. Methods* **68**, 273 (1969).

Bentley, R.D., Ph.D. Thesis, University of Colorado, Dept. of Physics and Astrophysics (1972).

Bewley, D.K., "Neutron Energy Spectra and their Implications," In: *Proc. Advisory Group Mtg. on Nuclear and Atomic Data for Radiotherapy and Related Radiobiology*, International Atomic Energy Agency, Vienna, 129 (1987).

Chaudri87 Chaudri, M.A., "Production of Fast Neutron Beams for Therapy," In: *Proc. Advisory Group Mtg. on Nuclear and Atomic Data for Radiotherapy and Related Radiobiology*, International Atomic Energy Agency, Vienna, 155 (1987).

Clough, A.S., Batty, C.J., Bonner, B.E., and Williams, L.E., "A Microscopic Analysis of the (p,n) Reaction on 1p-Shell Nuclei," *Nucl. Phys. A* **143**, 385 (1970).

Cross, W.G., "Nuclear Data for Radiotherapy with Neutrons," In: *Proc. Int. Conf. on Neutron Physics and Nuclear Data for Reactors and other Applied Purposes*, Harwell, U.K., September 1978, 648 (1978).

Finlay, R.W., Fink, G., Abfalterer, W., Lisowski, P., Morgan, G.L., and Haight, R.C., "Neutron Cross Sections at Intermediate Energy," In: *Proc. Int. Conf. on Nuclear Data for Science and Technology*, Jülich, May 13-17, 1991, p. 720, S.M. Qaim (ed.) (1992).

Goodman, C.D., Austin, S.M., Bloom, S.D., Rapaport, J., and Satchler, G.R., "The (p,n) Reaction and the Nucleon-Nucleon Force," Plenum Publishing Corp., New York, 149 (1980).

Johnsen, S.W., "Proton-beryllium Neutron Production at 25-55 MeV," *Med. Phys.* 4, 255 (1977).

Jungerman, J.A., Brady, F.P., Knox, W.J., Montgomery, T., McGie, M.R., Romero,

J.L., and Ishizaki, Y., "Production of Medium-Energy Neutrons from Proton Bombardment of Light Elements," *Nucl. Instr. Methods* 94, 421 (1971).

Pugh, Jr., B.G., "The (p,n) Reaction on ^9Be and ^{17}O at 135 MeV," Ph.D. Thesis, Massachusetts Institute of Technology (1985).

Romero, J.L., Brady, F.P., and Jungerman, J.A., "Production of Medium-Energy Neutrons from Proton Bombardment of Light Elements Using Revised Neutron-Proton Differential Cross Sections," *Nucl. Instr. Methods* 134, 537 (1976).

Trabandt, M., "Pre-compound Reactions with 80-160 MeV Projectiles," Ph.D. Thesis, University of Hamburg (1989).

5 Collimation and Shielding

5.1 Introduction

The subjects of this section are the uses and needs of nuclear data to optimize the design of collimators and shields. Neutrons for radiotherapy are produced by nuclear reactions such as p+Be. The neutrons emitted are broadly distributed in energy and angle of emission relative to the initial charged-particle beam. To localize these neutrons to the therapy volume, a collimator is placed between the source and the patient. Additional shielding is used in order to protect other parts of the patient and to confine radiation to the therapy room.

For modern neutron therapy facilities (other than those using boron-neutron therapy), sources producing neutrons in the 20-100 MeV range are employed. These energies are chosen for better penetration and because (n,α) reactions on carbon, nitrogen, and oxygen are more probable than at lower energies. The resulting alpha particles have a high LET, which is advantageous in killing slow-growing, hypoxic cells of the type found in some tumors. A detailed description of the clinical experience is given in Chapter 2 on the Status and Success of Neutron Therapy.

Collimators are designed to be adjustable so that the volume to be irradiated is fully covered and adjacent, healthy tissue is spared as much as possible. A typically irregular tumor volume and a schematic design of an adjustable collimator are shown in Figure 7 of Chapter 2. Because of the high penetrating power of neutrons, collimators must present a thickness of several mean free paths of material with a high neutron cross section. This amounts often to nearly 1 meter of material. Several designs of adjustable collimators are now in use. Included are iron "leaf" designs such as at Louvain-la-Neuve in Belgium, iron "bookend" type at Chiba Japan (Kawashima, 1991), and tungsten rods at Harper Grace Hospital in Detroit, Michigan, USA (Maughan *et al.*, 1989; Maughan, 1991). Some collimators also include polyethylene or borated polyethylene inserts to close the "windows" (see below) in the iron total cross section, especially the window near 25 keV. The mechanical complexity and the mass of the assembly lead to costs for these collimators on the order of US$500,000 or more.

The adjustable collimator is located close to the patient for best definition of the radiation dose. Between neutron source and collimator, there are fixed precollimators of materials such as iron, lead, tungsten, copper, concrete, polyethylene, and Benelex (a compressed wood product).

Shielding of irradiation facilities is accomplished by building materials such as concrete, the composition of which is carefully chosen for shielding characteristics. For example, concrete that is limestone based ($CaCO_3$) is preferred to silicaceous concrete (NCRP, 1977). Several reports of the US National Council on Radiation Protection (NCRP, 1977; NCRP, 1984) summarize the neutron shielding characteristics of common materials. These guidelines are based on integral measurements and "rules of thumb" from experience with accelerator shielding. Although they predate more modern data bases and calculational methods described below, they are used to certify the adequacy of shields to governmental radiation protection agencies, (*e.g.* Maughan, 1986).

This chapter outlines the physical processes of neutron interactions with matter, methods for calculating the transport of neutrons through collimation and shields, benchmark experiments to validate such calculations, and the problem of induced radioactivity in collimators, shields, tissue and air.

NEUTRON INTERACTIONS IN THE MeV
REGION
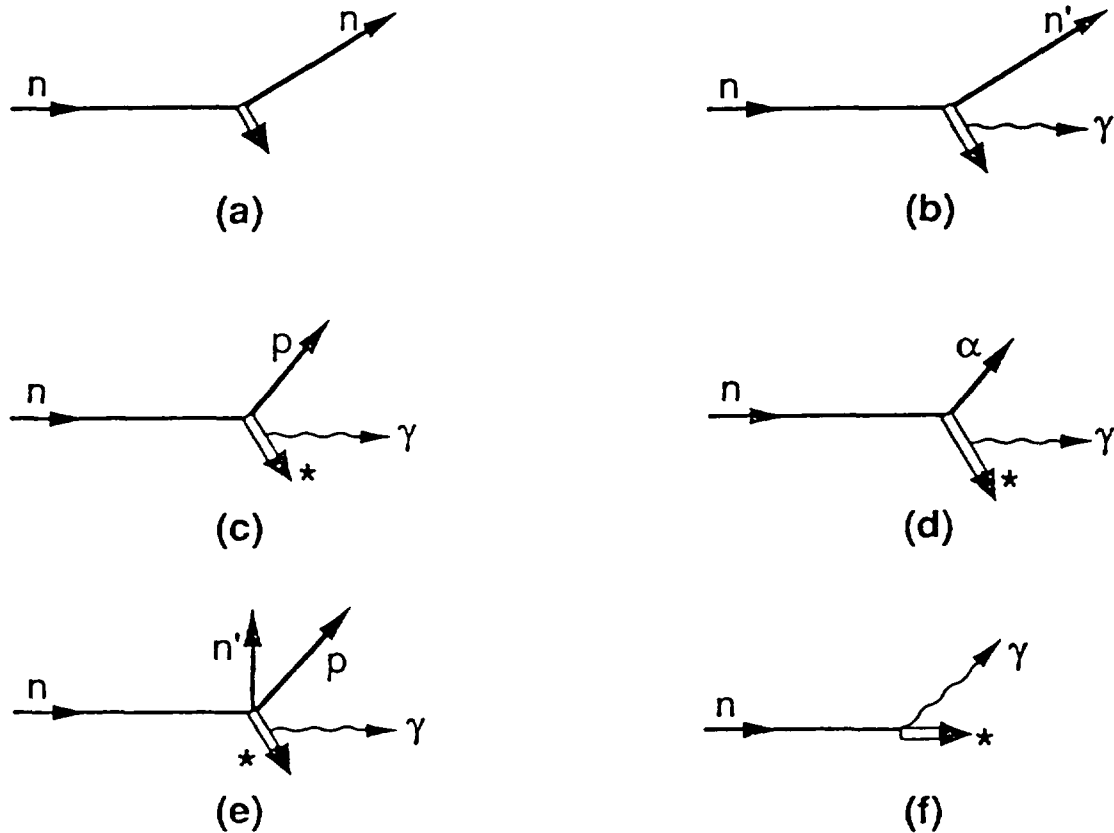
$^\star \equiv$ possibly radioactive residual nucleus

Figure 22: Examples of neutron scattering and reactions in the energy range up to 100 MeV: (a) Elastic scattering where the total kinetic energy after scattering equals the initial kinetic energy; (b) Inelastic scattering where the nucleus is excited and subsequently decays by gamma-ray emission; (c) Reaction resulting in absorption of the neutron and emission of a proton; (d) Reaction resulting in absorption of the neutron and emission of an alpha particle; (e) Reaction where a proton, neutron, and gamma-ray are emitted in the final state; and (f) Capture of the neutron with the emission of a gamma ray. In some reactions the product nuclei are radioactive.

5.2   Physical Processes in Neutron Interactions

Neutrons travel through materials until they scatter or react with a nucleus of one of the constituent elements. These interactions are to be contrasted with those of charged particles (electrons, protons, alpha particles, etc.) which transfer their energy mostly by long range interactions with the atomic electrons.

In the energy range of interest here, with neutrons up to 100 MeV, many different processes need to be considered. Several examples are given in Figure 22, but these represent only a few of the many reaction channels available at neutron energies of 50 to 100 MeV. Fortunately, each individual reaction channel need not be described

fully for a reliable calculation of collimators or shields, or indeed for the interaction of neutrons with tissue. Nevertheless, for collimators and shields, the more penetrating radiations following nuclear interactions (neutrons, gamma-rays, and perhaps the high energy protons) do need to be known well. This information is complementary to that needed to study radiation effects in tissue where the less penetrating and higher LET reaction products (recoil nuclei, alpha particles and lower energy protons) are more important.

To study the transport of neutrons, an important concept is the "mean free path", that is the mean distance between interactions of a neutron in the material. This quantity varies with the material and with the neutron energy. Typical values are given in Table XIV. In general, the mean free path increases with neutron energy so that the design of collimators and shields for this energy range (up to 70 MeV) is more difficult than for fission-spectrum neutrons (up to 10 MeV).

Table XIV: Neutron mean-free paths versus neutron energy. Mean-free-path, λ, values were derived from data from Plechaty et al. (1976), and Finlay et al. (1991).

| Material | Density [g cm^{-3}] | En[MeV] | | | | | |
| | | 1 | 5 | 10 | 20 | 50 | 100 |
		λ [cm]					
CH$_2$	0.96	2.3	5.5	8.1	9.7	19.4	38.2
H$_2$O	1.00	2.4	6.4	9.5	11.3	19.7	37.6
Al	2.70	4.8	7.6	9.5	9.3	9.9	16.8
Fe	7.87	4.4	3.3	3.7	5.1	4.8	6.4
Cu	8.96	3.3	3.2	3.4	4.7	4.4	5.9
W	19.30	2.4	2.7	3.1	2.9	3.9	3.7
Pb	11.36	6.1	4.2	6.0	5.2	7.1	6.7

Secondary particles emitted in the reactions are generally easier to shield against. Heavy charged particles (alpha particles and recoiling nuclei for example) have ranges of at most 100 mg/cm^2. Protons can have ranges up to about 1 g/cm^2. Gamma rays are generally in the range 0.1 to 10 MeV and can contribute to the dose to the patient or to the therapy staff. Scattered or emitted secondary neutrons generally have lower energy than the incident neutron and are therefore somewhat easier to shield against.

There are two important exceptions to the above statement that scattered or emitted neutrons are easier to shield against. In the case of elastic scattering, the scattered neutrons have very nearly the same energy as the initial neutron. Shielding these scattered neutrons is therefore no easier than for the incident neutrons. Furthermore elastically scattered neutrons are peaked in the forward direction, especially as the incident neutron energy increases. Hence the mean-free-paths given in Table XIV should not be used to calculate neutron attenuation. Rather a "transport-corrected-mean-free-path" should be used. For neutron energies less than 20 MeV, values for the corrected mean-free-path are given for example by Plechaty et al. (1976).

The second exception is that for some materials, the mean free path varies strongly with energy below 5 MeV and there exist "windows" where the mean-free-path is longer than usual. The window in iron near 25 keV is one example. (See Figure 23). To counteract such possibilities for neutron transport, combinations of different materials can be chosen, one closing the window of the other.

A FETOT.DAT   NEUTRON MEAN-FREE-PATH IN IRON   SCALE FACTOR 1

Figure 23: Mean-free-path for neutrons in iron in the region of the 25-keV window.

5.3   Transport Codes and Evaluated Data

Nuclear data and radiation transport codes are needed to calculate the performance of collimators and shields. The status of data and of calculational approaches has been reviewed recently (IAEA, 1991).

For neutron data, the region between 20 and 100 MeV is an intermediate region that is difficult to describe with simple theories or with complete data bases. Nuclear reaction mechanisms such as compound nucleus formation with statistical decay, direct processes, and intermediate or "pre-compound" processes all are important in this energy range. Nuclear reaction models must therefore take into account all of these processes and, where appropriate, the competition between them.

If, despite the modelling complexity, there were numerical data bases that described the processes, neutron transport could be calculated and effects tallied at interaction sites. Nearly all existing data bases, however, were intended for use in the development of nuclear fission and fusion energy sources and have 20 MeV as their upper limit. This limit is generally not a result of the fundamental structure of the files but rather the conventional upper limit defined for applications to fission and fusion energy. The following files have complete evaluations up to 20 MeV but, with a few exceptions do not extend to higher energies:

1. **ENDF/B-VI, USA, Canada**
   (although there is a special intermediate energy data base for selected materials)

2. **ENDL, USA (Lawrence Livermore National Laboratory)**
   (this data base is being extended to 250 MeV for certain tissue-resident and structural materials)

3. **JEF, Europe**

4. **BROND, USSR**

5. **JENDL-3, Japan**

6. **CENDL, China**

7. **FENDL, IAEA**
   (this data base is derived from several of the above data bases)

In the last few years, researchers have begun to address calculating neutron transport in the 20-100 MeV region through two approaches. One approach has been to extend nuclear model codes into this energy region, usually from approaches that work well at much higher energies. That is, intranuclear cascade codes are enhanced by adding additional physics to account for pre-equilibrium and direct processes. Many of these codes already treat not only the microscopic interaction of neutrons with nuclei but also the transport of radiation, in particular neutrons and charged particles. The following codes incorporate nuclear reaction models as well as transport:

1. **LAHET** (R. Prael, Los Alamos, USA) is a system of codes (Prael and Lichtenstein, 1989). MCNP is used for transport below 20 MeV with ENDF/B cross sections; intranuclear cascade and pre-compound codes are used above 20 MeV. At the higher energies, this code originated from the HETC code described below. Additional physics has been added more recently. This code has been tested against (p,n) data at 115 and 230 MeV and shows good agreement (Prael 1989, 1990).

2. **HETC** (Oak Ridge National Laboratory, USA) uses the code O5R up to 15 MeV and intranuclear cascade code above 15 MeV (Alsmiller *et al.*, 1988; Armstrong *et al.*, 1972; Chandler and Armstrong, 1972).

3. **HERMES** (KFA, Jülich, Germany) is also based on HETC. It couples neutron and photon transport.

The other approach has been to extend evaluated cross section data bases well beyond 20 MeV. Again, many of the required data are not available by experiments and must be calculated using reaction models. With the development of these more extensive data bases, however, the nuclear cross section calculation can be separated from the transport calculation. In addition, for the few cases where experimental cross section measurements do exist, they can be used to ensure that the evaluated data bases provide the most accurate possible representation of the cross sections. These evaluated data bases can also be benchmarked in an integral way be ensuring that they account for measured kerma factors. Another advantage is that the transport calculation is faster when the required cross section data do not need to be calculated

but rather can simply be looked up. An example of such an approach is the program currently being carried out at Lawrence Livermore National Laboratory to simulate dose deposition in radiation therapy using Monte Carlo transport techniques which access high-energy evaluated data libraries (White, 1994) . Transport codes that can be adapted for the energy range up to 100 MeV are:

1. **MCNP** (Los Alamos, USA)

2. **MCNP-4**, tested by J. Arkuszewski at PSI in Switzerland. This uses ENDF/B-VI as well as experimental data for H, N, O, Al, Ca, and Fe up to 100 MeV.

3. **COG** (T. Wilcox, Lawrence Livermore National Laboratory)

These codes use data bases, most of which are based mainly on model calculations. Codes used to calculate cross sections and emission spectra at energies up to 100 MeV (and often beyond) include (IAEA 1991):

1. **GNASH**, LANL

2. **FKK-GNASH**, LLNL and LANL

3. **LAHET**, LANL

4. **Bertini HETC**, USA

5. **ALICE**, LLNL

6. **NAUSICA**, ENEA-Italy

7. **HERMES**, Jülich, Germany

8. **ISABEL**, Weizmann Institute, Israel

9. **KAPSIES**, ECN Petten

Recently, modern data bases for neutron data above 20 MeV have been created for many materials used in collimators and shields. The calculational approaches include intranuclear cascade models, *e.g.*, Alsmiller and Barish (1981); Wilson and Costner (1975); and Alsmiller *et al.* (1988) and detailed models of precompound and Hauser-Feshbach mechanisms, *e.g.*, Young *et al.* (1990), Chadwick *et al.* (1994); and Pearstein (1989). In the case of neutrons on ^{1}H, phase-shift analyses have served for many years as a source of evaluated data. Below we describe the available neutron cross section data bases for individual elements:

1. ^{1}**H**: Phase shift analyses are good up to the inelastic threshold (about 280 MeV). These data are not given in a format for transport calculations but they could be used easily to create such a data base. Recent references are Arndt *et al.* (1983); Arndt *et al.* (1987); Arndt (1988); and Young *et al.* (1990). The status of n-p cross section data above 20 MeV is reviewed in an NEANDC Specialists' Meeting on Neutron Cross Section Standards for the Energy Region above 20 MeV (NEANDC, 1991).

2. ^{9}**Be**: An evaluation for neutrons and protons up to 100 MeV is available from Young *et al.* (1990).

3. **C:** Brenner and Prael (1989) have tabulated production cross sections for neutron energies up to 60 MeV obtained from model calculations. An evaluation of cross section data up to 32 MeV has been made by E. J. Axton in cooperation with the National Institute of Standards and Technology but the results have not been published yet (Axton, 1990). An evaluation for neutrons and protons up to 100 MeV for ^{12}C has been completed by Young et al. (1990). A recent evaluation by Chadwick et al. (1994) extends the Livermore data base up to 100 MeV.

4. **N:** Young et al. (1994) have recently extended the ENDF evaluation on nitrogen up to 40 MeV. A recent evaluation by Chadwick et al. (1994) extends the Livermore data base up to 100 MeV.

5. **O:** Brenner and Prael (1989) have tabulated production cross sections for neutron energies up to 60 MeV obtained from model calculations. An evaluation for neutrons and protons up to 100 MeV on ^{16}O is available from Young et al. (1990). A recent evaluation by Chadwick et al. (1994) extends the Livermore data base up to 100 MeV.

6. **Al:** An evaluation for neutrons and protons up to 100 MeV is available from Young et al. (1990).

7. **^{28}Si:** An evaluation for neutrons and protons up to 100 MeV is available from Young et al. (1990).

8. **^{40}Ca:** The ENDF evaluation has been extended to 40 MeV by Hetrick et al. (1982).

9. **Fe:** Young et al. (1990), have completed an evaluation to 100 MeV for both protons and neutrons.

10. **^{54,56}Fe:** 3.6 to 40 MeV: Isotopic evaluations are available from 3.6 to 40 MeV by Arthur and others (Arthur and Young, 1980a; Young et al., 1979; Arthur and Young, 1980b; Arthur and Young, 1980c).

11. **^{56}Fe:** Pearlstein gives calculational results and experimental comparisons from 1 to 1000 MeV (Pearlstein, 1989).

12. **^{56}Fe:** Calculational results are given by Hida and Iijima (1990) from 20 to 300 MeV.

13. **Cu:** From 1 to 50 MeV, see Arthur et al. (1987).

14. **W:** A new evaluation extends to 100 MeV by Young et al. (1990).

15. **Pb:** An evaluation to 100 MeV has been presented by Fukahori and Pearlstein (1991).

16. **^{238}U:** Young et al. (1990), have evaluated this material to 100 MeV.

Some of these evaluations are available from the National Nuclear Data Center at Brookhaven National Laboratory, USA, in the ENDF intermediate energy file.

Several new measurements in the range 20-100 MeV should also be noted:

Total cross sections: Finlay *et al.* (1991) measured total neutron cross sections on 18 target nuclides from 5 to 550 MeV with high accuracy. Together with other references cited in that work, this study provides an extremely accurate data base for applications.

Scattering: Elastic and inelastic scattering studies in the range 16 to 22 MeV have been carried out by Olsson and co-workers (Olsson *et al.*, 1987, 1989, 1990a, 1990b). Elements studied included Be, C, N, O, Mg, Al, Si, S, Ca, Cr, Fe, Co, Co, Ni, Y, Ce, Pb, and Bi. At 65 MeV, elastic scattering on C, Si, Ca, Fe, Sn, and Pb and inelastic scattering on Fe, Sn, and Pb have been studied (Hjort, 1990). A program at Ohio University has studied neutron elastic scattering on carbon (Meigooni, 1984) , nitrogen, oxygen, and calcium (Islam, 1988) in the 19 - 26 MeV range. There also exist elastic scattering data for 30 and 40 MeV *neutrons on biologically-important elements from Michigan State University* (DeVito, 79) .

Reactions: Using a white neutron source, Sorenson *et al.*, studied the (n,p) reaction on carbon isotopes from 50 to 250 MeV and for protons emitted in the forward direction (Sorenson, 1993). Similar studies on ^{64}Ni have been carried out by Ling and coworkers (Ling *et al.*, 1991). For neutron energies up to 30 MeV preliminary measurements on ^{12}C(n,α) and ^{27}Al(n,α) have been reported (Pedroni *et al.*, 1989; Grimes and Haight, 1989; Sterbenz *et al.*, 1991). Light charged particle production cross sections for 27,40, and 60 MeV neutrons on carbon, nitrogen and oxygen have been measured at UC-Davis (Subramanian *et al.*, 1983, 1986) . Recently the Louvain-La-Neuve group have presented charged particle production cross sections for 43, 63, and 73 MeV neutrons on carbon (Slypen, 1994) , and plan to measure similar cross sections on oxygen in the near future.

5.4   Benchmarks

To gain confidence in calculational approaches, it is necessary to have benchmark experiments with which to compare the calculations. For neutron energies below 20 MeV there are many integral tests of neutron and photon emission from macroscopic samples and of attenuation through shields. Above 20 MeV the number of integral tests is much smaller.

Examples of shielding benchmark tests for therapy applications have been published (Meulders *et al.*, 1975; Attix *et al.*, 1976; Smathers *et al.*, 1978a). The d+Be neutron source was used at several deuteron energies and materials tested included steel, lead, tungsten, polyethylene, concrete, borated paraffin, and several commercial products. Both broad beam and narrow beam geometries were explored. Detectors were tissue-equivalent ion chambers and liquid scintillators with neutron-gamma discrimination. The narrow beam results were consistent with exponential attenuation calculated from total cross section data. To certify shielding for facilities, the broad beam results are more relevant, but these were made only with tissue equivalent ion chambers. The relative contributions of neutrons and photons are therefore not available from these data. Thus the available benchmark tests are not sufficient for stringent tests of calculational models.

Neutron and photon spectra can be determined by unfolding of pulse height spectra obtained by measurements with organic scintillators (Brooks *et al.*, 1990). Brooks

et al. measured spectra in phantoms and therefore provide valuable information on the radiation quality and the absorbed dose given to a patient. They do not give much information on the performance of the collimator, however, even though the collimator opening was one variable in the study.

Obviously, more benchmark experiments need to be done to check the accuracy of transport calculations through the collimators. A well-defined geometry for these experiments is essential. One could imagine pulsed-sphere experiments of the type done at 14 MeV but with the higher energy neutron sources used in therapy facilities (Wong *et al.*, 1972; Goldberg *et al.*, 1990). Both neutron and gamma-ray emission should be studied. This type of experiment was carried out by Condé *et al.* (1987), who were interested in the moderation of neutrons up to 70 MeV in a water sphere. The source was a 72-MeV proton beam on a stopping copper target and neutrons emitted below 1 MeV were measured. An extension of this approach to materials of collimators and shields and to the full spectrum of emitted neutrons and photons would be most useful.

An opportunity to test calculations is offered by the experience with existing facilities. If neutron and photon spectra were measured at various locations relative to the collimator as well as outside the shield, the results could be compared with calculations that included the complex geometry of the as-built facility. The authors of this report are not aware of any work to date to take advantage of this opportunity.

A closely-related approach has been to measure the dose distributions in phantoms (ICRU, 1989). Although the results are important for calculating neutron transport, but the effects of the collimators are masked by transport in the phantom.

Of the relatively few benchmark experiments to test the calculated cross sections, several have been done at LAMPF (Prael, 1989b; Prael, 1990). These often have been at somewhat higher energies than 100 MeV. When necessary, the transport codes have been modified, sometimes to include new reaction processes, in order to reproduce results of the benchmarks.

Efficiencies of neutron detectors also can be considered as integral tests of the data and transport. Several studies (Sailor *et al.*, 1989; Dickens, 1991; Buffler, 1990; Antolkovic *et al.*, 1991) of organic scintillators (containing just carbon and hydrogen) conclude that much more data are needed for neutron interactions with carbon to obtain efficiencies with good confidence.

Facility shielding is guided often by rules of thumb since there already is a considerable body of experience in shielding such facilities. In a hospital setting, the shielding design is often constrained by pre-existing boundaries such as the size of the room in which the facility is to be installed. Optimization of the shielding is rarely done by detailed calculation, although significant cost savings could result by reducing the volume of the shield. Different shield constructions could also be investigated, such as the concrete and steel-ball shield used recently in a neutron source facility (Lisowski *et al.*, 1990).

Clearly there is a need for many more calculational studies and for benchmark experiments against which the calculations can be compared. The present integral experiments are useful beginnings, but often they stop short of offering stringent tests of nuclear data and transport calculations. To optimize collimators and shields in neutron therapy facilities, the present state of the data and codes allows one to begin calculational studies, which until very recently were impossible. The need for further benchmark tests is therefore great.

5.5 Activation of Collimators, Shields, and Other Materials

Neutrons in the energy range of interest interact with materials to produce radioactive isotopes (see Figure 22). Depending on the materials selected for collimators and shields, the isotopes can have long or short half-lives and can emit energetic or low-energy radiations. Although the added dose to the patient from this induced activity is very small compared with the therapeutic dose, the medical staff and accelerator technicians will receive a dose above background.

Doses from radioactive products at one therapy facility have been reported by Smathers et al. (1978b), who conclude that the major sources of exposure are the activated target assembly and the activated target end of the collimator inserts. They suggest operational methods to reduce the exposure. The annualized radiation doses are in the region of several hundred mRem.

The relative activation of tungsten, iron, and mild steel have been compared by Bonnett, 1986. He shows the buildup of radioactivity over a number of irradiations. There is a tradeoff therefore of one material over another depending on the number of irradiations that are planned per day. Another factor is the neutron spectral shape and, in particular, the contribution of thermal neutrons. Activation in tungsten is reduced, for example, if the thermal neutron flux can be reduced.

Activation of air and tissue is yet another concern. Ten Haken et al. (1983) have studied these processes with a p(66)Be(49) neutron source. The added dose to the patient from residual radioactivity in tissue is very small. Only in special circumstances would the activity in the air necessitate a waiting period before the treatment room is entered by the medical staff. It appears that this problem, at least, is well understood and not of major importance.

Acknowledgment: We thank Dr. Richard L. Maughan of the Radiation Oncology Center at Harper Grace Hospital for supplying much detailed information on the design of collimation and shielding for the cyclotron-based neutron therapy center there.

References

Alsmiller, Jr., R.G. and Berish, J., "Neutron-Photon Multigroup Cross Sections for Neutron Energies $\leq$ 400 MeV," *Nucl. Sci. Eng.* **80**, 448 (1981).

Alsmiller, Jr., R.G., Alsmiller, F.S., Gabriel, T.A., Hermann, O.W., and Bishop, B.L., Trans. Am. Nucl. Soc. annual meeting, San Diego, California (1988).

Antolković, B., Dietze, G., and Klein, H., "Reaction Cross Sections on Carbon for Neutron Energies from 11.5 to 19 MeV," *Nucl. Sci. Eng.* **107**, 1 (1991).

Armstrong, T.W., Alsmiller, R.G., Jr., Chandler, K.C., and Bishop, B.L., "Monte Carlo Calculations of High-Energy Nucleon-Meson Cascades and Comparison with Experiment," *Nucl. Sci. Eng.* **49**, 82 (1972).

Arndt, R.A., Roper, L.D., Bryan, R.A., VerWest, B.J., and Signell, P., Nucleon-Nucleon Partial-Wave Analysis to 1 GeV," *Phys. Rev. D* **28**, 97 (1983).

Arndt, R.A., Hyslop III, J.S., and Roper, L.D., Nucleon-Nucleon Partial-Wave Analysis to 1100 MeV," *Phys. Rev. D* **35**, 128 (1987).

Arndt, R.A., "Uncertainties in the np Interaction at Medium Energies," *Phys. Rev. D* **37**, 2665 (1988).

Arthur, E. and Young, P.G., "Evaluation of Neutron Cross Sections for ^{54}Fe and ^{56}Fe," In: *Proc. Symp. on Neutron Cross Sections from 10 to 50 MeV*, M.R. Bhat and S. Pearlstein (eds.), Brookhaven, 1980, p. 731, Brookhaven National Laboratory Report BNL-NCS-51245 (1980a).

Arthur, E.D. and Young, P.G., "Calculation of Neutron Cross Sections on Iron up to 40 MeV," *Trans. Am. Nucl. Soc.* **34**, 656 (1980b).

Arthur, E.D. and Young, P.G., *Evaluated Neutron-Induced Cross Sections for ^{54,56}Fe to 40 MeV*, Los Alamos National Laboratory Report LA-8626-MS (1980c).

Arthur, E.D., Young, P.G., and Perry, R.T., "Calculation of Higher Neutron Reactions on Al, Fe, Ni, and Cu," In: *Applied Nuclear Science Research and Development Progress Report*, E.D. Arthur and A. D. Mutschlecner (eds.), p. 8, Los Alamos National Laboratory Progress Report LA-10915-PR, (1987).

Attix, F.H., Theus, R.B., and Miller, G.E., "Attenuation Measurements of a Fast Neutron Radiotherapy Beam," *Phys. Med. Biol.* **21**, 530 (1976).

Axton, E.J., Private Communication (1990); "An Evaluation of Kerma in Carbon and the Carbon Cross Sections," NIST Report NISTIR 4838.

Bonnett, D.E., Private Communication to H. Blosser (19 August 1986).

Brenner, D.J., and Prael, R.E., "Calculated Differential Secondary Particle Production Cross Sections after Nonelastic Neutron Interactions with Carbon and Oxygen Between 15 and 60 MeV," *Atomic Data and Nucl. Data Tables* **41**, 71 (1989).

Brooks, F.D., Jones, D.T.L., Nchodu, R., and Buffler, A., National Accelerator Centre Annual Report, pp. 191-194 (Faure, Republic of South Africa, 1990).

Buffler, A., "The Response of Organic Scintillators to Neutrons of Energy 14-63 MeV," Ph.D. Thesis, University of Cape Town (1990).

Chadwick, M.B., Blann, M., Young, P.G., Reffo, G., "Model Calculations of Nuclear Data for Biologically-Important Elements," Lawrence Livermore National Laboratory Report UCRL-JC-117173 (1994).

Chandler, K.C. and Armstrong, T.W.,"Operating Instructions for the High-Energy Nucleon Meson Transport Code HETC," Oak Ridge National Laboratory Report ORNL-4744 (1972).

Condé, H., Grusell, E., Larsson, B., Pettersson, C.-B., Thuresson, L., Crawford, J., Reist, H., Dahl, B., and Sjostrand, N.G., "Time-of-Flight Measurements of the Energy Spectrum of Neutrons Emitted from a Spallation Source and Moderated in Water," *Nucl. Instrum. Methods in Phys. Research A* **261**, 587 (1987).

DeVito, R.P., Ph.D. Thesis, Michigan State University (1979).

Dickens, J.K., "Scintillation Detection Efficiencies for Neutrons in the Energy Region above 20 MeV," In: *Proc. NEANDC Specialists' Meeting on Neutron Cross Sections Standards for the Energy Region above 20 MeV*, Uppsala, Sweden, May, 1991, p. 142, Nuclear Energy Agency Nuclear Data Committee report NEANDC-305/U (1991).

Finlay, R.W., Fink, G., Abfalterer, W., Lisowski, P., Morgan, G.L., and Haight, R.C., "Neutron Total Cross Section Measurements at Intermediate Energy," In: *Proc. Int. Conf. on Nuclear Data for Science and Technology*, Jülich, May 13-17, 1991, p. 720, S.M. Qaim (ed.) (1992).

Fukahori, T. and Pearlstein, S., "Evaluation at the Medium Energy Region for Pb-208 and Bi-209," In: *Proc. Advisory Group Meeting on Intermediate Nuclear Data for Applications*, IAEA, Vienna, October 9-12, 1990, N.P. Kocherov (ed.), IAEA Report INDC(NDS)-245, International Atomic Energy Agency, Vienna (1991).

Goldberg, E., Hansen, L.F., Komoto, T.T., Pohl, B.A., Howerton, R.J., Dye, R.E., Plechaty, E.F., and Warren, W.E., "Neutron and Gamma-ray Spectra from a Variety of Materials Bombarded with 14-MeV Neutrons," *Nucl. Sci. Eng.* **105**, 319 (1990).

Grimes, S.M. and Haight, R.C., "Facilities for Measuring (n,z) Reactions," In: *Proc. Int. Conf. on Nuclear Data for Science and Technology*, Jülich, May 13-17, 1991, p. 410, S.M. Qaim (ed.) (1992).

Hetrick, D.M., Fu, C.Y., and Larson, D.C., *Evaluated Neutron-Induced Cross Sections for ^{40}Ca from 20 to 40 MeV*, Oak Ridge National Laboratory Report ORNL/TM-8290 (1982).

Hida, K. and Iijima, S., Nuclear Engineering Laboratory of Toshiba, "Calculation of ^{56}Fe Reactions Induced by High Energy Neutrons and Protons," In: *Proc. 2nd International Symposium on Advanced Nuclear Energy Research*, Mito, March 12-16, 1990, p. 710; and *Proc. 1989 Seminar on Nuclear Data*, Y. Nakajima and M. Igashira (eds.), NEANDC(U)-149/U, INDC(JPN)-136/L (1990).

Hjort, E.L., Ph.D. Thesis, University of California at Davis (unpublished); and Hjort, E.L., Brady, F.P., Romero, J.L., Drummond, J.R., Hamilton, M.A., McEachern, B., Smith, R.D., Brown, V.R., Petrovich, F., and Madsen, V.A., "Pb(n,n'x) a + 65 MeV and the Isospin Structure of the Giant Quadrupole Resonance Region," *Phys. Rev. Letters* **62**, 870 (1989).

International Atomic Energy Agency, *Proc. Advisory Group Meeting on Intermediate Energy Nuclear Data for Applications*, Vienna, 9-12 October 1990, N.P. Kocherov (ed.), IAEA Report INDC(NDS)-245, International Atomic Energy Agency, Vienna (1991).

International Commission on Radiation Units and Measurements, *Clinical Dosimetry Part I: Determination of Absorbed Dose in a Patient Treated by External Beams of Fast Neutrons*, Report 45 (International Commission on Radiation Units and Measurements, Bethesda, MD) (1989).

Islam, M.S., Finlay, R.W., Petler, J.S., Rapaport, J., Alarcon, R., and Wierzbicki, J., "Neutron Scattering Cross Sections and Partial Kerma Values for Oxygen, Nitrogen, and Calcium at $18 < E_n < 60$ MeV," *Phys. Med. Biol.* **33**, 315 (1988).

Kawashima, K., "Collimator Design for the Neutron Irradiation Facility at Chiba, Japan," Private Communication (1991).

Ling, A., Aslanoglou, X., Brady, F.P., Finlay, R.W., Haight, R.C., Howell, C.R.,

King, N.S.P., Lisowski, P.W., Park, B.K., Rapaport, J., Romero, J.L., Sorenson, D.S., Tornow, W., and Ullmann, J.L., "Ground-state Gammow-Teller Strength in ^{64}Ni,(n,p)^{64}Co Cross Sections at 90-249 MeV," *Phys. Rev. C* **44**, 2794 (1991).

Lisowski, P.W., Bowman, C.D., Russell, G.J., and Wender, S.A., "The Los Alamos National Laboratory Spallation Neutron Sources," *Nucl. Sci. Eng.* **106**, 208 (1990).

Maughan, R.J., "Report on the Shielding and Radiation Protection Requirements of the Superconducting Cyclotron to be Installed in the Gershenson Radiation Oncology Center at Harper Hospital," Wayne State University, Harper-Grace Hospital, Detroit Medical Center (1986).

Maughan, R.L., Blosser, G.F., Blosser, E.B., Blosser, H.G., and Powers, W.E., "Transmission Measurements in Multi-rod Arrays: A Design Study for a Multi-rod Collimator," *Radiotherapy and Oncology* **15**, 125 (1989).

Maughan, R.L., "Collimator Design," Private Communication (1991).

Meigooni, A.S., Petler, J.S., and Finlay, R.W., "Scattering Cross Sections and Partial Kerma Factors for Neutron Interactions with Carbon at $20 < E_n < 65$ MeV," *Phys. Med. Biol.* **29**, 643 (1984).

Meulders, J.P., Leleux, P., Marq, P.C., Pirart, C., and Valenduc, G., "Intensity Measurements and Shieldings of a Fast-Neutron Beam for Biological and Medical Applications," *Nucl. Instr. Methods* **126**, 81 (1975).

National Council on Radiation Protection and Measurements, *Radiation Protection Design Guidelines for 0.1 to 100 MeV Particle Accelerator Facilities*, NCRP Report No. 51, NCRP, Washington (1977).

National Council on Radiation Protection and Measurements, *Neutron Contamination from Medical Electron Accelerators*, NCRP Report No. 51, NCRP, Washington (1984).

Nuclear Energy Agency Nuclear Data Committee, *Proc. NEANDC Specialists' Meeting on Neutron Cross Sections Standards for the Energy Region above 20 MeV*, Uppsala, Sweden, May, 1991, Nuclear Energy Agency Nuclear Data Committee Report NEANDC-305/U (1991).

Olsson, N., Trostell, B., Ramstrom, E., Holmqvist, B., and Dietrich, F.S., "Microscopic and Conventional Optical Model Analysis of Neutron Elastic Scattering at 21.6 MeV Over a Wide Mass Range," *Nucl. Phys. A* **472**, 237 (1987).

Olsson, N., Trostell, B., and Ramstrom, E., "Neutron Elastic and Inelastic Scattering from Carbon in the Energy Range 16.5-22.0 MeV," *Nucl. Phys. A* **496**, 505 (1989); *Phys. Med. Biol.* **34**, 909 (1989).

Olsson, N., Ramstrom, E., and Trostell, B., "Neutron Elastic and Inelastic Scattering from Beryllium, Nitrogen and Oxygen at En = 21.6 MeV," *Nucl. Phys. A* **509**, 161 (1990); *Phys. Med. Biol.* **35**, 1255 (1990a).

Olsson, N., Ramstrom, E., and Trostell, B., "Neutron Elastic and Inelastic Scattering from Mg, Si, S, Ca, Cr, Fe, and Ni at En = 21.6 MeV," *Nucl. Phys. A* **513**, 205 (1990b).

Pearlstein, S., "Medium-Energy Data Libraries: A Case Study, Neutron- and Proton-Induce Reactions in ^{56}FE," *The Astrophysical Journal* **346**, 1049 (1989).

Pedroni, R.S., Boukharouba, N., Grimes, S.M., Mishra, V., and Haight, R.C., "A Facility for Measuring Charged Particles Emitted in Neutron-Induced Reactions up to 50 MeV," *Bull. Am. Phys. Soc.* **33**, 1577 (1988).

Plechaty, E., Cullen, D.E., Howerton, R.J., and Kimlinger, J.R., *Tabular and Graphical Presentation of 175 Neutron-Group Constants Derived from the LLL Evaluated Nuclear Data Library*, Lawrence Livermore National Laboratory Report UCRL 50400, Vol. 16, Rev. 2 (1976).

Prael, R.E., "LAHET Benchmark Calculations of Differential Neutron Production Cross Sections for 113 and 256 MeV Protons," Los Alamos National Laboratory Report LA-UR-89-3347 (1989).

Prael, R.E. and Lichtenstein, H., "Users Guide to LCS: The LAHET Code System," Los Alamos National Laboratory Report LA-UR-89-3014 (1989).

Prael, R.E., "LAHET Benchmark Calculations of Neutron Yields from Stopping-Length Targets for 113 and 256 MeV Protons," Los Alamos National Laboratory Report LA-UR-90-1620 (1990).

Sailor, W., Byrd, R.C., and Yariv, Y., "Calculation of the Pulse-Height Response of Organic Scintillators for Neutron Energies $28 \leq En \leq 492$ MeV," *Nucl. Inst. Meth. in Phys. Research* **A277**, 599 (1989).

Smathers, J.B., Graves, R.G., Sandel, P.S., Almond, P.R., Otte, V.A., and Grant, W.H., "Radiation Dose Received by TAM VEC Neutron Therapy Staff," *Health Phys.* **35**, 271 (1978a).

Smathers, J.B., Graves, R.G., Wilson, W.B., Almond, P.R., Grant, W.H., and Otte, V.A., "Shielding for Neutron Radiotherapy Sources Created by the Be, (d,n) Reaction," *Health Phys.* **35**, 807 (1978b).

Sorenson, D.S., Aslanoglou, X., Brady, F.P., Drummond, D.R., Haight, R.C., Howell, C.R., King, N.S.P., Ling, A., Lisowski, P.W., Park, B.K., Rapaport, J., Romero, J.L., Tornow, W., and Ullmann, J.L., "Energy Dependence of the Gamow-Teller Strength in p-Shell Nuclei Observed in the (n, p) Reactions," *Phys. Rev. C* **45** R500 (1992).

Sterbenz, S.M., Haight, R.C., Lee, T.M., Bateman, F., Boukharouba, N., Doctor, K., Mishra, V., Pedroni, R.S., Grimes, S.M., and Vonach, H., "Spallation Neutron Source Measurements of the (n, alpha) Cross Section for 27 Al," *Bull. Am. Phys. Soc.* **36**, 1349 (1991).

Subramanian, T.S., Romero, J.L., Brady, F.P., Watson, J. W., Fitzgerald, D.H., Garrett, R., Needham, G.A., Ullmann, J.L., Zanelli, C.I., Brenner, D.J., and Prael, R.E., "Double differential inclusive hydrogen and helium spectra from neutron-induced reactions on carbon at 27.4, 39.7, and 60.7 MeV," *Phys. Rev. C* **28**, 521 (1983); *Phys. Rev. C* **34**, 1580 (1986).

Slypen, I., Corcalciuc, V., Ninane, A., and Meulders, J.P., "Charged Particles Produced in Fast Neutron Induced Reactions on ^{12}C in the 45-80 MeV Energy Range'," *Nucl. Instr. Methods in Phys. Research A* **337**, 431 (1994).

Ten Haken, R.K., Awschalom, M., and Rosenberg, I., "Activation of the Major Constituents of Tissue and Air by a Fast Neutron Radiation Therapy Beam," *Med. Phys.* **10**, 636 (1983).

White, R.M., Chadwick, M.B., Hartmann Siantar, C.L., and Chandler, W.P., "Nuclear Data Needed for Applications in Radiation Oncology," Lawrence Livermore National Laboratory Report UCRL-JC-117412 (1994).

Wilson, J.W. and Costner, C.M., "Nucleon and Heavy-Ion Total and Absorption Cross Sections for Nuclei," NASA Report NASA-TN D8107 (1975).

Wong, C., Anderson, J.D., Brown, P., Hansen, L.F., Kammerdiener, J.L., Logan, C., and Pohl, B.A., "Livermore Pulsed Sphere Program: Program Summary Through July 1971," Lawrence Livermore National Laboratory Report UCRL-51144, Rev. I (1972).

Young, P.G., Arthur, E.D., and Madland, D.G., In: *Proc. Int. Conf. on Nuclear Cross Sections for Technology*, J.L. Fowler, C.H. Johnson, and C.D. Bowman (eds.),

Knoxville, 1979, p. 639, National Bureau of Standards Publication 594 (1980).

Young, P.G., Arthur, E.D., Bozoian, M., England, T.R., Hale, G.M., LaBauve, R.J., Little, R.C., MacFarlane, R.E., Madland, D.G., Perry, R.T., and Wilson, W.B., Los Alamos National Laboratory Report LA-11753-MS (1990).

Young, P.G., Hale, G.M., and Chadwick, M.B., ENDF/B-VI ^{14}N Evaluation up to 40 MeV, Rev.3, 1994, available from the Brookhaven NNDC.

6 Kerma Factors

6.1 Introduction

Effects on matter produced by the interactions of fast neutrons occurs by means of the charged particles produced. In fact this is a two-step process: [1] the initial production of charged particle energy by neutron interactions and [2] the subsequent interaction of these charged particles with matter depositing energy by ionization and excitation. The former is called KERMA, an acronym for **K**inetic **E**nergy **R**eleased in **MA**tter, and represents the sum of all the initial energy transferred to charged particles by indirectly ionizing radiation neutrons, while the latter corresponds to absorbed dose, that is the energy deposited per unit mass (ICRU, 1980). The kerma factor is the kerma produced per unit neutron fluence. Quantification of neutron absorbed dose is accomplished most accurately when measurements are carried out in the media of interest. For biological purposes this is wet tissue. Such a medium is not amenable to the construction of detector apparatus and *tissue substitute* materials more suitable for measurement purposes are required. If these materials replicate the exact atomic composition of tissue, the measurement yields the absorbed dose in tissue. As this is never the case for neutrons, the tissue absorbed dose determination depends upon knowledge of the relative rate of charged particle energy production per unit mass for the *tissue substitute* material and tissue, *i.e.* the kerma or kerma factor ratio. As this kerma ratio is a function of the neutron energy, information about the neutron energy spectrum is also needed. Hence, neutron dose determinations with *tissue substitute* materials require accurate kerma factor values for all constituent materials for the entire neutron energy range of interest.

Table X in Section 3 summarizes the values of elemental mass fractions for wet tissue and some common solid, liquid, and gaseous tissue substitutes. Notice that hydrogen, which contributes most to the kerma and absorbed dose at neutron energies above 1 MeV, is well matched for each mixture. For solid materials, carbon is exchanged for oxygen. To a lesser extent this is also true for gas mixtures. Thus, information about the ratio of oxygen-to-carbon kerma is most important for fast neutron absorbed dose measurements.

Kerma factors can be calculated directly from microscopic reaction cross section information. Complete cross-section information is needed for all energetic charged particles as a function of emission angle and neutron bombarding energy – achievable only in principle. *In lieu* of these data, suitable nuclear models can be employed to provide the missing cross-section information allowing the calculation of kerma factors. Finally, kerma factors can be inferred from direct absorbed dose measurements in appropriate materials.

Below 10 MeV neutron energy, kerma is dominated by elastic and inelastic reactions. Extensive cross-section information is available in this energy region for most low-Z elements as well as many common heavier nuclei. Kerma factors are well established for these fast neutron energies. At higher neutron energies, only limited cross-section information is available. Charged particle emission becomes increasingly important, yet few reaction channels have been measured completely even for such important elements as carbon and oxygen. Tabulated kerma factors based on these cross sections are limited to 20 or 30 MeV neutron energy. Kerma factor values deduced from nuclear model calculations are reported for several elements up to 100-200 MeV neutron energy. Of course such models are themselves based upon information

about the nuclei deduced from limited measurements. Nonetheless, such calculations are useful for indicating the energy dependence of kerma factors. Measured kerma factor values are even more sparse, confined to carbon, oxygen, aluminum, magnesium, silicon, and iron at a few neutron energies below 30 MeV.

6.2 Microscopic Data

The quantity measured in nuclear physics experiments is often the microscopic cross section for the reaction type studied. If a charged particle spectrometer is employed to measure the energy and/or angle of the emitted ejectile(s), differential or double differential cross section information is obtained. Other experiments quantify observables related to nuclear structure (*e.g.*, spin), which are required for input to nuclear models used to calculate cross section:

In energy domains where experimental data are lacking, nuclear models can be used to calculate the cross sections and emission spectra. The results of such calculations become more and more uncertain the further they extrapolate from measured data. At low energies, where elastic and inelastic scattering dominate the total cross section, the optical model in combination with a statistical Hauser-Feshbach calculation can be used to describe the data (*i.e.* within a few tenths of a percent). At higher energies, the optical model can be used to estimate the elastic scattering cross section, but the precision is lower (about 50%) since there are fewer data that can be used to fix the many parameters of that model. A more important problem at higher energies ($15 < E_n < 100$ MeV) is the rapidly increasing number of more complicated reaction channels, which necessitate calculations involving both the statistical compound mechanism and direct processes, as well as all the possibilities in between, *i.e.* the pre-compound or pre-equilibrium processes. The calculated results for these reactions are credible to within a factor of about two in the absence of measurements.

The available experimental data in conjunction with model calculations and less formalized systematics are used by experienced physicists to produce evaluated data files. At the present time most of these files extend to 20 or 30 MeV neutron energy. The different existing evaluations together with commonly used nuclear model codes were presented in the previous section.

Some of the best known nuclear data in neutron physics pertains to the elastic scattering of neutrons by hydrogen. This reaction is often used as a primary cross section standard in measurements of other cross sections, and while its uncertainty is thereby introduced into these data, the uncertainty is small enough to be a minor effect when compared with other uncertainties. Moreover, the n-p scattering is in itself an important contribution to the kerma in tissue. The total cross section for this reaction is at present known to better than 0.5% up to 20 MeV and less accurately at higher energies. The angular distribution, which deviates from isotropy in the center of mass system above about 10 MeV, is considered to be accurate to within 2–3% up to 20 MeV. In the energy range 20–100 MeV, where there are very few experimental data points, the uncertainty can be considerable. The reaction has been modelled in terms of phase shift analyses of experimental data (Hopkins and Breit, 1971; Arndt *et al.*, 1983; Arndt *et al.*, 1987; Arndt, 1988). These calculations can be used to extract cross section information in energy regions where no data exist.

The kerma factor, k_f, is related to the microscopic nuclear cross sections by the following expression

$$k_f(E_n) = \sum_L N_L \sum_J \epsilon_{L,J}(E_n)\sigma_{L,J}(E_n),\qquad(7)$$

where the index L identifies the nuclide or element, and the index J identifies the type of nuclear reaction (elastic or inelastic scattering, (n,α), *etc.*). N_L is the number of nuclei of the L-th species per unit mass, $\epsilon_{L,J}(E_n)$ is the average energy transferred to charged particle kinetic energy in an interaction whose cross section is $\sigma_{L,J}(E_n)$ (ICRU, 1980). It is important that all secondary charged particles are included, *i.e.* residual nuclei recoils, p, d, t, ^{3}He, *etc.* For reaction channels in which both intermediate and final states are defined, *e.g.*, elastic scattering and inelastic scattering to discrete final states, the average transferred energy ϵ is easily accessible from the reaction kinematics. For other reaction channels explicit distributions of secondary particles must be used.

It is important to emphasize that the kerma factor is only a measure of how much energy per unit fluence is given to light charged particles and residual nuclei in a certain volume, regardless of the energy spectrum of the secondary particles. Since biological response varies dramatically with ionization capability, *i.e.* the particle type and energy, the secondary charged particle spectra are of importance in the context of radiation quality. These problems will be discussed in more detail in Chapter VII.

6.3 Experimental Determinations

As noted above, a direct measurement of kerma involves determination of the initial energies of all charged particles produced per unit mass by neutron bombardment. With the exception of elastic and inelastic scattering, such measurements pose a formidable problem above 10 MeV neutron energy even for few nucleon systems. An important example is fast neutron bombardment of carbon, where recoil ^{12}C and ^{9}Be nuclei, one or more α particles and other charged particles can be produced. Hence, experiments have concentrated upon measurements of limited reaction channels, *e.g.*, (n,p), (n,d), (n,α), total α-particle production, *etc.* As such, these experiments constitute a *partial* kerma factor determination. Partial kerma factors are combined with total cross-section information to estimate the kerma factor.

6.4 Integral Kerma Factor Measurements

Integral measurement of the total kerma offers an alternative procedure for kerma factor determinations. Usually the charged particle energy **deposited** per unit mass, the absorbed dose, is measured rather than the total charged particle energy produced, the kerma. For conditions of charged particle equilibrium, kerma and absorbed dose are equal. By measuring the absorbed dose per unit neutron fluence, corrected for any contributions due to γ-rays or off-energy neutrons, the kerma factor is determined. This procedure then involves two determinations: absorbed dose and neutron fluence.

Absorbed dose can be measured by calorimetric or cavity-ionization techniques. McDonald made a direct measurement of absorbed dose by a calorimetric procedure (McDonald, 1987). A calorimetric measurement is largely independent of the details of radiation metrology such as the interaction of the secondary charged particles with the detection medium. Rather, the calibration can be based upon the specific heat of the calorimeter material and resistively deposited energy. For precise determinations,

1-10 $\frac{mW}{kg}$ of ionizing power are required – corresponding to a large neutron flux. Additionally, no discrimination amongst the energy and type of bombarding ionizing radiation is possible.

Bühler, DeLuca, Goldberg and Wuu employed cavity-ionization chambers (Bühler *et al.*, 1985; DeLuca *et al.*, 1984; Goldberg *et al.*, 1978; Wuu and Milavickas, 1960). In each case the absorbed dose is measured in the material of interest, *e.g* carbon, magnesium, aluminum, A-150 plastic, *etc*. For the case of oxygen, a matched pair of instruments constructed of ZrO_2 and Zr yield the oxygen kerma by subtraction. Ionization chambers operated as low pressure proportional counters have proved to be particularly advantageous for these measurements. The small gas cavity minimally perturbs the equilibrium charged particle spectrum emanating from the wall. Using filling gases with small neutron kerma factors relative to the counter wall material results in minimal contribution to dose by neutron interactions with the gas. In this way, their response is due almost exclusively to charged particles produced in the wall, ensuring that energy absorbed in the gas is due to the particles of interest. Even though energy depositions in the counter gas result from an integral spectrum of charged particles produced in the wall, considerable information can be deduced about the initiating spectrum of indirectly ionizing particles bombarding the counter, *i.e.* γ-rays and neutrons. For example, energy depositions due to γ-ray induced electron recoils are distinguished from α-particle and heavier ion recoils and to a certain extent from energetic protons on the basis of their very different rates of energy loss to the gas stopping power.

6.5 Partial Kerma Factor Determinations

A few of the reaction channels that have been experimentally studied in order to obtain partial kerma factors will be discussed in more detail in this section.

Measurements of the neutron elastic scattering cross section provide a reliable determination of the reaction cross section since this quantity is just the difference between the total and the elastic cross sections, and the total cross section is normally well known. Measurements of inelastic scattering are also important since any fraction of the non-elastic cross section arising from inelastic scattering from particle-stable states is not available for charged-particle production. Thus, one can estimate an upper limit for these reactions which can be used as a constraint in model calculations. Moreover, differential elastic and inelastic scattering cross sections provide direct information on the high LET ($> 10^3$ keV/μm) heavy-ion recoil contribution to the kerma.

Scattering cross sections are experimentally measured by utilizing the neutron time-of-flight techniques. Traditionally, most measurements have been performed below 10 MeV, but also at about 15 MeV, where D-T neutron generators have been employed. Recently, scattering cross sections and partial kerma factors for carbon in the neutron energy range of 10–40 MeV and for oxygen at 10–26 MeV have been published (Börker *et al.*, 1988; Olsson *et al.*, 1989a, 1989b; Olsson *et al.*, 1990a; Meigooni *et al.*, 1984; Finlay *et al.*, 1985; Meigooni *et al.*, 1985; Islam *et al.*, 1987; Islam *et al.*, 1988; Glasgow *et al.*, 1976; DeVito, 1979). Above the neutron energies given, no experimental data exist at present.

To illustrate the quality of this kind of partial data and the model calculations that can be obtained by fitting to the experimental data, an example of partial kerma factors for elastic and inelastic (4.44 MeV) scattering for carbon up to 40 MeV is shown in Figures 24 and 25, respectively.
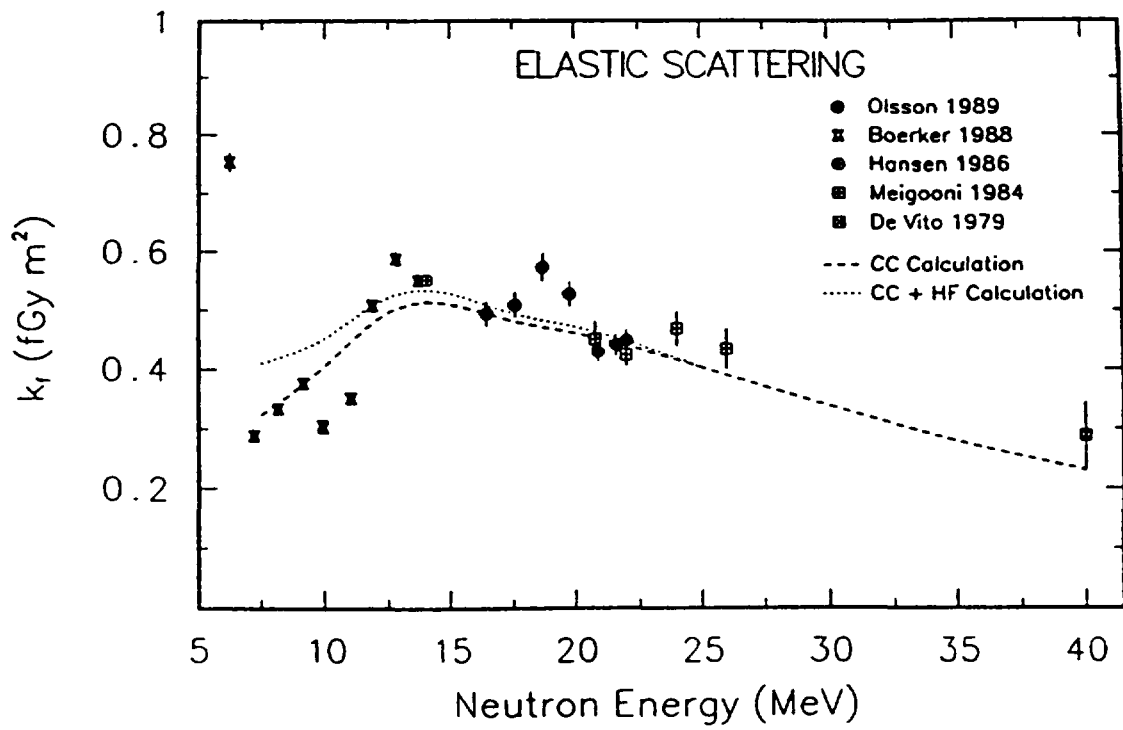
Figure 24: Measured partial carbon kerma factors for elastic neutron scattering from 5 to 40 MeV (Börker *et al.*, 1988; Hansen, 1986; Olsson *et al.*, 1989a, 1989b; Meigooni *et al.*, 1984; DeVito, 1979). The curves are model calculations (see text).
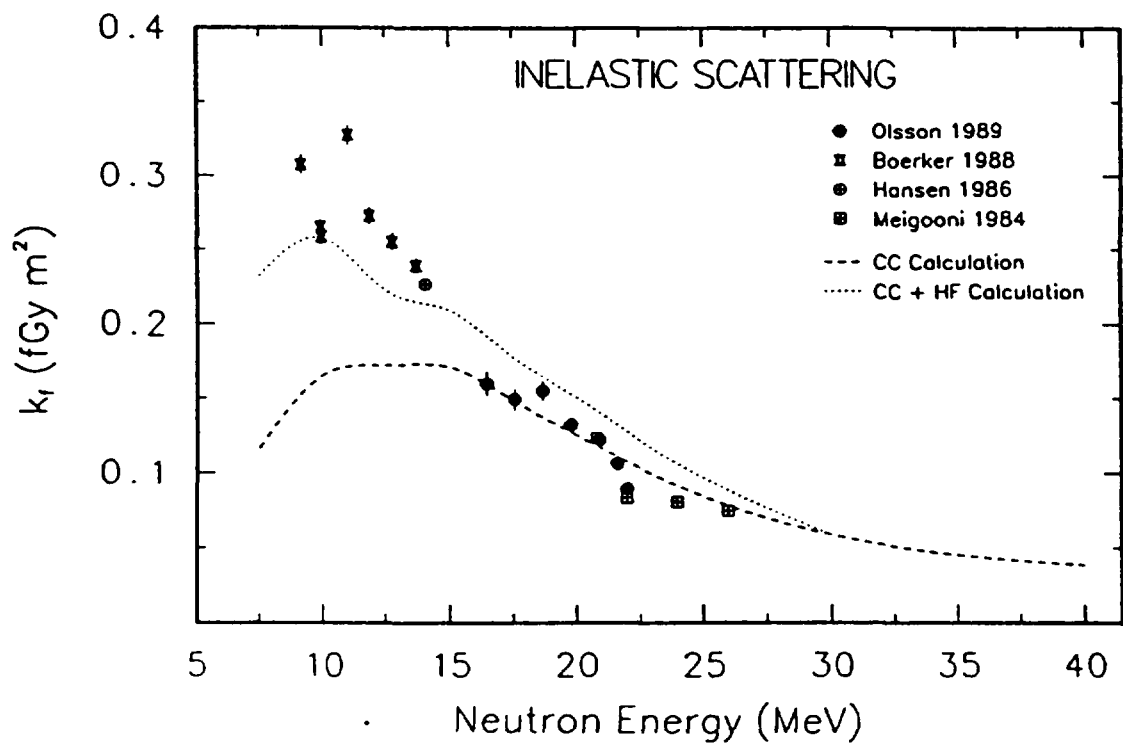
Figure 25: Measured partial carbon kerma factors for inelastic (4.44 MeV) neutron scattering from 5 to 40 MeV (Börker *et al.*, 1988; Hansen, 1986; Olsson *et al.*, 1989a, 1989b; Meigooni *et al.*, 1984). The curves are model calculations (see text).

As can be seen, the different data sets are in good agreement. The dashed lines were calculated with the coupled channels (CC) formalism, using a deformed optical model potential (Olsson, 1989a, 1989b). For elastic scattering the model calculation gives a good description of the data from 8 to about 40 MeV. A good description is also obtained for inelastic scattering above 15 MeV, whereas the kerma factors are increasingly underpredicted at lower energies. Compound nucleus contributions were determined in a Hauser-Feshbach (HF) calculation. The sum of the CC and HF calculations are shown as dotted lines in the figures. It is obvious that the HF contribution to elastic scattering is small above 8 MeV, while it is considerable for inelastic scattering up to more than 15 MeV. Similar calculations in the energy range 20-65 MeV have been published by Meigooni *et al.* (1984).

Measurements of charged particle production are difficult to perform, especially when there are more than one particle in the exit channel. This is the case for the most important reactions contributing to the kerma above 10-15 MeV in carbon and oxygen, *i.e.* the $^{12}C(n,n')3\alpha$ and $^{16}O(n,n'\alpha)^{12}C$ reactions. The former reaction has recently been studied up to 35 MeV by Antolković *et al.* (1975, 1983, 1990), when using the nuclear emulsion technique. The problem is not only to measure the cross section, but also to determine the energies of the three α-particles. For the $^{16}O(n,n'\alpha)^{12}C$ reaction the data base is still meager.

In the higher energy range, double differential cross sections of (n,p), (n,d), (n,t), $(n,\,^3He)$ and (n,α) reactions on carbon, nitrogen and oxygen at 27, 40 and 61 MeV have been reported by the group at the University of California-Davis (Brady, 1979; Romero *et al.*, 1986). These are the only available experimental data in this energy region. Preliminary reports of ongoing experiments with a white neutron source have been given by Pedroni *et al.* (1988).

6.6 Neutron Fluence

Besides measurement of the neutron kerma or partial kerma, the experimental determination of kerma factors requires accurate measurement of the neutron fluence. This poses two difficulties: [1] the absolute fluence measurement and [2] the energy fluence spectrum of the neutron source. Below 20-MeV energy, intense essentially monochromatic, sources of neutrons can be produced by the $^3H(d,n)$, $^2H(d,n)$, and $^3H(p,n)$ reactions (Brolley, 1960). While these same reactions can be employed to produce more energetic neutrons, disintegration of ^2H and ^3H into multiple particles creates a large flux of lower energy contaminating neutrons (Poppe *et al.*, 1963). Bombardment of other low-Z elements by 20-100-MeV protons or deuterons, *e.g.*, $Li(p,n)$ or $Be(p,n)$, generates intense fluxes of neutrons. However, even for thin targets, copious quantities of low energy neutrons are produced. In either case, these "off-energy" neutrons pose a significant complication to kerma determinations by integral techniques.

Neutron fluence measurements contribute on an equal basis with kerma measurements to the kerma factor uncertainty. Ultimately, the neutron fluence is deduced by comparison to an established measured cross-section value. For neutrons below 20 MeV, $^{27}Al(n,\alpha)^4Na$, $^{197}Au(n,2n)^{196}Au$, and $^{19}F(n,2n)^{18}F$ can serve to measure the neutron fluence to < 5% through activation techniques. Proton recoil counters and fission ionization chambers can give somewhat better accuracy through $H(n,p)$ scattering and $^{235,238}U(n,f)$ reactions, respectively. At higher energies, cross-section information is much less certain, perhaps 10-20%.

6.7 Results

Kerma factor measurements by any of the aforementioned techniques are sparse. With the exception of Brady and Romero's values at higher energies (Brady and Romero, 1979; Romero, 1986), measurements have concentrated on a few elements for neutron bombarding energies below 30 MeV. Kerma factor values deduced from microscopic cross-section information are available below 30-MeV neutron energy for many elements (Caswell et al., 1980). Several calculations, based upon nuclear models, are available below 100 MeV for some elements (Alsmiller and Barish, 1977; Behrooz and Watt, 1981; Brenner, 1983; Dimbylow, 1982; Wells, 1979). In subsequent sections, kerma factor values are compared by element and type of determination. For the results of Brady and Romero, in each case the values reported employ a correction for the detection thresholds as discussed by Dimbylow, 1982. These constitute corrections of 28, 16, and 8% at neutron energies of 27.4, 39.7, and 60.7 MeV, respectively.

6.7.1 Carbon

Carbon kerma factor measurements are more extensive than for any other element. Integral determinations were done using calorimetric (McDonald, 1987) and ionization techniques (Binns and Hough, 1990; Bühler et al., 1985; DeLuca et al., 1984; DeLuca et al., 1986; Goldberg et al., 1978; Hartmann et al., 1992; Pihet et al., 1993; Schell et al., 1990; Schrewe et al. 1992; Schuhmacher et al. 1992, Wuu and Milavickas, 1987). Haight et al. (1984) made a partial kerma determination by measuring α-particle production at several emission angles for 14.1 MeV neutron bombardment. At higher neutron energies, Brady and Romero deduced kerma factor values from their charged particle measurements at 27, 40, and 61 MeV (Brady and Romero, 1979). Antolković et al. (1983) measured α-particle production and energy from 11- to 35-MeV neutron energy using photographic emulsions. Using these data, an exact kinematic model, and the partial kerma factor results of Brady and Romero, 1979, a kerma factor value for 27.4 MeV was deduced (Antolković et al., 1984). Below 30-MeV neutron energy, measured kerma factor values from all techniques are in agreement, albeit with experimental uncertainties of 5-10%. Tables XV and XVI summarize these kerma factor values, while Figure 26 plots these values as well as values calculated from microscopic cross-section information (Caswell et al., 1980; Howerton et al., 1986; Gerstenberg et al., 1988) and from theoretical estimates (Alsmiller et al., 1977; Behrooz et al., 1981; Brenner, 1985; Dimbylow, 1982; Wells, 1979).

In the 15- to 30-MeV energy region, measured values are systematically lower than values based on evaluated microscopic cross-section information from ENDF/B-IV,V (Caswell et al., 1980). Gerstenberg et al. (1988) noted that this is largely due to the $^{12}C(n, n')3\alpha$ and $^{12}C(n, \alpha)$ reaction cross sections, which comprise about 24% of the total cross section but contribute more than 70% of the kerma. Gerstenberg's kerma factor values use a recent evaluation of these cross sections combined with ENDF/B-V values for other reaction components and include the measured kerma factor values shown in Tables XV and XVI. Hence, the agreement in values from microscopic cross sections and integral determinations is expected.

Kerma factor estimates based on nuclear models show considerable variance. Values from several estimates are plotted in Figure 26. Differences of 20-40% are apparent above 20-MeV neutron energy. The values of Dimbylow (1982) and Wells (1979) are in fair agreement with measured values in the 20- to 25-MeV region.

Table XV: Measured Kerma Factors at Several Measurements and Neutron Energy
Below 20 MeV

Energy [MeV]	Material/K_f [fGy m^2]							
	C	N	O	Mg	Al	Si	Fe	A-150
13.9	1.93±0.14[60]							6.86±4%[52]
14.1	1.78±0.11[22]							
14.1	1.84±0.16[38]							
14.6	1.80±0.16[48]							
14.7	2.19±0.18[69]			1.22±0.03[69]			0.48±0.22[69]	6.60±0.27[69]
14.7	2.38±0.19[60]							
14.8	2.11±0.42[63]							6.06±1.03[63]
14.9	2.10±0.16[23]							
15.0	2.25±0.49[36]		1.22±0.18[25]	1.52±0.50[36]	1.25±0.11[19]	1.23±0.18[25]	0.59±0.23[36]	7.19±4%[52]
15.0	2.26±0.17[60]							
15.0	2.35±0.24[19]			1.39±0.13[19]	1.35±0.20[24]			
17.0	2.46±0.24[19]				1.24±0.12[19]			7.61±4%[52]
17.0	2.79±0.19[60]							
17.5	2.70±0.20[60]		1.63±0.25[25]		1.58±0.23[24]	1.59±0.23[25]		
17.8	2.92±0.22[24]							
17.9	2.97±0.30[23]							
18.0	2.95±0.42[40]		2.14±0.37[40]					
18.1	3.13±0.23[60]		1.71±0.26[25]		1.57±0.23[24]	1.35±0.20[25]		
18.4	2.93±0.20[60]							5.7± 10%[11]
19.0	2.99±0.20[60]							7.27±4%[52]
19.1			2.22±0.37[25]		1.52±0.25[24]	1.60±0.26[25]		
19.8	3.55±0.28[24]							
20.0	3.24±0.25[60]							

Table XVI: Measured Kerma Factors at Several Measurements and Neutron Energy Above 20 MeV

Energy [MeV]	Material/K_f [fGy m^2]							
	C	N	O	Mg	Al	Si	Fe	A-150
23.0	3.46±0.81[?]		2.01±0.54[?]					
25.0	3.85±1.15[?]		2.58±0.86[?]	2.20±0.40[?]			1.75±0.35[?]	
26.3	3.47±0.29[?]							
27.4	4.68±0.94[?]	3.00±0.20[?]	2.30±0.10[?]					
27.4	4.00±0.10[?]							
37.8	4.10±0.37[?]							
39.7	4.10±0.10[?]	4.20±0.10[?]	3.00±0.20[?]					
58.0	4.80±0.90[?]							
60.7	5.60±0.20[?]	6.10±0.60[?]	5.10±0.50[?]					
66.0	5.00±0.90[?]							
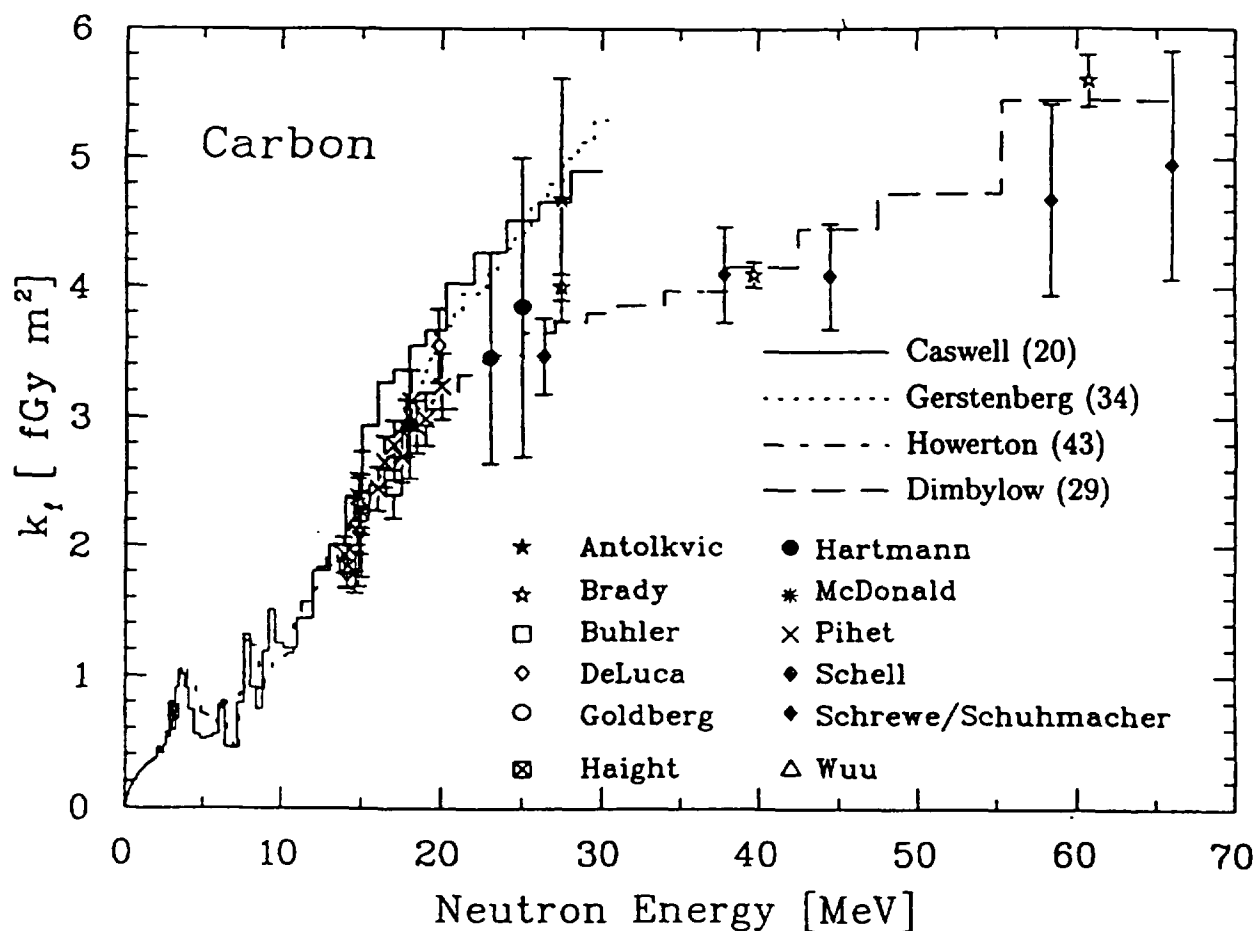
Figure 26: Measured carbon kerma factor values plotted *versus* neutron energy. Also plotted are values based on evaluated microscopic cross sections and nuclear model calculations. See text for references to these results.

Partial kerma factor values or cross sections for elastic and inelastic scattering from discrete states in the energy range 10–40 MeV have recently been published by Börker *et al.* (1988) 6–14 MeV; Glasgow *et al.* (1976) 9–15 MeV; Olsson *et al.* (1989a, 1989b) 16–22 MeV; and Meigooni *et al.* (1984, 1985) 21–26 MeV and also at 40 MeV with data from DeVito (1979). For elastic scattering the data agree quite well with existing evaluations (ENDF/B-VI, 1990) up to about 20 MeV, while for inelastic scattering, especially from the higher excited states, the discrepancies are considerable.

Based on the available experimental measurements and the results of model calculations, we have evaluated the total kerma factor for carbon, for energies between 10 and 70 MeV. Based upon the thresholds of reactions on carbon, their probable cross sections, and numerous modeling calculations, we consider it likely that the kerma factor measured by Brady at the highest energy point (60.7 MeV) is too high. Our evaluation, shown in Figure 27, agrees well with the measurements by Schrewe (1992). We have assigned ±8% as the *minimum* uncertainty in the recommended kerma factor up to neutron energies of 50 MeV. By minimum uncertainty, we mean that given the current database, no realistic uncertainty less than ±8% can be assigned to the recommended value. Above 50 MeV we have assigned a minimum uncertainty of ±16% based on the only two sets of experimental data available. While the errors reported by Schrewe are significantly larger than those of Brady, we have given more weight to the shape and normalization of the Schrewe data based partially on guidance from the change in slope of several model calculations. Table XVII gives the recommended values of the carbon kerma factor as a function of neutron energy from 10 to 70 MeV. Further details can be found in the paper by White *et. al.* (1992) .
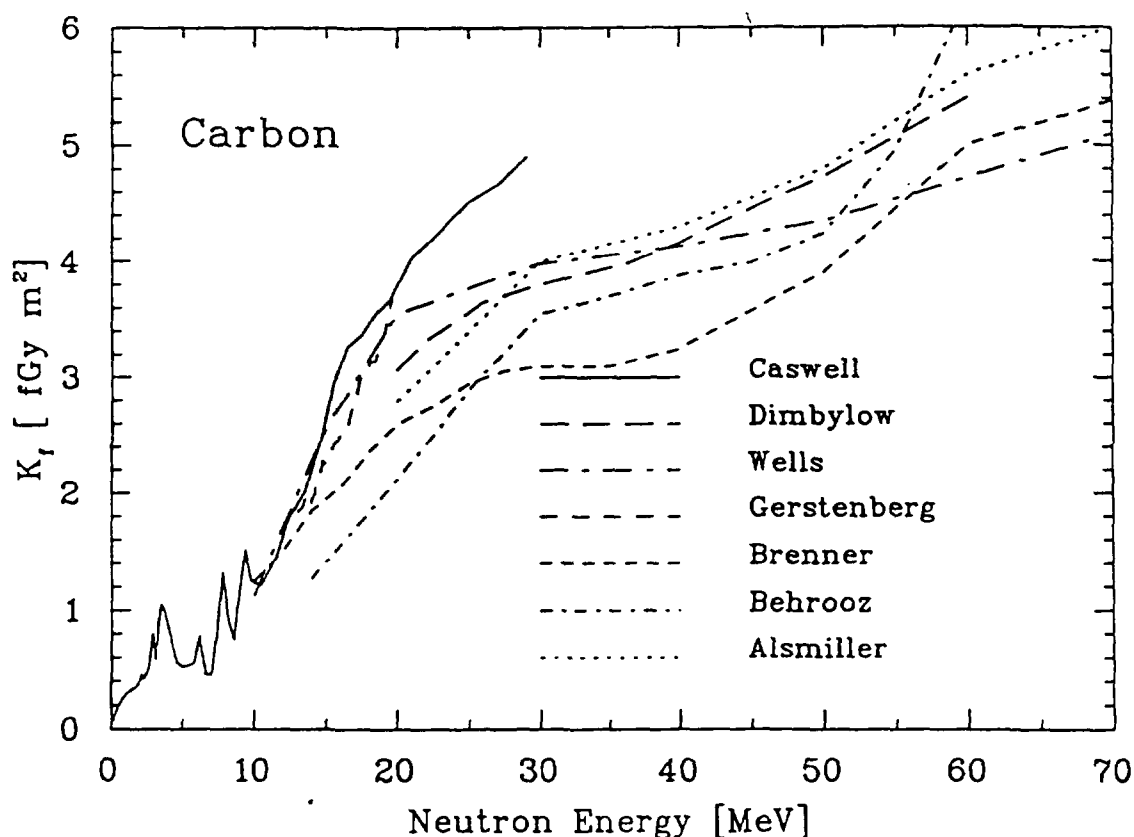
Figure 27: Recommended carbon kerma factor values as a function of incident neutron energy from 10 to 70 MeV. See Fig. 26 for key to experimental measurements.

Table XVII: Recommended neutron kerma factor for carbon. The table is designed for linear-linear interpolation. The minimum uncertainty (see text) is ±8% below 50 MeV and ± 16% above 50 MeV.

E_n (MeV)	K_f (Gy.m^2.10^{-15})
10.0	1.20
12.1	1.75
19.5	3.12
23.1	3.51
30.1	3.86
70.0	5.14

6.7.2 Nitrogen

Nitrogen is a small fraction of tissue composition, see Table X, and contributes minimally to the kerma in tissue. The only measured kerma factors are the partial kerma factor determinations of Brady and Romero (1979) which are summarized in Table XVI, and compared to values deduced from microscopic cross sections in Figure 28.

In addition, partial kerma factors for elastic and inelastic scattering have recently been published by Islam *et al.* (1988) 20 and 25 MeV and by Olsson *et al.* (1990a, 1990b) 21.6 MeV.
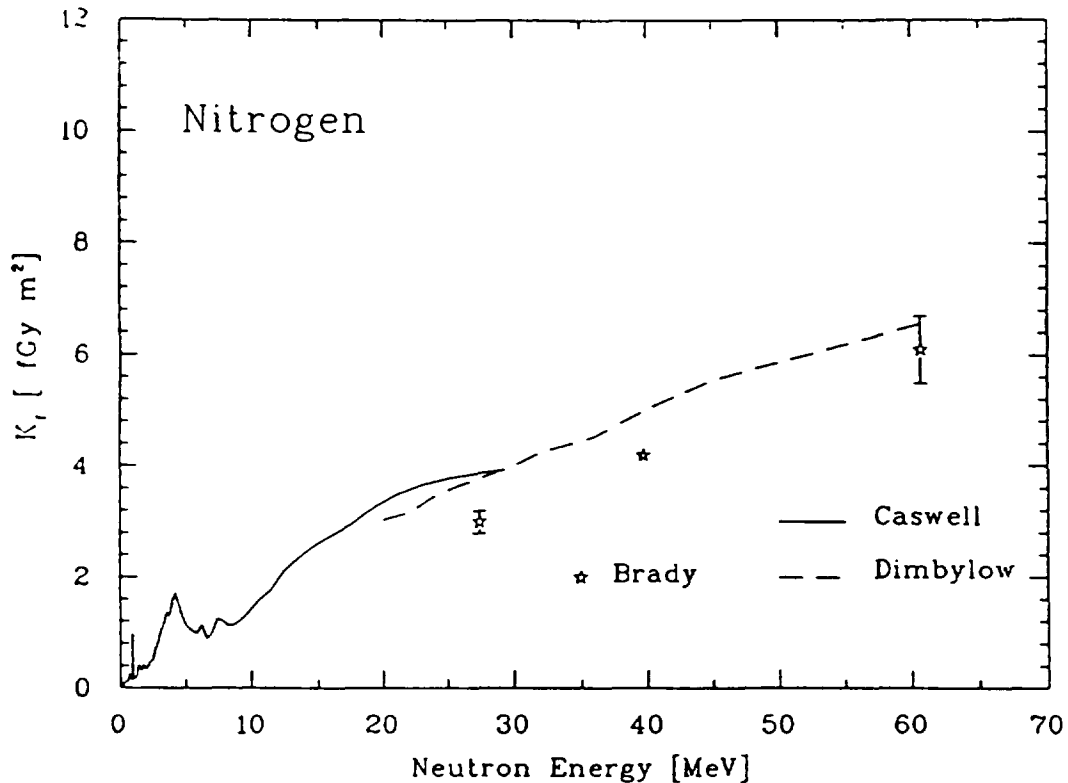
Figure 28: Measured nitrogen kerma factor values plotted *versus* neutron energy. Kerma factor values based on evaluated microscopic cross sections (Caswell *et al.*, 1980), are also shown.

6.7.3 Oxygen and the Carbon-to-Oxygen Kerma Ratio

Next to hydrogen, oxygen is the most important element contributing to tissue kerma. As mentioned above, knowledge of the oxygen-to-carbon kerma factor ratio is essential for conversion of measured dose in tissue-mimicking materials to absorbed dose in tissue. Integral kerma factor determinations were made using matched ZrO_2 and Zr proportional counters (DeLuca et al., 1988; Hartmann, 1990). Brady and Romero (1979) deduced kerma factors from partial charged particle production cross section measurements above 25 MeV. Table XVI summarizes these kerma factor values.

Figure 29 plots measured kerma factors as well as values based upon microscopic cross sections (Caswell et al., 1980; Howerton, (1986)) and nuclear model calculations (Behrooz and Watt, 1981; Alsmiller and Barish, 1977; Dimbylow, 1980; Wells, 1979). As was the case for carbon, measured values for oxygen are for the most part less than values calculated from microscopic cross sections. The model predictions show differences of 10-30%.
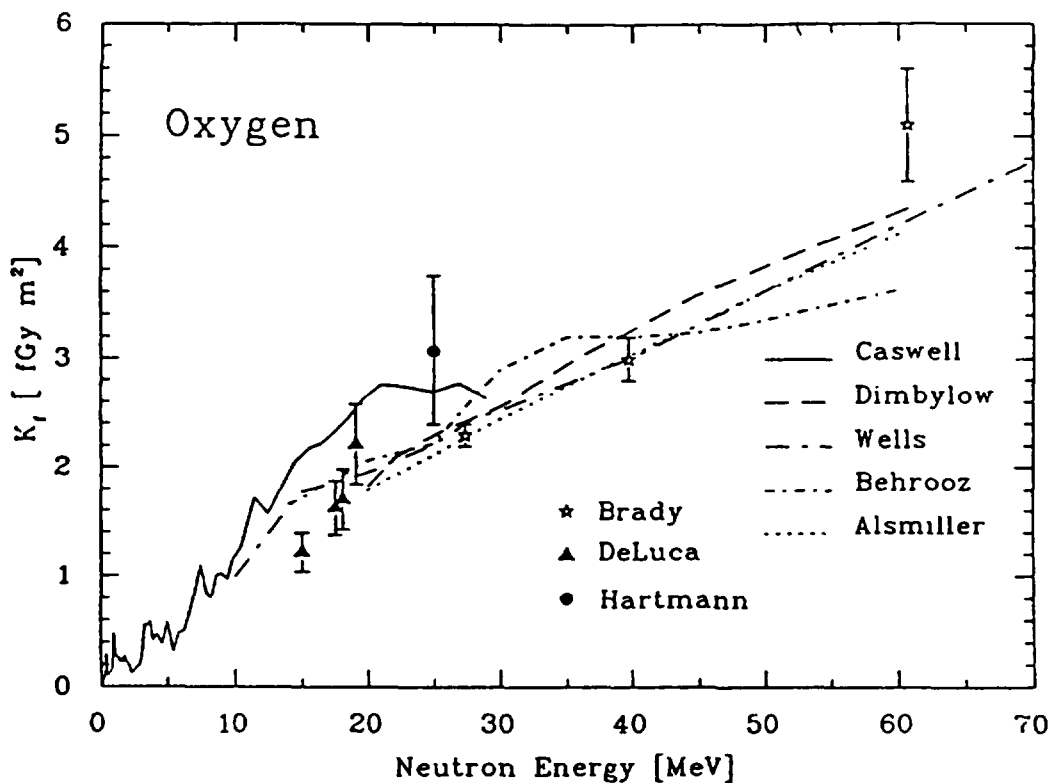
Figure 29: Measured oxygen kerma factor values plotted versus neutron energy. Also plotted are values based on evaluated microscopic cross sections and nuclear model calculations. See text for references to these results.

Recently measured partial kerma factors for elastic and inelastic scattering up to 26 MeV have been published by Börker *et al.* (1988), 6–15 MeV; Islam *et al.* (1987, 1988), 18–26 MeV; and Olsson *et al.* (1990a, 1990b), 21.6 MeV.

Based on the available experimental measurements and the results of model calculations shown in Figure 29 we have evaluated the total kerma factor for oxygen, for energies between 10 and 70 MeV. Since the experimental database for oxygen is so limited, the uncertainties in the total kerma factor are much larger than for carbon. Figure 30 shows our recommended values for the oxygen kerma factors from 10 to 70 MeV. The assignment of ±15% from 10 to 30 MeV for the minimum uncertainty in the recommended kerma factors is dictated by the spread in the experimental data.

Above 30 MeV, a minimum uncertainty of ±20% has been assigned based on our belief that the 60.7 MeV measurement of Brady is high. We based this belief upon knowledge of thresholds of reactions, the systematics of cross sections for these reactions, several model calculations, and the fact that the same energy point for Brady's carbon value is higher than the Schrewe measurements. However, it is the *only* experimental point available at this high energy and, until further measurements are carried out, must fall within the minimum uncertainty estimates on our recommended values. Values of the recommended kerma factors for oxygen are given in Table XVIII. Further details can be found in the paper by White *et. al.* (1992) .

In Figure 31 we plot the recommended carbon-to-oxygen kerma ratio for neutrons from 10 to 70 MeV. The corresponding numerical values are given in Table XIX. These values can be interpolated linearly to obtain the kerma factor ratio at energies other than those listed. Because the recommended carbon and oxygen kerma values each had two (non-overlapping) regions where the minimum assigned uncertainty changed, the recommended ratio has three regions of differing uncertainties, as indicated in Figure 31. Because Brady (1979) and Hartmann (1992) each measured carbon and oxygen at the same energies, Figure 31 includes their ratios with their corresponding uncertainties. Also plotted is the ratio of DeLuca's (1985) carbon measurement at 14.9 MeV to his (1988) measurement of oxygen at 15 MeV. DeLuca's (1988) measurements of oxygen at 17.5 and 18.1 MeV were interpolated linearly and used with his carbon measurement (1986) at 17.8 MeV to obtain the ratio point at 17.8 MeV. DeLuca's (1986) measurement of carbon at 19.8 MeV was used with his (1988) oxygen measurement at 19.1 MeV and plotted as 19.45 MeV. These ratio data are plotted in Figure 31 for informational purposes only and were not used to determine the recommended carbon-to-oxygen kerma ratios. the recommended ratio was determined from the separate evaluations of carbon and oxygen.

The purpose of this carbon-to-oxygen ratio evaluation is two-fold: (1) to establish a recommended value for this ratio based upon all available direct measurements and model calculations currently known to us; and (2) to give an uncertainty estimate to this ratio. We have chosen a minimum uncertainty which is only meant to indicate that no lesser uncertainty could reasonably be placed on the values. It does not mean that the uncertainty is not greater. It is not a precise definition, but only meant to serve as a guide to the current state-of-the-art and to indicate where further measurements are needed.
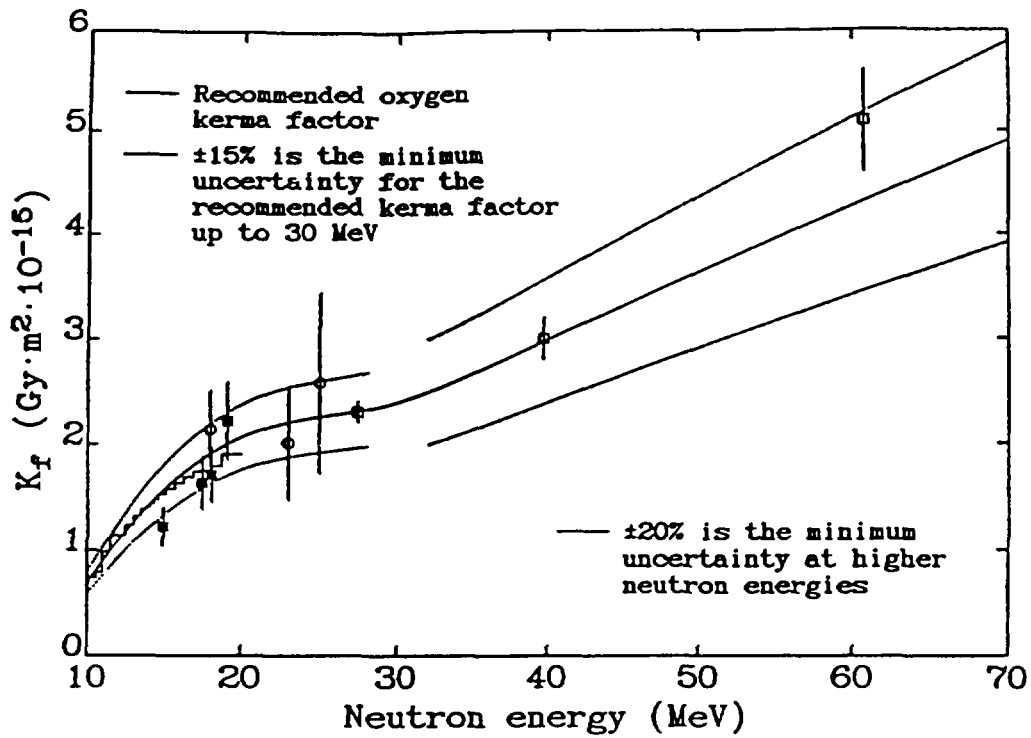
Figure 30: Recommended oxygen kerma factor values as a function of incident neutron energy from 10 to 70 MeV. See Fig. 31 for key to experimental measurements.
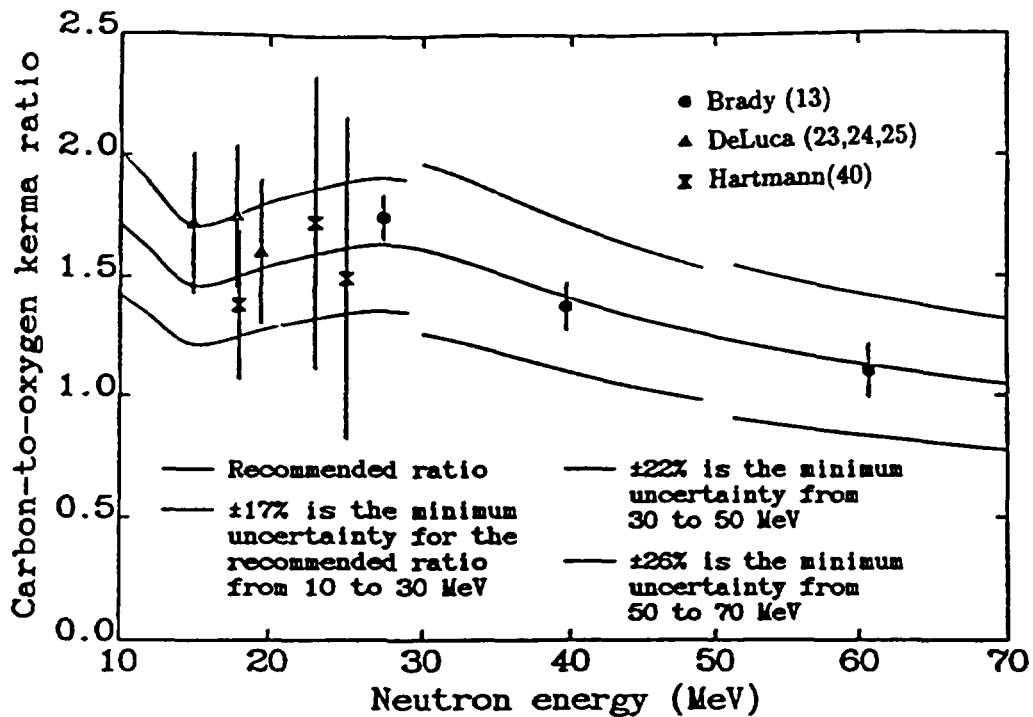
Figure 31: Recommended carbon-to-oxygen kerma factor ratio from 10 to 70 MeV with the ratios of specific data included. See text for details.

Table XVIII: Recommended neutron kerma factor for oxygen. The table is designed for linear-linear interpolation. The minimum uncertainty (see text) is ±15% below 30 MeV and ± 20% above 30 MeV.

E_n (MeV)	K_f (Gy.m^2.10^{-15})
10.0	0.70
13.2	1.28
15.8	1.67
18.9	1.99
22.5	2.19
30.5	2.42
40.7	3.03
70.0	4.91

Table XIX: Recommended ratio of carbon to oxygen kerma factors. The table is designed for linear-linear interpolation. The minimum uncertainty (see text) is ±17% below 30 MeV, ± 22% between 30 and 50 MeV, and ± 26% above 50 MeV.

E_n (MeV)	Ratio
10.0	1.72
14.6	1.47
17.3	1.49
26.1	1.62
30.9	1.60
46.0	1.30
61.5	1.12
70.0	1.05

6.7.4 Magnesium

Integral kerma factor determinations are available below 30-MeV neutron energy using proportional counters and ionization chambers. The measured values near 15 MeV are in good agreement and consistent with values based on microscopic cross sections, see Table XV and Figure 32. The single measured value at 25 MeV is somewhat larger than the predictions of Dimbylow, (1982), and significantly greater than that based on microscopic cross sections (Caswell et al., 1980).

6.7.5 Aluminum

As was the case for magnesium, integral aluminum kerma factor determinations were made below 30-MeV neutron energy using low pressure proportional counters and values are reported in Table XVI. Kerma factor values deduced from microscopic cross-section information (Caswell et al., 1980) indicate a trend opposite to the only model calculation of Dimbylow (1982). Measurements near 15 MeV are in good agreement, while those at higher energies are more consistent with the model predictions of Dimbylow. Figure 33 plots measured and calculated values versus neutron energy.

6.7.6 Silicon

Several integral kerma factor determinations have been made using proportional counters in the 15 to 25 MeV neutron energy range (DeLuca et al., 1988; Hartmann, 1990).
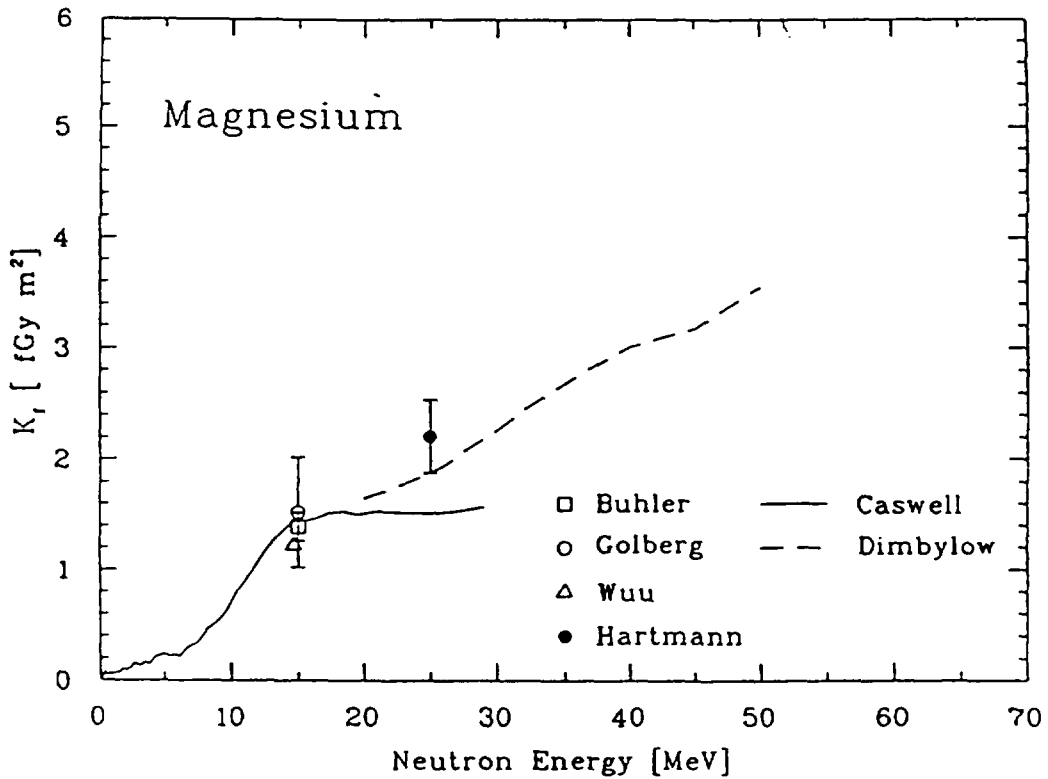
Figure 32: Measured magnesium kerma factor values plotted *versus* neutron energy. Also shown are values based on evaluated microscopic cross sections (Caswell *et al.*, 1980) and the model calculation of Dimbylow (1982).
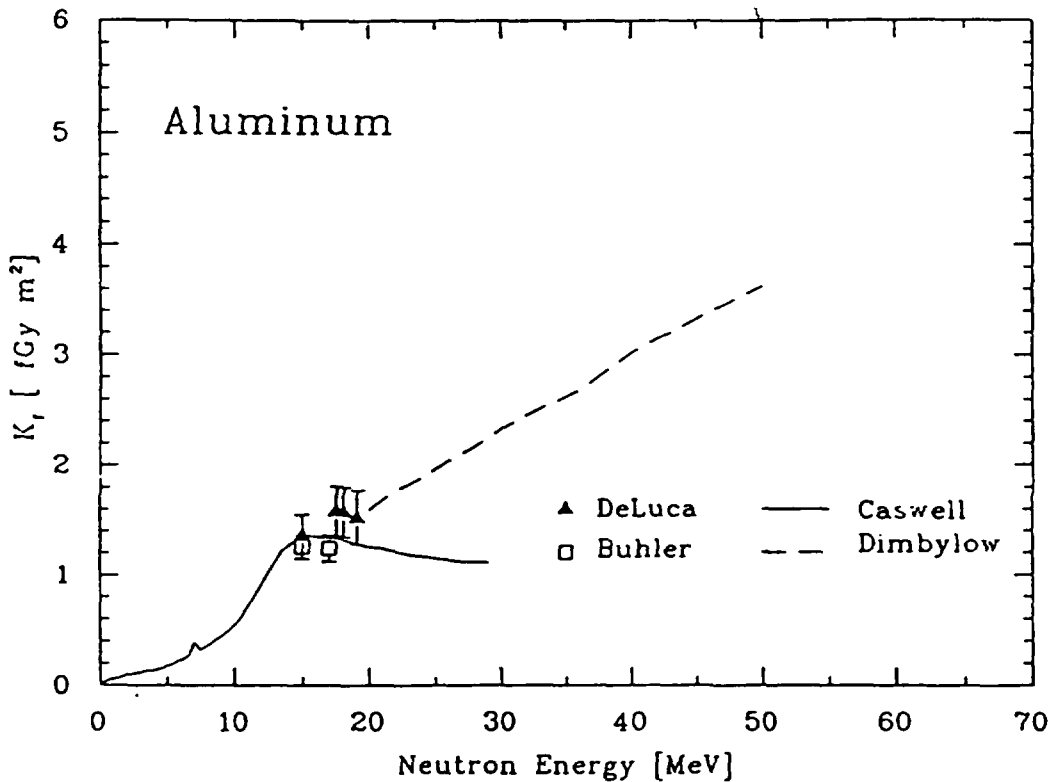
Figure 33: Measured aluminum kerma factor values plotted *versus* neutron energy. Also shown are values based on evaluated microscopic cross sections (Caswell *et al.*, 1980) and the model calculation of Dimbylow (1982).

Tables XV and XVI indicate these values, which are also plotted in Figure 34 along with tabulated values based upon microscopic cross-section information (Caswell *et al.*, 1980).

6.7.7 Calcium

Elastic and inelastic scattering partial kerma factors for four energies in the range 20–26 MeV have been determined by Islam *et al.* (1988) and at 21.6 MeV by Olsson *et al.* (1987, 1990a). Partial kerma factors for elastic scattering at 30 and 40 MeV have been deduced by Islam *et al.* (1988) from data measured by DeVito, (1979).

6.7.8 Iron

Very little experimental information is available for iron. Wuu and Milavickas (1960) and Goldberg *et al.* (1978) made integral determinations near 15 MeV using low pressure proportional counters and ionization chambers, respectively. These values are indicated in Table XV and plotted in Figure 35. Also plotted are values based on microscopic cross-section information (Caswell *et al.*, 1980). For iron the experimental and calculated values are in agreement.

6.7.9 A-150 Tissue Equivalent Plastic

A-150 tissue equivalent plastic is commonly employed in ionization chamber construction for devices used in neutron dosimetry. Neutron tissue dose is deduced by converting the response in the A-150 instrument to tissue, usually by the ratio of
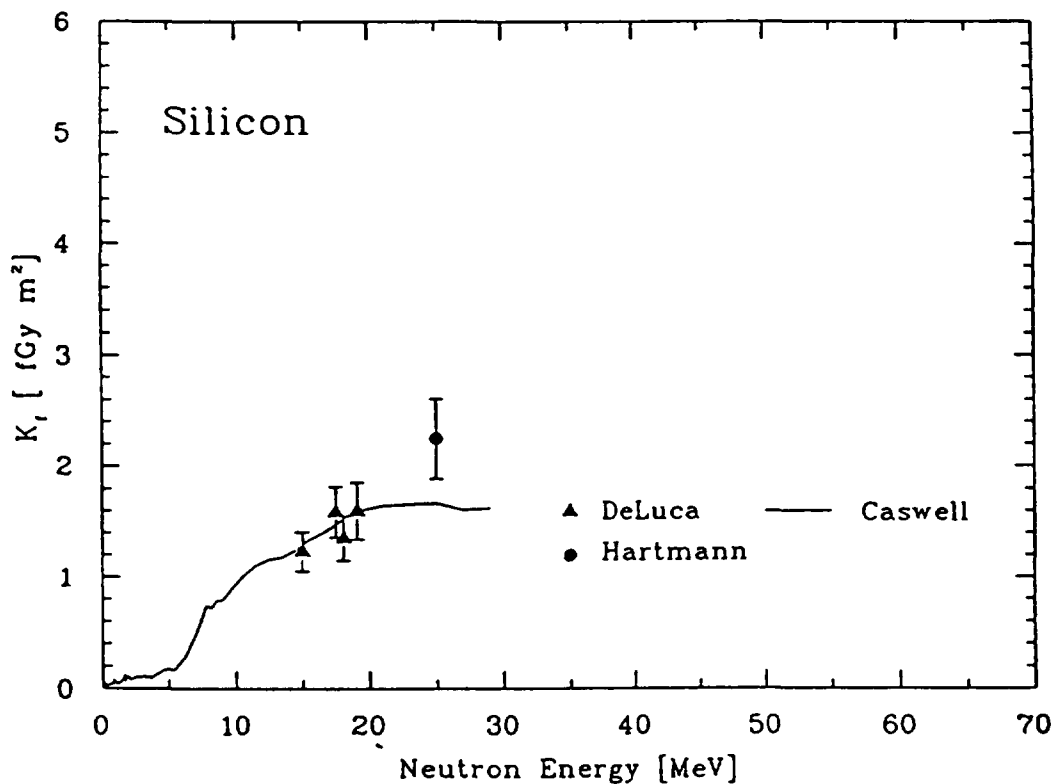
Figure 34: Measured silicon kerma factor values plotted *versus* neutron energy. Also shown are values based on evaluated microscopic cross sections (Caswell *et al.*, 1980).

collision kerma factors for tissue-to-A-150. In a manner similar to other integral ionization measurements, A-150 kerma factors have been determined. Table XV lists the available measured values. Menzel *et al.* (1984); Wuu and Milavikas (1960); and Binns and Hough (1990) employed spherical A-150 plastic proportional counters, while Schell *et al.* (1990) used a hemispherical A-150-walled counter telescope to deduce A-150 kerma. A-150 kerma factor values, along with those calculated from microscopic cross-section information are plotted in Figure 36. With the exception of the value reported by Binns and Hough (1990), measured values are in agreement. As the A-150 kerma is dominated by hydrogen, 10.2% by mass fraction and ≈ 70% by kerma factor, uncertainties due to the carbon kerma factor contribution are obscured. Hence, the agreement between measured and microscopic-based kerma factors is not unexpected.
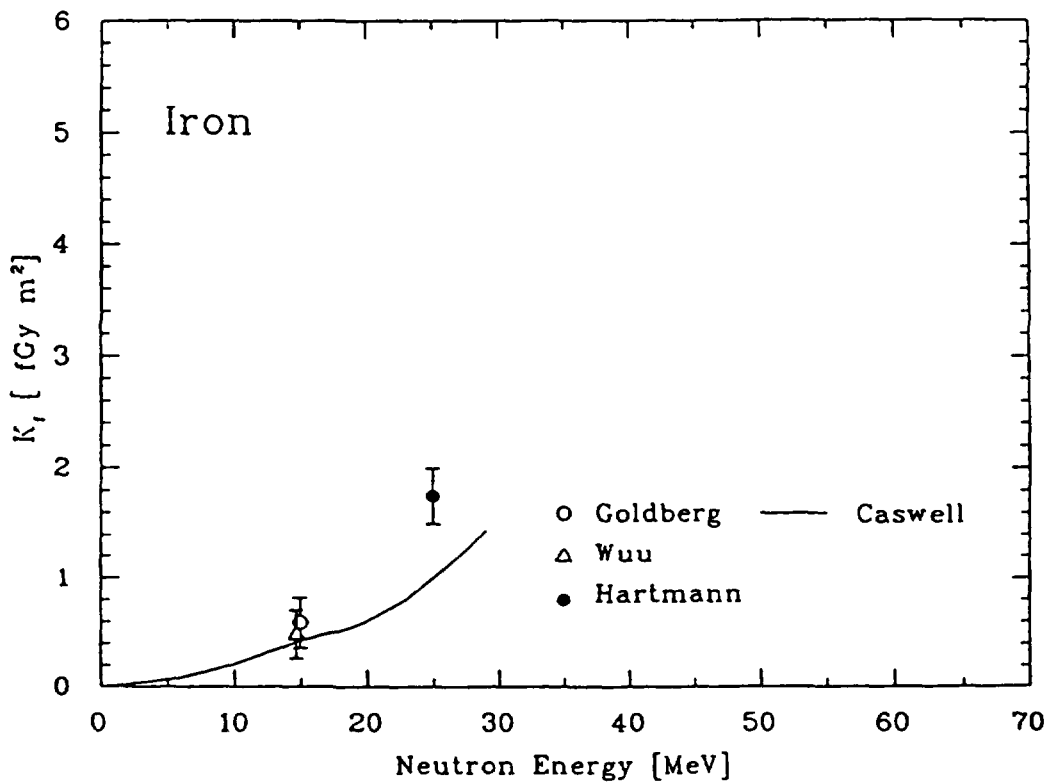
Figure 35: Measured iron kerma factor values plotted *versus* neutron energy. Also shown are values based on evaluated microscopic cross sections (Caswell *et al.*, 1980).
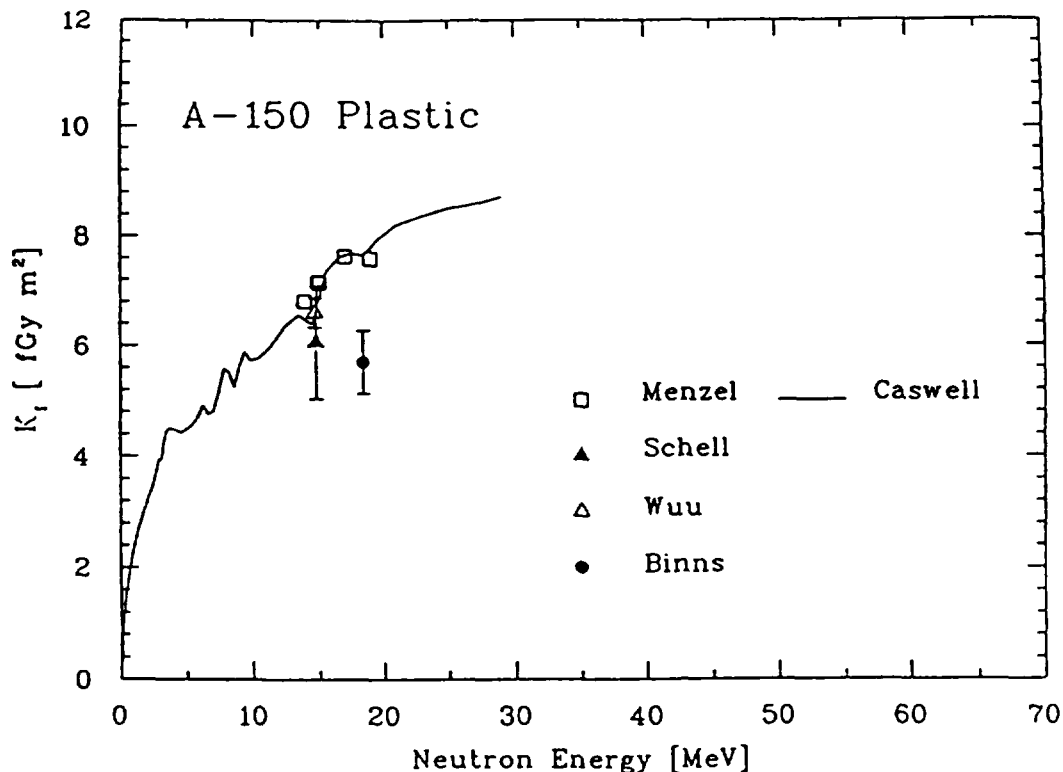
Figure 36: Measured A-150 plastic kerma factor values plotted *versus* neutron energy. Also shown are values based on evaluated microscopic cross sections (Caswell *et al.*, 1980).

References

Alarcon, R., and Rapaport, J., "Neutron Elastic and Inelastic Scattering from ^{28}Si, ^{32}S, and ^{34}S," *Nucl. Phys. A* **458**, 502 (1986).

Alsmiller, R.G., Jr., and Barish, J., "Neutron Kerma Factors for H, C, N, O, and Tissue in the Energy Range of 20-70 MeV," *Health Phys.* **33**, 98 (1977).

Antolković, B., and Dolenec, Z., "The Neutron-induced ^{12}C(n,n'3α) Reaction at 14.4 MeV in a Kinematically Complete Experiment," *Nucl. Phys. A* **237**, 235 (1975).

Antolković, B., Šlaus, I., and Plenković, D., "Study of the Reaction ^{12}C(n,3α)n from Threshold to E_n=35 MeV," *Nucl. Phys. A* **394**, 87 (1983).

Antolković, B., Šlaus, I., and Plenković, D., "Experimental Determination of the Kerma Factors for the Reaction ^{12}C(n,n'3α) at E_n=10-35 MeV," *Radiat. Res.* **97**, 253 (1984).

Antolković, B., Dietze, G., and Klein, H., "Reaction Cross Sections on Carbon for Neutron Energies From 11.5 MeV to 19 MeV," *Nucl. Sci. Eng.* **107**(1), 1-21 (1991).

Arndt, R.A., Roper, L.D., Bryan, R.A., VerWest, B.J., and Signell, P., "Nucleon-Nucleon Partial-Wave Analysis to 1 GeV," *Phys. Rev. D* **28**, 97 (1983).

Arndt, R.A., Hyslop III, J.S., and Roper, L.D., "Nucleon-Nucleon Partial-Wave Analysis to 1100 MeV," *Phys. Rev. D* **35**, 128 (1987).

Arndt, R.A., "Uncertainties in the np Interaction at Medium Energies," *Phys. Rev. D* **37**, 2665 (1988).

Behrooz, M.A., and Watt, D.E., "An Appraisal of Partial Kerma Factors for Neutrons Up to 60 MeV," In: *Proc. 4th Symposium on Neutron Dosimetry*, Munich/Neuherberg, FRG, EUR-7448, 353 (Commission of the European Communities, Luxembourg) (1981).

Binns, P.J. and Hough, J.H., "Determination of Neutron Kerma Factors for A150 Plastic and Carbon at 18.4 MeV," *NAC Annual Report*, NAC/AR/90-01, June 1990 (National Accelerator Center, Faure, RSA) (1990).

Börker, G., Bottger, R., Brede, H.J., Klein, H., and Siebert, B.R.L., "Partial Kerma Factors for Carbon and Oxygen Obtained From Cross Section Measurements," *Radiat. Prot. Dosim.* **23**, 23-26 (1988).

Brady, F.P. and Romero, J.L., "Neutron Induced Reactions in Tissue Resident Elements," Final Report to the National Cancer Institute, Grant No. 1R01 CA16261, University of California, Davis, CA (1979).

Brenner, D.J., Prael, R.E., Dicello, J.F., and Zaider, M., "Improved Calculations of Energy Deposition from Fast Neutrons," In: *Proc. 4th Symposium on Neutron Dosimetry*, Munich/Neuherberg, FRG, EUR-7448, 103 (Commission of the European Communities, Luxembourg) (1981).

Brenner, D.J., "Neutron Kerma Values Above 15 MeV Calculated with a Nuclear Model Applicable to Light Nuclei," *Phys. Med. Biol.* **29**, 437 (1983).

Brenner, D.J. and Prael, R.E., "Calculated Differential Secondary-Particle Production Cross Sections after Nonelastic Neutron Interactions with Carbon and Oxygen between 15 and 60 MeV," *Atomic Data and Nuclear Data Tables* **41**, 71 (1989).

Brolley, J.E., Jr. and Fowler, J.L., "Monoenergetic Neutron Sources: Reactions with Light Nuclei", In: *Fast Neutron Physics: Part I: Techniques*, J.B. Marion and J.L. Fowler (eds.), p. 73, Interscience Publishers, Inc., New York (1960).

Bühler, G., Menzel, H., Schuhmacher, H., and Guldbakke, S., "Dosimetric Studies with Non-hydrogenous Proportional Counters in Well Defined High Energy Neutron Fields," In: *Proc. 5th Symposium on Neutron Dosimetry*, Munich/Neuherberg, FRG, EUR-9762, 309 (Commission of the European Communities, Luxembourg) (1985).

Bühler, G., Menzel, H., Schuhmacher, H., Dietze, G., and Guldbakke, S., "Neutron Kerma Factors for Magnesium and Aluminum Measured with Low-pressure Proportional Counters," *Phys. Med. Biol.* **31(6)**, 601 (1986).

Caswell, R.L., Coyne, J.J., and Randolph, M.L., "Kerma Factors for Neutron Energies below 30 MeV," *Radiat. Res.* **83**, 217-254 (1980).

Cocu, F., Haout, G., Lachkar, J., Patin, Y., Sigaud, J., and Dalbera, G., "Sections Efficaces Diferentielles et Totale de la Reaction $^{12}C(n,n'3\alpha)$ a E_n=14.2 MeV," CEA-R-4746, Center d'Etudes de Buyères-le-Châtel (1976).

DeLuca, P.M., Jr., Barschall, H.H., Haight, R.C., and McDonald, J.C., "Kerma Factor of Carbon for 14.1 MeV Neutrons," *Radiat. Res.* **100**, 78 (1984).

DeLuca, P.M., Jr., Barschall, H.H., Haight, R.C., and McDonald, J.C., "Measured Neutron Carbon Kerma Factors from 14.1 MeV to 18 MeV," In: *Proc. Fifth Symposium on Neutron Dosimetry*, Schraube, H., Burger, G., and Booz, J. (eds.), ENDIP-2, pp. 193-200, EUR 9762 (Commission of the European Communities, Luxembourg)(1985).

DeLuca, P.M., Jr., Barschall, H.H., Burhoe, M., and Haight, R.C., "Carbon Kerma Factor for 18- and 20-MeV Neutrons," *Nucl. Sci. Eng.* **94**, 192 (1986).

DeLuca, P.M., Jr., Barschall, H.H., Sun, Y., and Haight, R.C., "Kerma Factor of Oxygen, Aluminum, and Silicon for 15- and 20-MeV Neutrons," *Radiat. Prot. Dos.* **23**, 27 (1988).

DeLuca, P.M., Jr., Barschall, H.H., Hartmann, C.L., and Pearson, D.W., "Corrections to Kerma Factor Measurements Made by Integral Techniques," *Nucl. Inst. Meth.* **40/41**, 1279 (1989).

Dev79 DeVito, R.P., Ph.D. Thesis, Michigan State University (1979).

Dimbylow, P.J., "Neutron Cross-section and Kerma Values for Carbon, Nitrogen, and Oxygen from 20 to 50 MeV," *Phys. Med. Biol.* **25(4)**, 673 (1980).

Dimbylow, P.J., "Neutron Cross-section and Kerma Value Calculations for C, N, O, Mg, Al, P, S, Ar, and Ca from 20 to 50 MeV," *Phys. Med. Biol.* **27(8)**, 989 (1982).

ENDF/B-VI, "Evaluated Nuclear Data File," National Nuclear Data Center, Brookhaven National Laboratory, Upton, NY (1990).

Fabian, H., "Interaction of 14.0 MeV-Neutrons with ^{12}C in Stilbene," *Z. Naturforsch.* **26A**, 317 (1971).

Finlay, R.W., Meigooni, A.S., Petler, J.S., and Delaroche, J.P., "Partial Kerma Factors for Neutron Interactions with ^{12}c Between 9 and 12 MeV," *Nucl. Instrum. Methods* **B10/11**, 396 (1985).

Frye, G.M., Rosen, L., and Stewart, L., "Disintegration of Carbon into Three Alpha Particles by 12-20 MeV Neutrons," *Phys. Rev.* **99**, 1375 (1955).

Gerstenberg, H.M., Caswell, R.L., and Coyne, J.J., "Initial Spectra of Neutron-Induced Secondary Charged Particles," *Radiat. Prot. Dosim.* **23(1)**, 41 (1988).

Glasgow, D.W., Purser, F.O., Hogue, H., Clement, J.C., Steltzer, K., Mack, G., Boyce, J.R., Epperson, D.H., Buccino, S.G., Lisowski, P.W., Glendinning, S.G., Bilpuch, E.G., Newson, H.W., and Gould, C.R., "Differential Elastic and Inelastic Scattering of 9 to 15 MeV Neutrons from Carbon," *Nucl. Sci. Eng.* **61**, 521 (1976) (revised in 1982 by C.R. Gould).

Goldberg, E., Slaughter, D.R., and Howell, R.H., "Experimental Determination of Kerma Factors at E_n=15 MeV," Report UCID-17789 (Lawrence Livermore Laboratory, Livermore, CA) (1978).

Grin, G., Vaucher, B., Alder, J., and Joseph, C., "^{12}C(n,n), (n,n'), (n,n')3α Reactions at 14.1 MeV," *Helvetica Physica Acta* **42**, 990 (1969).

Haight, R.C., Grimes, S.M., Johnson, R.G., and Barschall, H.H., "The ^{12}C(n,α) Reaction and the Kerma Factor of Carbon at E_n = 14.1 MeV," *Nucl. Sci. Eng.* **87**, 41 (1984).

Hansen, L.F., "Recommended Set of Neutron Differential Cross Sections for Carbon at 14.1 MeV," Lawrence Livermore National Laboratory Report UCRL-95890 (1986); Hansen, L.F. and Meigooni, A., "Coupled-channel Analysis of Neutron Scattering from Carbon Between 9 and 15 MeV," Proceedings of an International Conference on Fast Neutron Physics, Dubrovnik, Yugoslavia, May 26-31 (1986).

Hartmann, C.L., DeLuca, Jr., P.M., and Pearson, D.W., "Measurement of Neutron Kerma Factors in C, O, and Si at 18, 23, and 25 MeV," *Radiat. Prot. Dos.* **44**(1/4), 25-30 (1992).

Hauser, W. and Feshbach, H., "The Inelastic Scattering of Neutrons," *Phys. Rev.* **87**(2), 366 (1952).

Hopkins, J.C. and Breit, G., "The ^{1}H(n,n)^{1}H Scattering Observables Required for High-precision Fast-neutron Measurements," *Nucl. Data Tables A* **9**, 137 (1971).

Howerton, R.J., "Calculated Neutron KERMA Factors Based on the LLNL ENDL File. Lowrence Livermore National Laboratory Report UCRL-50400 27: revised (1986).

International Commission on Radiation Units and Measurements, *Radiation Quantities and Units*, Report 33, (International Commission on Radiation Units and Measurements, Bethesda, MD) (1980).

International Commission on Radiation Units and Measurements, *Microdosimetry*, Report 36, (International Commission on Radiation Units and Measurements, Bethesda, MD) (1983).

Islam, M.S., Finlay, R.W., and Petler, J.S., "Elastic and Inelastic Scattering of Nucleons from ^{16}O," *Nucl. Phys. A* **464**, 395 (1987).

Islam, M.S., Finlay, R.W., Petler, J.S., Rapaport, J., Alarcon, R., and Wierzbicki, J., "Neutron Scattering Cross Sections and Partial Kerma Values for Oxygen, Nitrogen and Calcium at 18 < E_n < 60 MeV," *Phys. Med. Biol.* **33**, 315-328 (1988).

McDonald, J.C., "Calorimetric Measurements for the Carbon Kerma Factor for 14.6-MeV Neutrons," *Radiat. Res.* **109**(1), 28-35 (1987).

Meigooni, A.S., Petler, J.S., and Finlay, R.W., "Scattering Cross-sections and Partial Kerma Factors for Neutron Interactions with Carbon at 20 < E_n < 65 MeV," *Phys. Med. Biol.* **29**, 643-659 (1984).

Meigooni, A.S., Finlay, R.W., Petler, J.S., and Delaroche, J.P., "Nucleon-induced Excitation of Collective Bands in ^{12}c," *Nucl. Phys. A* **445**, 304 (1985).

Mellema, S., Finlay, R.W., Dietrich, F.S., and Petrovich, F., "Microscopic and Conventional Optical Model Analysis of Fast Neutron Scattering from ^{54,56}Fe," *Phys. Rev. C* **28(6)**, 2267 (1983).

Menzel, H., Bühler, G., Schumacher, H., Muth, H., Dietze, G., and Guldbakke, S., "Ionization Distributions and A-150 Plastic Kerma for Neutrons Between 13.9 and 19.0 MeV Measured with a Low Pressure Proportional Counter," *Phys. Med. Biol.* **29**, 1537 (1984).

Olsson, N., Trostell, B., and Ramström, E., Holmqvist, B., and Dietrich, F.S., "Microscopic and Conventional Optical Model Analysis of Neutron Elastic Scattering at 21.6 MeV over a Wide Mass Range," *Nucl. Phys. A* **472**, 237-268 (1987).

Olsson, N., Trostell, B., and Ramström, E., "Cross Sections and Partial Kerma Factors for Elastic and Inelastic Neutron Scattering From Carbon in the Energy Range 16.5-22.0 MeV," *Phys. Med. Biol.* **34**, 909-926 (1989a).

Olsson, N., Trostell, B., and Ramström, E., "Neutron Elastic and Inelastic Scattering from Carbon in the Energy Range 16.5-22.0 MeV," *Nucl. Phys. A* **496**, 505-529 (1989b).

Olsson, N., Ramström, E., and Trostell, B., "Neutron Elastic and Inelastic Scattering from Mg, Si, S, Ca, Cr, Fe and Ni at E_n = 21.6 MeV," *Nucl. Phys. A* **513**, 205-238 (1990a).

Olsson, N., Ramström, E., and Trostell, B., "Cross Sections and Partial Kerma Factors for Elastic and Inelastic Neutron Scattering From Nitrogen, Oxygen and Calcium at E_n = 21.6 MeV," *Phys. Med. Biol.* **35**, 1255-1270 (1990b).

Petler, J.S., Islam, M.S., Finlay, R.W., and Dietrich, F.S., "Microscopic Optical Model Analysis of Nucleon Scattering from Light Nuclei," *Phys. Rev. C* **32(3)**, 673 (1985).

Pedroni, R.S., Boukharouba, N., Grimes, S.M., Mishra, V., and Haight, R.C., "A Facility for Measuring Charged Particles Emitted in Neutron-Induced Reactions up to 50 MeV," *Bull. Am. Phys. Soc.* **33**, 1577 (1988).

Pihet, P., Guldbakke, S., Menzel, H.G., and Schuhmacher, H., "Measurement of Kerma Factors for Carbon and A-150 Plastic: Neutron Energies From 13.9 MeV to 20.0 MeV," *Phys. Med. Biol.* **37**, 1957-1976 (1992).

Poppe, C.H., Holbrow, C.H., and Borchers, R.R., "Neutrons from $D+T$ and $D+H^*$," *Phys. Rev.* **129(2)**, 733 (1963).

Romero, J.L., Brady, F.P., and Subramanian, T.S., "Neutron Induced Charged Particle Spectra and Kerma From 25 to 60 MeV," In: *Proc. Int. Conf. on Nuclear Data for Basic and Applied Science*, Santa Fe, NM, P.G. Young *et al.* (eds.), Vol. 1, pp. 687-699, Gordon and Breach Science Publishers, New York (1986).

Schell, M.C., Pearson, D.W., DeLuca, Jr., P.M., and Haight, R.C., "Measurement of Dose Distributions of Linear Energy Transfer in Matter Irradiated by Fast Neutrons," *Med. Phys.* **17(1)**, 1 (1990).

Schrewe, U.J., O'Brede, H.J., Gerdung, S, Nolte, R., Pihet, P., Schmelzbach, P., and Schuhmacher, H., "Determination of Kerma Factors of A-150 Plastic and Carbon at Neutron Energies Between 145 and 66 MeV, *Radiat. Prot. Dos.* **44**(1/4), 21-24 (1992).

Schuhmacher, H., Brede, H.J., Henneck,R., Kunz, A., Meulders, J.P., Pihet, P., and Schrewe, U.J., "Measurement of Neutron Kerma Factors for Carbon and A-150 Plastic at Neutron Energies of 26.3 MeV and 37.8 MeV," *Phys. Med. Biol.* **37**(6), 1265 (1992).

Vasilév, S., Lomarov, V., and Popova, A., "Dissociation of C^{12} into Three Alpha Particles by 12-20 MeV Neutrons," *Soviet Physics JETP* **6**, 1016 (1958).

Wells, A.H., "A Consistent Set of Kerma Values for H, C, N, and O for Neutrons of Energies from *10 to 80 MeV*," *Radiat. Res.* **80**, 1 (1979).

White, R.M., Broerse, J.J., DeLuca Jr., P.M., Dietze, G., Haight, R.C., Kawashima, K., Menzel, H.G., Olsson, N., and Wambersie, A., "Status of Nuclear data for use in Neutron Therapy," *Radiat. Prot. Dos.* **44**(1/4), 11-20 (1992).

Wuu, C., and Milavickas, L., "Determination of the Kerma Factors in Tissue-equivalent Plastic, C, Mg, and Fe for 14.7 MeV Neutrons," *Med. Phys.* **14**(6), 1007-1014 (1960).

7 Absorbed Dose and Radiation Quality

7.1 Introduction

In radiation therapy of malignant tumors, the prescription of doses to the tumor itself ("gross tumor volume"), the doses delivered to the normal tissue and the related treatment planning are based on the quantity absorbed dose. This quantity has proven to be suitable in photon and electron radiation therapy because the biological effects observed in radiobiological experiments and in clinical experience are uniquely related to absorbed dose (for a given time pattern or "fractionation"). Reporting and recording of radiation treatments, and therefore the transfer of clinical experience, are based entirely on absorbed dose and its distribution within malignant and normal tissue.

The dose prescription is based on such clinical experience and for curative treatment, *i.e.* the intended eradication of all clonogenic tumor cells, the absorbed dose must exceed a certain limit over the entire clinical target volume. The maximum dose which can be delivered to a given tumor depends on the dose received by so called organs at risk or, more generally, on the tolerance of the irradiated normal tissue. The probability of local tumor control depends on this maximum dose and the uniformity of the absorbed dose within the clinical target volume. Treatment planning is used in order to optimize the beam arrangement with regard to these two aspects.

The requirement of high accuracy in the delivery of absorbed dose to the clinical target volume is determined by the steepness of the dose-response curves for tumor control and complications in normal tissues (see Figure 37). With respect to the quality control of therapeutic irradiations, it also includes the requirement of reproducibility.

All these considerations based on experience in photon radiation therapy are also applicable in principle to neutron radiation therapy. However, there are additional aspects to be taken into account. The particular problems of clinical neutron dosimetry with regard to the requirement of basic nuclear data have been addressed in preceding sections, and the more practical problems of clinical neutron dosimetry are discussed in length in ICRU Report 45 (1989).

In this section, the role of radiation quality for neutron radiation therapy is summarized. In contrast to photons (above several 100 keV), neutrons do not produce the same biological effect for a given absorbed dose. The effectiveness of the radiation depends on the energy (spectrum) of the neutrons, and on the fraction of dose due to gamma rays in a given beam. This phenomenon is usually described by the beam radiation quality. It is generally accepted that radiation quality is related to the microscopic pattern of the discontinuously distributed points of interactions and interaction products along the path of charged particles on a molecular and cellular level. The investigation of these patterns and their relevance for the subsequent chemical and biological processes is the subject of the field of microdosimetry (ICRU, 1983).

7.1.1 The Microdosimetric Approach

In phenomenological terms, biological effectiveness, example expressed as RBE, increases with the LET of a charged particle or its ionization density within its track up to a maximum above which the RBE decreases again. This decrease is generally attributed to saturation effects. In spite of considerable progress in microdosime-
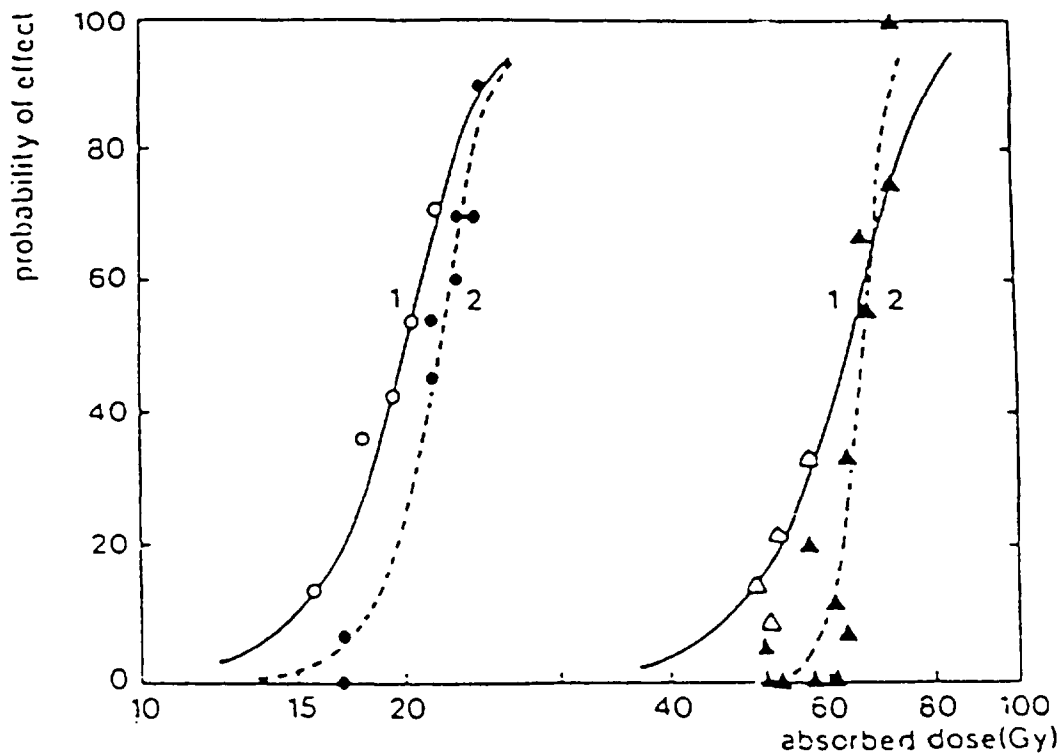
Figure 37: Dose-effect relationships for tumor control (solid line) and normal tissue complications (dashed line) after photon (triangle) and neutron (circle) irradiations. The steepness of the curves is similar for both radiation qualities implying that the same level of accuracy is required for dose delivery. Modified from Batterman *et al.* (1981).

try and radiation biology, it has not been possible to derive principal or generally accepted quantities and concepts to account quantitatively for radiation quality. In practical situations, therefore, pragmatic solutions using empirical procedures have to be established. In radiation protection, the introduction of a quality factor, defined in dependence of LET, and the quantity dose equivalent, defined as product of absorbed dose and quality factor, is a practicable approach. This approach, however, cannot be transferred to high-LET radiation therapy because of the very much higher accuracy requirements.

The neutron beams used by various therapy centres are of widely differing energies and, correspondingly, variations of up to 50 percent in the RBE between different beams have been found in radiobiological experiments (Hall and Kellerer, 1979; Zywietz *et al.*, 1982; Beauduin *et al.*, 1989). In addition, at some facilities RBE variations have been observed inside irradiated phantoms, in particular with increasing depth (Zeitz *et al.*, 1975; Gueulette *et al.*, 1984; Bewley *et al.*, 1989). In spite of this radiobiological evidence, there is no quantitative and widely accepted specification of radiation quality used in neutron therapy practice. The obvious discrepancy between the accuracy requirement for absorbed dose delivery and the lack of an adequate method for accounting for radiation quality differences and variations calls for an urgent practical solution to this problem.

The radiation quality problem in fast neutron therapy is composed of three distinct aspects: 1) the RBE of neutrons compared with that of photons, 2) the difference of RBE between neutron beams of different energy used at different therapy centres and 3) the variation of radiation quality with respect to different irradiation conditions. Historically, the first aspect has been considered as the most important one because neutron therapy beams have relatively high RBE values (of the order of 3) compared with gamma rays because of the large reaction of absorbed dose delivered by high-LET secondaries. The problem was investigated by means of radiobiological experiments using various biological end-points relevant for therapy (early and late effects in normal tissues). The second aspect is an urgent present problem of neutron therapy owing to the increasing number of neutron therapy centres and to the widely differing energies used (Wambersie et al., 1990). The necessity arises to compare clinical results and therapeutic protocols between different centres and therefore to take into account the differences in radiation quality for the specification of the absorbed dose delivered. The third problem was recognized very early on (Wilson and Field, 1970). Initially, these investigations were focused on radiation quality variations within the irradiated patient or phantoms. With the first generation of neutron therapy facilities (mean neutron energies < 10 MeV) the observed variations of radiation quality and RBE were rather small, at least compared with the RBE difference between neutrons and photons, so that ignoring the variation of radiation quality in tissue (except taking account of variations of the gamma-dose fraction) was considered acceptable. However, considering the accuracy requirement for dose delivery, variations in radiation quality of the order of 5 percent may not be neglected any more and are relevant for treatment planning calculations. Furthermore, with the new generation of high-energy neutron therapy facilities (neutron beams produced using high-energy neutron on Be-targets), significant (5-10 percent) RBE variations can no longer be excluded (Pihet et al., 1988; Pihet, 1989).

Although the RBE difference between photons and neutrons was initially the main motivation for radiation quality investigations, at present priority is given to the determination of the RBE ratio between neutron beams at different facilities.

RBE differences between 10 and 50 percent need to be taken into account for specifying the dose delivered, otherwise the transfer of clinical information is not meaningful. The conversion factor used to account for RBE differences between neutron therapy beams of different energies has been given the name clinical neutron intercomparison factor (CNIF) (Wambersie and Battermann, 1985). This factor compares the biological effectiveness of each neutron beam for identical conditions (same field size, same depth, on the beam axis) with that of another neutron beam chosen as a reference. Considering the accuracy requirement accepted in neutron therapy, the CNIF needs to be specified with an uncertainty of not more than about 3 percent.

Figure 1 in Section 2 illustrates the relevant physical aspects for the differences in radiation quality in terms of microdosimetric spectra between ^{60}Co gamma rays and neutrons and between lower energy neutrons d(14)Be, as used in the initial phase of neutron therapy trials, and a modern high energy therapy facility p(65)Be. The experimental method employed to determine the spectra is the use of (spherical) low pressure proportional counters with walls made of tissue-like material and of the same construction as those used in kerma measurements (see Section 6). The spectra represent the distributions of energy deposited by single (secondary) charged particles when traversing the counter gas cavity. The gas pressure is chosen to "simulate" a sphere diameter of 2 μm of tissue, i.e. the energy loss of charged particles traversing

the cavity along its diameter corresponds to that over a distance of 2 μm in tissue. The microdosimetric quantity lineal energy, y, (ICRU, 1983) is used to express the energy imparted to the mass of the gas. It is defined as the quotient of the energy imparted by single charged particles and 2/3 of the diameter of the spherical counter (= mean chord length). The energy imparted is correlated to the LET of the particles and the actual chord length and is influenced by energy loss straggling and other factors. For the range of energies of interest in neutron therapy, lineal energy spectra can be taken as an approximation for LET distributions.

The shape of microdosimetric spectra for neutrons is related to the types and energy spectra of the charged particles released in neutron interactions with the tissue-like detector material. The distributions extend over a large range of y reflecting the complexity of the secondary charged particle spectra and the related LET distributions. A brief physical explanation for the spectra is given in the figure caption of *Figure 1 in Section 2.*

Comparing spectra such as those in Figure 1 there is an obvious qualitative correlation between the shape of the spectra and their respective radiation quality. However, the quantitative specification of radiation quality for applications in neutron radiation therapy is a very difficult task due to the accuracy requirements. This problem has been investigated since the initial phase of neutron therapy.

Several microdosimetric studies have been carried out by different groups since the early 1970s in close connection with the development of neutron therapy (Wilson and Field, 1970; Oliver *et al.*, 1975; Bridier and Fache, 1975; Menzel *et al.*, 1976; Amols *et al.*, 1977; Heintz *et al.*, 1977; Weaver *et al.*, 1977; Menzel and Schuhmacher, 1981; Booz and Fidorra, 1981; Zywietz *et al.*, 1982; Beach and Milavickas, 1982; Menzel, 1984; Waker and Maughan, 1986; Stinchcomb *et al.*, 1986; Stafford *et al.*, 1987; Binns and Hough, 1988; Schmidt and Hess, 1988; Pihet *et al.*, 1988; Pihet, 1989; Kliauga *et al.*, 1990; Pihet *et al.*, 1990). These studies were aimed at the investigation of changes in radiation quality between different neutron therapy beams and for a given beam between different irradiation conditions. Figures 38 through 42 show typical examples of the results obtained from these investigations.

- Comparison of the dose distributions in lineal energy measured in similar conditions for neutron beams of different energies at various therapy facilities (Figures 38, 39).

- Comparison of microdosimetric spectra obtained in a neutron beam with a given energy, at different depths in a phantom, on the axis of a standard 10 cm × 10 cm field (Figure 40).

- Comparison of microdosimetric spectra obtained in a neutron beam with a given energy, at the same depth in the phantom, on the beam axis and for different field sizes (Figure 41).

- Comparison of microdosimetric spectra obtained in a neutron beam with a given energy, outside the geometrical beam, and by using collimators made of different materials (Figure 42).
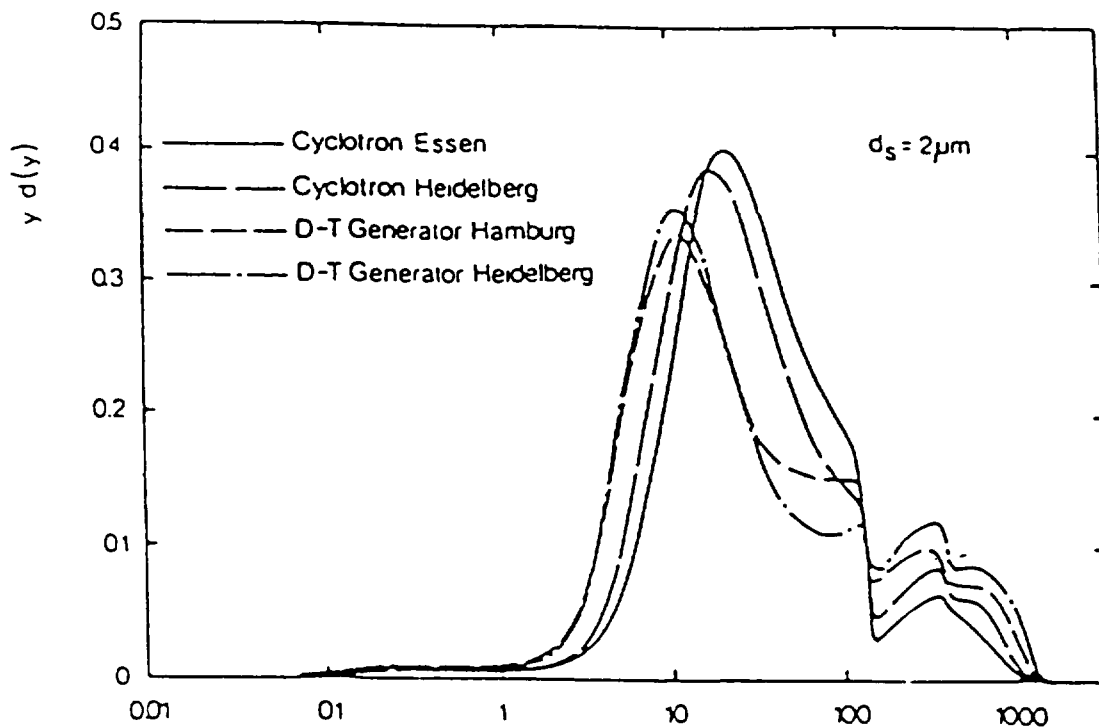
Figure 38: Comparison of microdosimetric distributions measured in the same conditions at three different neutron facilities for four different neutron therapy beams (Menzel and Schuhmacher, 1981).
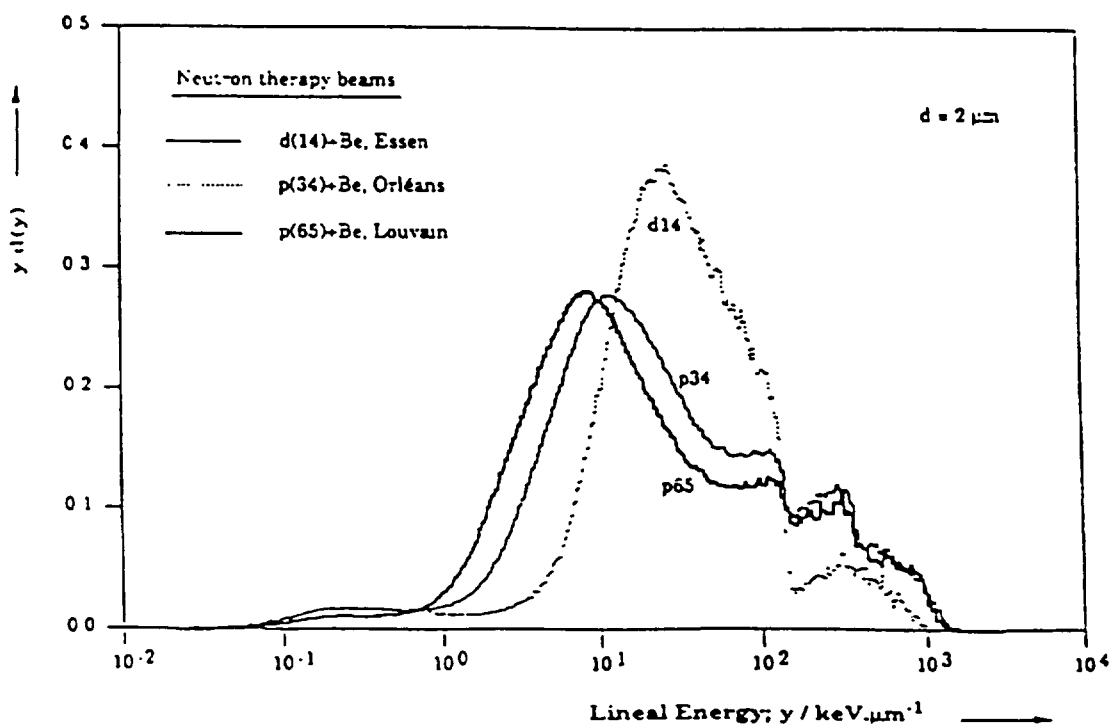
Figure 39: Microdosimetric intercomparison of neutron therapy beams at European facilities sponsored by the EORTC. Comparison of the lineal energy spectra obtained for a low-energy neutron beam and for two beams of the new generation (high-energy proton on Be-targets) neutron beams is shown. Modified from Pihet *et al.* (1988).

110
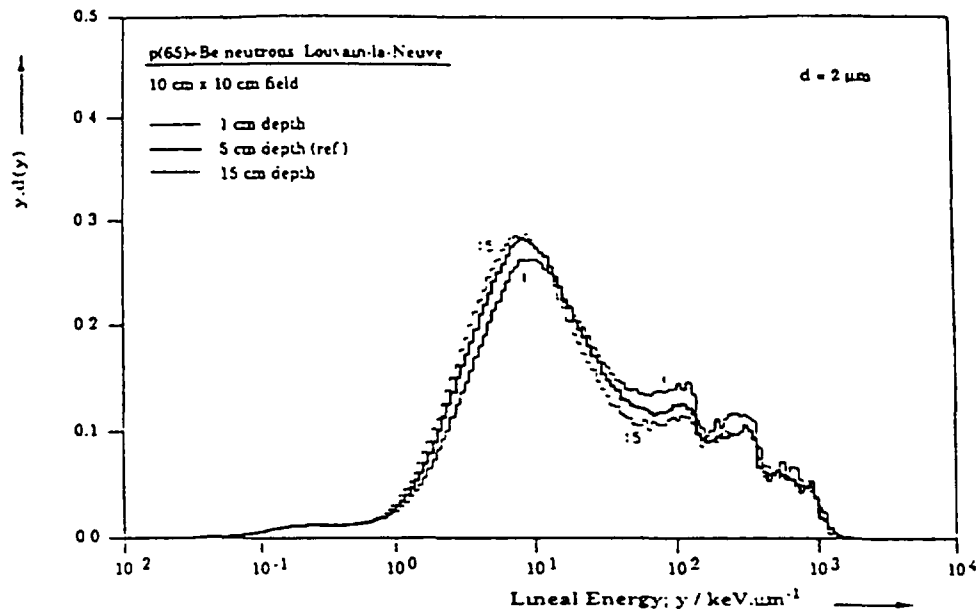
Figure 40: EORTC microdosimetric intercomparison showing comparison of microdosimetric spectra measured at different depths in a phantom on the axis of the p(65)Be neutron therapy beam used at Louvain-la-Neuve (Pihet, 1989).
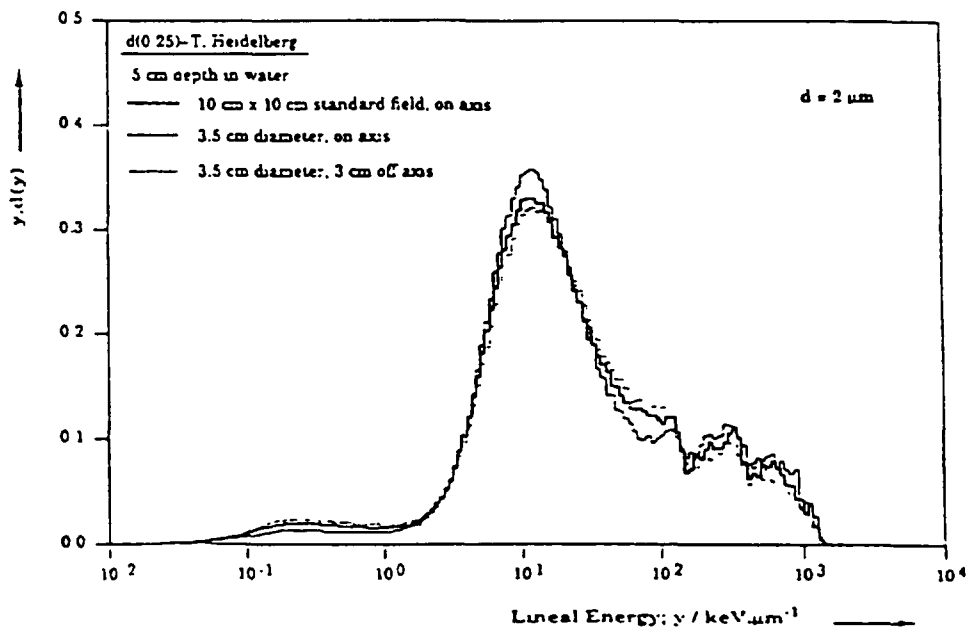
Figure 41: EORTC microdosimetric intercomparison showing comparison of microdosimetric spectra measured for the 14 MeV D-T neutron beam in Heidelberg for different field sizes (Pihet, 1989).
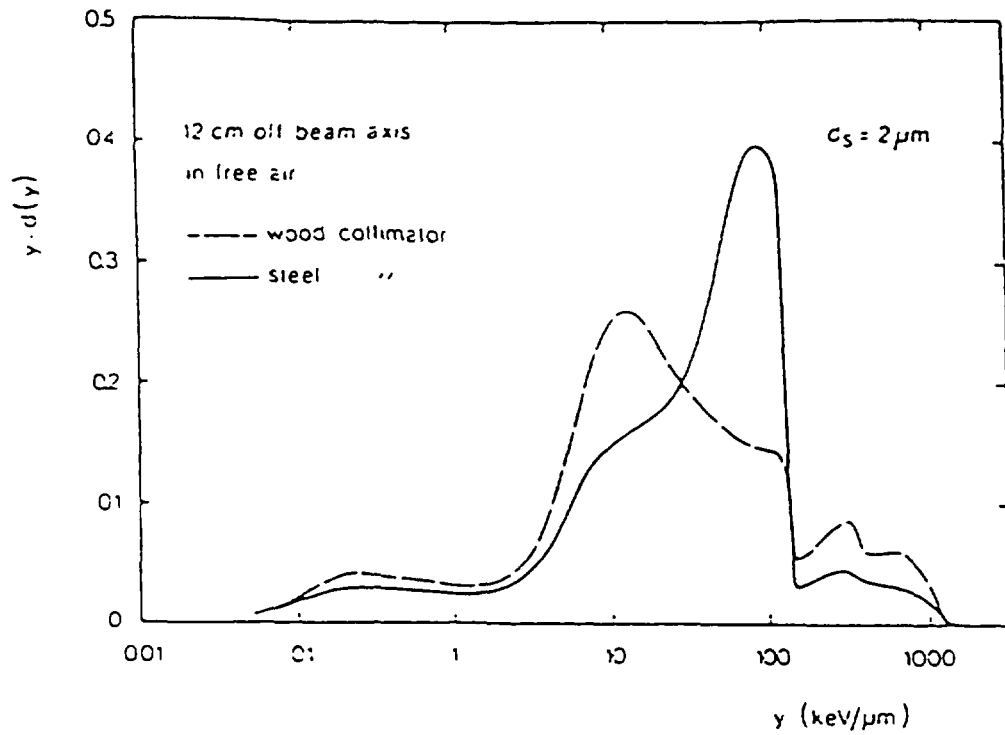
Figure 42: Comparison of microdosimetric spectra measured for 14 MeV D-T neutrons (DKFZ, Heidelberg) outside the geometrical beam for different types of collimator (Menzel, 1984).

These examples illustrate the potential of the microdosimetric approach to account implicitly for any factor related to the current clinical practice that may influence radiation quality.

7.1.2 One Parameter Specification of Radiation Quality

In order to solve the problem of specifying radiation quality in neutron therapy it would be useful to identify a parameter with a relative variation similar to that of RBE. It would then be necessary to prove that such a parameter can be determined with sufficiently low uncertainty. Using microdosimetric data, such a method is well known and consists of deriving mean values from weighted dose distributions in lineal energy. This solution was recognized in earlier studies when the microdosimetric parameter y was used. y is calculated according to Kellerer and Rossi (1972) by weighting the dose distribution in lineal energy with a function (Figure 43) representing the variation of RBE with lineal energy, *i.e.* taking the variation of RBE with LET into account (ICRU, 1983; Menzel, 1984):

$$y^* = y_{sat}(y) \times d(y) \times dy \qquad (8)$$

Phenomenologically, the calculation of y^* illustrates the general solution of the problem, *i.e.* a reasonably good correlation is found between y^* and RBE as a function of neutron energy for some biological endpoints (Pihet *et al.*, 1988). However, the accuracy achievable in specifying radiation quality using y^* (with a fixed weighting function y_{sat}) for neutron therapy is rather low, *i.e.* the ratio of y^* values for two different neutron beams may deviate distinctly from their RBE ratio. It is well known that the RBE versus LET curve critically depends on the level of effect and on the biological system (Barendsen, 1964; Cox *et al.*, 1977). In order to increase the accuracy on the weighted mean parameter, an adjustment of the biological weighting function used is therefore needed. This approach became possible recently by using the results of the microdosimetric intercomparison of European therapy facilities currently carried out by the Heavy Particle Therapy Group of the EORTC (European Organization on Research and Treatment of Cancer).

The problem of specifying the radiation quality for a neutron beam with a given energy compared with that of another neutron beam chosen as a reference may be solved by optimizing a weighting function $r(y)$ so that the integral R:

$$R = r(y) \times d(y) \times dy, \qquad (9)$$

reproduces the RBE ratio between the two neutron beams (Pihet *et al.*, 1990). This approach only assumes a correlation between the RBE of a given neutron beam and the shape of its microdosimetric dose distribution. It does not require further assumption regarding the biophysical meaning of the energy actually deposited in the side. However, the secondary particles are identified here by their lineal energy instead of their type and energy, which is expected to be more relevant for radiation quality specification.

The specification of radiation quality for neutron therapy beams requires that the parameter R is determined with an uncertainty of about 3 percent. The crucial problem therefore remains how accurately can the weighting function $r(y)$ be optimized in order to fulfill this requirement. During the 1980s, biological intercomparisons of neutron therapy facilities were limited most often to two neutron beams of different
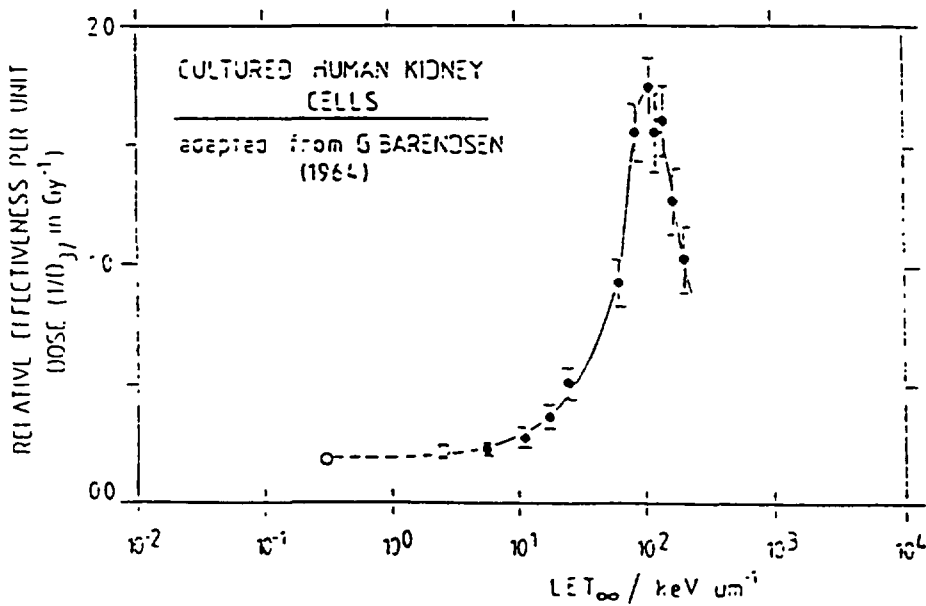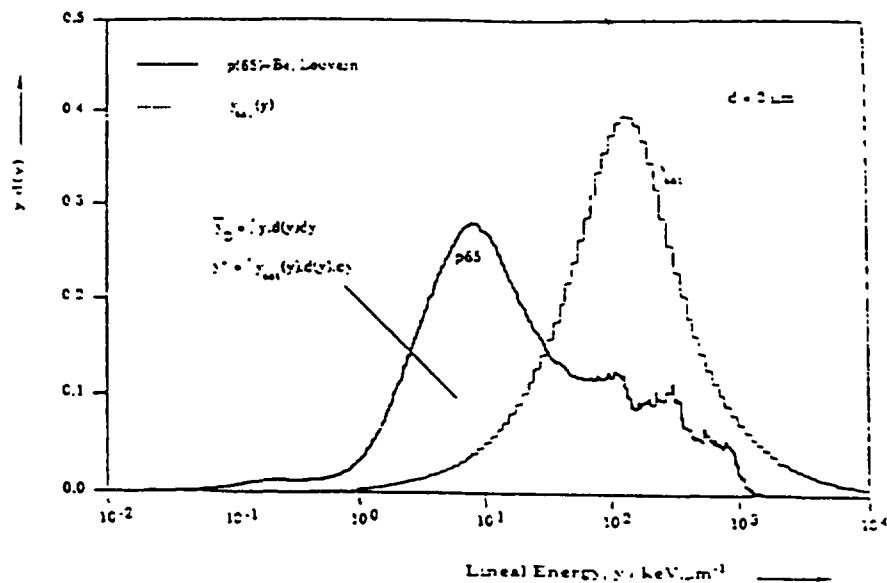
Figure 43: (Bottom) RBE values for mammalian cell survival as a function of LET (Barendsen, 1964). The curve shows a peak at about 100 keV μm^{-1}. This phenomenon is generally referred to as saturation effect.

(Top) The function $y_{sat}(y)$ used as biological weighting function for the calculation of the microdosimetric parameter y^* is similar to the RBE versus LET curve (see text). It is compared with the dose distribution in lineal energy for p(65)+Be neutrons at Louvain-la-Neuve.

energy, *e.g.*, Zywietz *et al.* (1982), Gueulette *et al.* (1984), Joiner and Field (1988). More recently, systematic biological intercomparisons of neutron therapy beams in the energy range between d(14)Be and p(65)Be became available (Beauduin *et al.*, 1989). At the same time, a microdosimetric intercomparison carried out by the EORTC enabled the measurement of the microdosimetric characteristics for 14 different neutron beams including those used in the biological experiments (Pihet *et al.*, 1988). By using the microdosimetric spectra and the RBE ratios determined for the same neutron beams as input data, the weighting function $r(y)$ could be optimized numerically by an iterative procedure. This unfolding method has been applied several times in microdosimetry to evaluate empirically biological weighting functions (Varma and Bond, 1982; Zaider and Brenner, 1985). Assuming an initial guess function, the parameters of the function $r(y)$ are optimized by successive iterations (see Equation 9) in order to match the calculated parameter type R and the experimental RBE ratio for each neutron beam. The main limitations of this approach are the energy range, the biological end-point and the dose level for the RBE values used as input data.

This calculation could be performed using the data for nine neutron beams of different energies ranging from d(4)Be to p(65)Be (Pihet *et al.*, 1990). The optimized weighting functions found by using two different series of RBE ratios are shown in Figure 44. Their shapes are similar to that of the RBE versus LET curves. The effect of the weighting function on the dose distribution in lineal energy is shown in Figure 44 for p(65)Be neutrons. The integral of the weighted dose distribution, R, gives an estimate of the RBE of the beam. In the case of p(65)Be neutrons, this

integral is equal to 1 as this neutron beam was taken as reference radiation according to the biological experiments (RBE ratio=1).

A statistical analysis of the uncertainty of the parameter R as compared to the experimental RBE values showed that an overall uncertainty of 3% (1 standard deviation) can be obtained (Menzel *et al.*, 1990). This proves that the combined microdosimetric and radiobiological approach can fulfill the accuracy requirements of radiation therapy in principle. However, there is a profound lack of systematic radiobiological results for malignant tissues and early and late effects in normal tissues

with an adequate characterization of the radiation field, which could be used for this procedure.

In practice, very pragmatic and unsatisfactory solutions to the problem of radiation quality are in use at present. They rely strongly on the clinical judgment of the involved radio-oncologists. As a kind of minimum requirement for radiation quality specification, it has been suggested to use the beam penetration expressed as half value thickness, HVT, measured in well-defined reference conditions. The justification for this approach can be derived from Figure 44 where RBE ratios are plotted against HVT. This approach is an improvement on current practice. However, it does not meet the accuracy requirements and does not account for variations of RBE within the patient or due to variation in radiation geometry.

7.1.3 Variance of Absorbed Dose at Cellular Level

The difference in radiation quality between neutrons and photons has also consequences with regard to the uniformity of absorbed dose in volumes of the size of biological cells or cell nuclei. The average 1-2 orders of magnitude larger energy deposition for neutrons per traversal of a charged particle means that at a given (macroscopic) absorbed dose the frequency of energy deposition events in microscopic volumes is 1-2 orders of magnitude lower for neutrons than for photons. As a consequence, the variance of absorbed dose in such small volumes is considerably larger for neutrons than for photons. It can be calculated on the basis of microdosmetric data (Lindborg and Brahme, 1990) that the relative standard deviation of energy depositions is in volumes with a diameter of 1 μm; 86% for 14-MeV neutrons and 8%
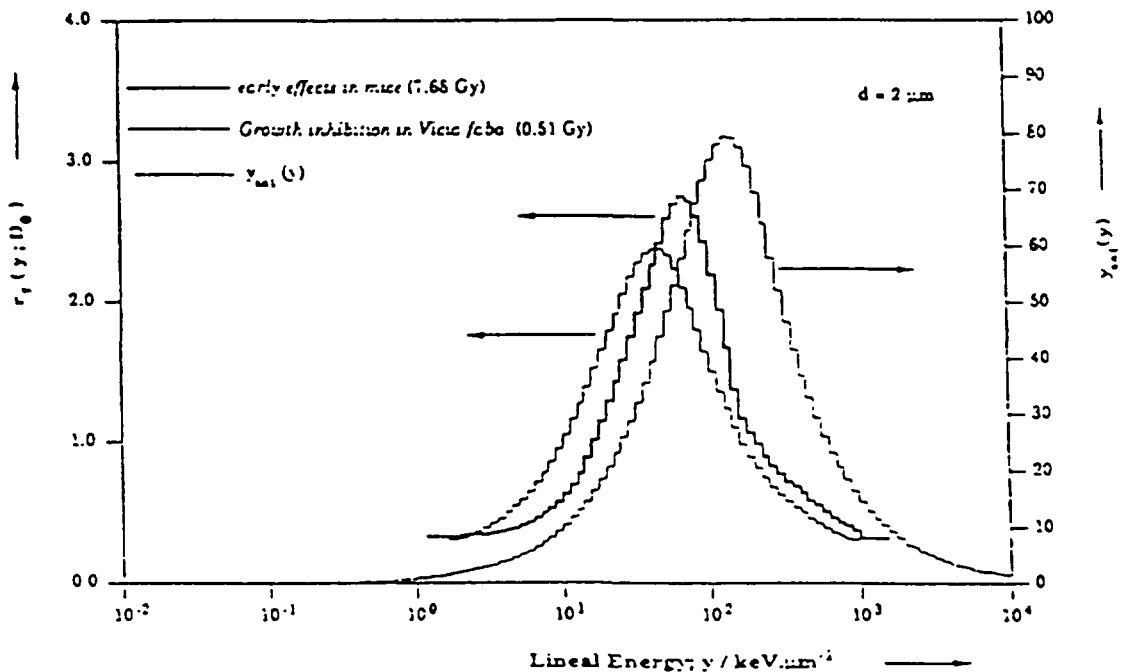
Figure 44: Biological weighting functions obtained numerically by unfolding calculation using RBE ratios and microdosimetric distributions obtained for the same neutron beams as experimental input data. The functions depend on the biological system and the dose level corresponding to the input RBE values. The curves are compared with the function $y_{sat}(y)$ used for the calculation of y^* (Pihet et al., 1990).

116

for ^{60}Co gamma rays. For a diameter of 4 μm the respective standard deviations are 20% and 1.5%. For this calculation a total dose of 22-Gy neutrons and 60-Gy gamma rays was assumed. Lindborg and Brahme (1990) addressed this to-date ignored problem of high-LET radiation therapy in the light of the general requirement of dose uniformity and dose-effect curves for cell killing. They concluded that a combination of photons and neutron therapy may be advantageous in order to achieve a better dose uniformity and improved tumor control.

References

Amols, H.I., Dicello, J.F., Awschalom, M., Coulson, L., Johnsen, S.W., and Theus, R.B., "Physical Characterization of Neutron Beams Produced by Protons and Deuterons of Various Energies Bombarding Beryllium and Lithium Targets of Several Thicknesses," *Med. Phys.* 4, 486-493 (1977).

Barendsen, G.W., "Impairment of the Proliferative Capacity of Human Cells in Culture by Alpha-particles with Differing Lineal-energy Transfer," *Int. J. of Rad. Biol.* 8, 453-466 (1964).

Battermann, J.J., Hart, A.A.M., and Breur, K., "Dose-effect Relations for Tumour Control and Complication Rate After Fast Neutron Therapy for Pelvic Tumours," *Brit. J. Rad.* 54, 899-904 (1981).

Beach, J.L. and Milavickas, L.R., "Microdosimetric Measurements of Radiation Quality Variations in Homogeneous Phantoms Irradiated by Fast Neutrons," *Med. Phys.* 9, 52-59 (1982).

Beauduin, M., Gueulette, J., De Coster, B.M., Gregoire, V., Octave-Prignot, M., Vynckier, S., and Wambersie, A., "Radiobiological Intercomparisons of Fast Neutron Beams Used in Therapy," In: *Proc. of the EORTC-Heavy Particles Therapy Group Meeting*, Munich, October 1987, *Strahlenth. Onk.* 165, 263-267 (1989).

Bewley, D.K., Cullen, B.M., Astor, M., Hall, E.J., Blake, S.W., Bonnett, D.E., and Zaider, M., "Changes in Biological Effectiveness of the Neutron Beam at Clatterbridge (62 MeV p on Be) Measured with Cells In Vitro," *Brit. J. of Rad.* 62, 344-347 (1989).

Binns, P.J. and Hough, J.H., "Lineal Energy Measurements in Two Fast Neutron Beams–d(16)+Be and p(66)," In: *Proc. of the 6th Symposium on Neutron Dosimetry*, Munchen, 1987, H. Schraube, G. Burger and J. Booz (eds.), *Rad. Prot. Dos.* 23, 385-388 (1988).

Booz, J. and Fidorra, J., "Microdosimetric Investigations on Collimated Fast Neutron Beams for Radiation Therapy: II. The Problem of Radiation Quality and RBE," *Phys. Med. Biol.* 26, 43-56 (1981).

Bridier, A. and Fache, P., "Etudes Dosimétriques et Microdosimétriques de Faisceaux de Particules á Transfer Linéique élevée, " Ph.D. Thesis, Université Paul Sabatier, Toulouse, Rapport CEA-R-4655 (1975).

Cox, R., Thacker, J., Goodhead, D.T., and Munson, R.J., "Mutation and Inactivation of Mammalian Cells by Various Ionising Radiations," *Nature* 267, 425-427 (1977).

Gueulette, J., Breteau, N., Sabatier, R., and Wambersie, A., "RBE of p(34)+Be Neutrons for Early Intestinal Tolerance in Mice. Radiobiological Intercomparison Between Orléans (p(34)+Be Neutrons)," In: *Proc. of the EORTC Workshop on High-LET Particles in Radiation Therapy*, Orléans, May 1983, J. Battermann, J.P. LeBourgeois, A. Wambersie, and N. Breteau (eds.), *J. Européen de Radiothérapie* 5, 175-179 (1984).

Hall, E.J. and Kellerer, A., "Review of RBE Data for Cells in Culture," In: *Proc. of the 3rd Meeting on 'Fundamental and Practical Aspects of the Application of Fast Neutrons and Other High LET Particles in Clinical Radiotherapy,'* G.W. Barendsen, J.J. Broerse and J.J. Breur (eds.), pp. 171-174 (1979).

Hartmann, G., Menzel, H.G., and Shuhmacher, H., "Different Approaches to Determine Effective Quality Factors and Dose Equivalent Using the Rossi-counter," In: *Proc. of the 4ᵗʰ Symposium on Neutron Dosimetry*, München, 1981, G. Burger and H.G. Eberg (eds.), (Luxembourg CEC), EUR 7448, pp. 225-236 (1981).

Heintz, P.H., Johnsen, S.W., and Peek, N.F., "Neutron Energy Spectra and Dose Distribution Spectra of Cyclotron Produced Neutron Beams," *Med. Phys.* 4, 250-254 (1977).

International Commission on Radiation Units and Measurements, *Microdosimetry*, Report 36, (International Commission on Radiation Units and Measurements, Bethesda, MD) (1983).

International Commission on Radiation Units and Measurements, *Clinical Neutron Dosimetry. Part I: Determination of Absorbed Dose in a Patient Treated by External Beams of Fast Neutrons*, Report 45, (International Commission on Radiation Units and Measurements, Bethesda, MD) (1989).

Joiner, M.C. and Field, S.B., "The Response of Mouse Skin to Irradiation with Neutrons from the 62 MeV Cyclotron at Clatterbridge, U.K.," *Radiotherapy and Onc.* 12, 153-166 (1988).

Kellerer, A.M. and Rossi, H.H., "The Theory of Dual Radiation Action," *Curr. Topics Radiat. Res. Q.* 8, 85-157 (1972).

Kliauga, P., Bonnett, D., and Waker, A., "A Microdosimetric Comparison of High Energy Neutron Therapy Facilities: Clatterbridge and M.D. Anderson," In: *Proc. of the 10ᵗʰ Symposium on Microdosimetry*, Rome, 1989, J. Booz, J.A. Dennis, and H. Menzel (eds.), *Rad. Prot. Dos.* 31, 449-451 (1990).

Lindborg, L. and Brahme, A., "Influence of Microdosimetric Quantities on Observed Dose-response Relationships in Radiation Therapy," *Rad. Res.* 124, 523-528 (1990).

Menzel, H.G., Pihet, P., and Wambersie, A., "Microdosimetric Specification of Radiation Quality in Neutron Radiation Therapy," *Int. J. Radiat. Biol.* 57(4), 865-883 (1990).

Menzel, H.G. and Schumacher, H., "Comparison of Microdosimetric Characteristics of Four Fast Neutron Therapy Facilities," In: *Proc. of the 7ᵗʰ Symposium on Microdosimetry*, Oxford, 1980, J. Booz, H.G. Ebert, and H.D. Hartfield (eds.), (Luxembourg: CEC, EUR 7147), 1217-1232 (1981).

Menzel, H.G., "Proportional Counter Measurements in Neutron Therapy Beams," IAEA STI/PUB/643, In: *Proc. of a Symposium on Advances in Dosimetry for Neutrons and Heavy Charged Particles for Therapy Applications*, Vienna, 1982 (Vienna: IAEA-AG-371/3), 105-126 (1984).

Menzel, H.G., Waker, A.J., and Hartmann, G., "Radiation Quality Studies of Fast Neutron Therapy Beam," In: *Proc. of the 5th Symposium on Microdosimetry*, J. Booz, H.G. Ebert, and B.R.G. Smith (eds.), (Luxembourg: CEC, EUR 5452), 591-608 (1976).

Oliver, G.D., Walter, J., Grant III, W.H., and Smathers, J.B., "Radiation Quality of Fields Produced by 16, 30, and 50 MeV Deuterons on Beryllium," *Rad. Res.* **61**, 366-373 (1975).

Pihet, P., Gueulette, J., Menzel, H.G., Grillmaier, R.E., and Wambersie, A., "Use of Microdosimetric Data of Clinical Relevance in Neutron Therapy Planning," In: *Proc. of the 7th Symposium on Neutron Dosimetry*, Munich, 1987, H. Schraube, G. Burger, and J. Booz (eds.) *Rad. Prot. Dos.* **23**, 471-474 (1988).

Pihet, P., "Etude Microdosimétrique de Faisceaux de Neutrons de Haute énergie. Applications Dosimétriques et Radiobiologiques," Ph.D. Thesis, Université Catholique de Louvain, Louvain-la-Neuve (1989).

Pihet, P., Menzel, H.G., Schmidt, R., Beauduin, M., Wambersie, A., "Biological Weighting Function for RBE Specification of Neutron Therapy Beams: Intercomparison of 9 European Centers," In: *Proc. of the 10th Symposium on Microdosimetry*, Rome, 1989, J. Booz, J.A. Dennis, and H. Menzel (eds.), *Rad. Prot. Dos.* **31**, 437-442 (1990).

Schmidt, R. and Hess, A., "Component Evaluation of Event Size Spectra for a Clinical 14 MeV Neutron Beam, *Med. Phys.* **15**, 343-347 (1988).

Stafford, M.P., Horton, J.L., and Almond, P.R., "A Microdosimetric Characterization of a Cyclotron-produced Therapeutic Neutron Beam," *Med. Phys.* **14**, 1015-1019 (1987).

Stinchcomb, T.G., Kuchnir, F.T., Myrianthopoulos, L.C., Horton, J.L., and Roberts, W.K., "Correlation of Microdosimetric Measurements with Relative Biological Effectiveness from Clinical Experience for Two Neutron Therapy Beams," *Med. Phys.* **13**, 201-206 (1986).

Varma, M.N. and Bond, V.P., "Emperical Evaluation of Cell Critical Volume Dose vs. Cell Response Function for Pink Mutations in Tradescantia," In: *Proc. of the 8th Symposium on Microdosimetry*, Jülich, September 1982 (Luxembourg: CEC, EUR 8395EN) 439-450 (1982).

Waker, A.J. and Maughan, R.L., "Microdosimetric Inveztigation of a Fast Neutron Radiobiology Facility Utilizing the $d(4)-{}^9Be$ Reaction," *Phys. Med. Biol.* **31**, 1281-1290 (1986).

119

Wambersie, A. and Gueulette, J., "Accuracy Required in Radiotherapy and in Neutron Therapy," IAEA STI/PUB/643, In: *Proc. of the Symposium on Advances in Dosimetry for Neutrons and Heavy Charged Particles for Therapy Applications*, Vienna 1982 (Vienna: IAEA), IAEA-AG-317/1, 11-26 (1984).

Wambersie, A. and Battermann, J.J., "Practical Problems Related to RBE in Neutron Therapy," In: *Proc. of the 3rd Meeting on Progress in Radio-Oncology*, Vienna, 1985 (ICRO), Progress in Radio-Oncology III, 155-162 (1985).

Wambersie, A., Pihet, P., and Menzel, H.G., "The Role of Microdosimetry in Radiotherapy," In: *Proc. of the 10th Symposium on Microdosimetry*, Rome, 1989, J. Booz, J.A. Dennis, and H. Menzel (eds.), *Rad. Prot. Dos.* **31**, 421-432 (1990).

Weaver, K., Bichsel, H., Eenmaa, J., and Wootton, P., "Measurement of Photon Dose Fraction in a Neutron Radiotherapy Beam, *Med. Phys.* **4**, 379-386 (1977).

Wilson, K.S.J. and Field, S.B., "Further Measurement of LET Spectra with a 10 cm Spherical Rossi Counter," In: *Proc. of the 2nd Symposium on Microdosimetry*, H.G. Ebert (ed.) (Luxembourg: CEC, EUR 4452) 137 (1970).

Zaider, M. and Brenner, D.J., "On the Microdosimetric Definition of Quality Factors," *Rad. Res.* **103**, 302-316 (1985).

Zeitz, L., Canada, T.R., Djordjevic, B., Dymbort, G., Freeman, R., McDonald, J.C., O'Neil, J., and Laughlin, J.S., "A Biological Determination of the Variation of Fast Neutron Field Quality with Depth, RBE and OER," *Rad. Res.* **63**, 211-225 (1975).

Zywietz, F., Menzel, H.G., Van Beuningen, D., and Schmidt, R., "A Biological and Microdosimetric Intercomparison of 14 MeV d-T Neutrons and 6 MeV Cyclotron Neutrons," *Int. J. Rad. Biol.* **42**, 223-228 (1982).

CONTRIBUTORS TO DRAFTING AND REVIEW

Broerse, J. J.　　　　Institute of Applied Radiobiology and
　　　　　　　　　　　　Immunology (ITRI) TNO
　　　　　　　　　　P. O. Box 5815
　　　　　　　　　　2280 HV Risjswijk
　　　　　　　　　　The Netherlands

DeLuca, Jr., P. M.　　University of Wisconsin
　　　　　　　　　　Department of Medical Physics
　　　　　　　　　　1530 Medical Sciences Center
　　　　　　　　　　1300 University Avenue
　　　　　　　　　　Madison, WI 53706
　　　　　　　　　　USA

Dietze, G.　　　　　Physikalisch-Technische Bundesanstalt
　　　　　　　　　　Bundesallee 100, Postfach 33 45
　　　　　　　　　　D-3300 Braunschweig
　　　　　　　　　　Germany

Haight, R. C.　　　　Los Alamos National Laboratory
　　　　　　　　　　Group P-15, MS-D406
　　　　　　　　　　Bikini Road
　　　　　　　　　　Los Alamos, NM 87545
　　　　　　　　　　USA

Hiraoka, T.　　　　National Institute of Radiological Sciences
　　　　　　　　　　Division of Physics
　　　　　　　　　　4-9-1 Anagawa, Chiba-shi
　　　　　　　　　　Chiba-ken 260
　　　　　　　　　　Japan

Kawashima, K.　　　National Institute of Radiological Sciences
　　　　　　　　　　Division of Physics
　　　　　　　　　　4-9-1 Anagawa, Chiba-shi
　　　　　　　　　　Chiba-ken 260
　　　　　　　　　　Japan

Kocherov, N.　　　　IAEA
　　　　　　　　　　Nuclear Data Section
　　　　　　　　　　Wagramerstrasse 5, P. O. Box 100
　　　　　　　　　　A-1400 Vienna
　　　　　　　　　　Austria

Menzel, H. G.　　　Commission of European Communities
　　　　　　　　　　DG XII/D/3
　　　　　　　　　　200 Rue de la Loi
　　　　　　　　　　B-1049 Brussels
　　　　　　　　　　Belgium

Olsson, N.
Uppsala University
Department of Neutron Research
Studsvik
S-611 82 Nyköping
Sweden

Wambersie, A.
Université Catholique de Louvain
Faculté de Medicine
Unité de Radiotherapie et Radioprotection
Avenue Hippocrate 54
B-1200 Brussels
Belgium

White, R. M.
Lawrence Livermore National Laboratory
Physics Department, L-298
Livermore, CA 94550
USA

Zoetelief, J.
Institute of Applied Radiobiology and
Immunology (ITRI) TNO
P. O. Box 5815
2280 HV Risjswijk
The Netherlands